# UNIVERSITY OF SOUTHAMPTON

FACULTY OF ENGINEERING AND PHYSICAL SCIENCES

School of Electronics and Computer Science

**Simulation of Brayton Cycle and Selection of Heat Exchangers for a Small High-Temperature Gas-Cooled Reactor**

by

**Donny Nurmayady**

1st Supervisor: Dr. Igor Golosnoy

2nd Supervisor: Professor George Chen

Thesis for the degree of Master of Philosophy

August 2022

**UNIVERSITY OF SOUTHAMPTON**

# ABSTRACT

FACULTY OF ENGINEERING AND PHYSICAL SCIENCES

Electronics and Computer Science

Thesis for a degree of Master of Philosophy

**SIMULATION OF BRAYTON CYCLE AND SELECTION OF HEAT EXCHANGERS FOR A SMALL HIGH TEMPERATURE GAS-COOLED REACTOR**

Donny Nurmayady

HTGR is an advanced gas-cooled reactor that utilized high temperature and high pressure. This work aims to understand the state of the art on HTGR Gas turbine plants with aim of identifying the research gaps and challenges. With this knowledge, we develop a model power conversion system (PCS) for a High-Temperature Gas-cooled reactor. HTGR technology which has been chosen by Indonesian authorities (sponsors of this work), is relatively small with only 10MWth-installed power. Thus, Small Medium Reactor(SMR)-HTGR would be described. This research investigated five different working gases in five PCS Brayton cycle configurations in HTGR 10MWth. Thermodynamic analysis using cold-gas standard assumption was applied to measure the efficiencies. This research also considered temperature interaction in heat exchangers and the capability of a turbine to drive a compressor. Particular gas would be suitable for a particular pressure ratio and PCS diagram. 1T2C diagram with pressure ratio 9 and carbon dioxide as the working gas were able to reach optimum thermal efficiency, which was about 43 %. Double pipe heat exchanger served in Intermediate Heat Exchanger (IHX) and recuperator. The sizing of the heat exchangers determined the dimension as well as pressure drop of this component. The pressure drop of IHX was 413580 Pa for the hot side and 64227 Pa for the cold side and the length was about 37 m. The pressure drop of the recuperator was 700883 Pa for the hot side and 824731 Pa for the cold side and the length was about 70 m.

# Declaration of Authorship

Print name : Donny Nurmayady

Title of thesis : Simulation of Brayton Cycle and Selection of Heat Exchangers for a Small High-Temperature Gas-Cooled Reactor

I declare that this thesis and the work presented in it are my own and has been generated by me as the result of my own original research.

I confirm that:

1. This work was done wholly or mainly while in candidature for a research degree at this University;

2. Where any part of this thesis has previously been submitted for a degree or any other qualification at this University or any other institution, this has been clearly stated;

3. Where I have consulted the published work of others, this is always clearly attributed;

4. Where I have quoted from the work of others, the source is always given. With the exception of such quotations, this thesis is entirely my own work;

5. I have acknowledged all main sources of help;

6. Where the thesis is based on work done by myself jointly with others, I have made clear exactly what was done by others and what I have contributed myself;

7. A part of this thesis, chapter four, had been presented and published in an international conference. The article is :

Donny Nurmayady, "Thermal Efficiency Modelling for HTGR GT 10 MWth" *4th International Conference on Nuclear Energy Technologies and Science 2021 (Iconets 2021 )*, 8th September 2021, Virtual Conference. https://doi.org/10.1063/5.0095613

Signed:

Date : 21st June 2022

# Table of Contents

**List of Tables** ..... **iii**

**List of Figures** ..... **iv**

**Abbreviations and Nomenclature** ..... **vi**

**Acknowkedgement** ..... **vix**

**Chapter 1 Introduction** ..... **ix**

1.1 Background ..... 1

1.2 Research Aim and Objectives ..... 2

1.3 Research Methodology ..... 2

1.4 Report Structure ..... 3

**Chapter 2 Literature review** ..... **5**

2.1 HTGR Development ..... 5

2.2 Brayton Cycle Configuration ..... 11

2.2.1 Direct vs Indirect Cycle ..... 12

2.2.2 Open Cycle vs Closed Cycle ..... 12

2.2.3 Working Fluid ..... 13

2.2.4 Modification Brayton Cycle Configuration ..... 14

2.3 Heat Exchanger ..... 16

2.4 Summary ..... 18

**Chapter 3 HTGR Modelling** ..... **19**

3.1 Thermodynamic Analysis ..... 19

**3.2** Sizing Heat Exchanger ..... 25

**Chapter 4. Thermal Efficiency Brayton cycle** ..... **34**

4.1. Thermodynamic Analysis of Open Cycle Configuration ..... 34

4.2. Thermodynamic Analysis of 1T1C Configuration ..... 40

4.3. Thermodynamic Analysis of 1T2C Configuration ..... 46

4.4. Thermodynamic Analysis of 2T2C Cycle Configuration ..... 52

4.5. Thermodynamic Analysis of Combined Cycle Configuration ..... 58

**Chapter 5. Double Pipe Heat Exchanger .....64**

**5.1.** Intermediate Heat Exchanger (IHX)..... 65

**5.2.** Recuperator..... 69

**Chapter 6. Conclusion.....72**

**List of References .....73**

# List of Tables

Table 2.1 Development HTGR design ..... 6

Table 3.1 Data assumption ..... 23

Table 4.1. Gas turbine open cycle diagram for pressure ratio 9 and turbine temperature inlet 1200 K ..... 36

Table 4.2. Optimum pressure ratio at minimum temperature (800K) for open-cycle diagram 39

Table 4.3. Gas turbine 1T1C diagram for pressure ratio 9 and turbine temperature inlet 1200K.42

Table 4.4. Optimum pressure ratio at minimum temperature (800K) for 1T1C diagram ..... 45

Table 4.5. Gas turbine 1T2C diagram for pressure ratio 9 and turbine temperature inlet 1200K.48

Table 4.6. Optimum pressure ratio at minimum temperature (800K) for 1T2C diagram ..... 51

Table 4.7. Gas turbine 2T2C diagram for pressure ratio 9 and turbine temperature inlet 1200K. 54

Table 4.8. Optimum pressure ratio at minimum temperature (800K) for 2T2C diagram ..... 57

Table 4.9. Combined cycle diagram for pressure ratio 9 and turbine temperature inlet 1200K. 60

Table 4.10. Optimum pressure ratio vs efficiency.....63

Table 5.1 Properties of the gases .....65

Table 5.2 Result calculation sizing IHX..... 67

Table 5.3 Result calculation sizing Recuperator.....70

# List of Figures

Figure 2.1 Variations in Brayton cycle configuration ..... 11

Figure 2.2 Two-stage Brayton cycle ..... 15

Figure 3.1 Flowchart Brayton cycle thermal calculation ..... 24

Figure 3.2 Heat transfer in double pipe ..... 25

Figure 3.3 Heat transfer energy in a medium surface and electrical resistance analogy ..... 27

Figure 3.4 Procedure sizing a double pipe heat exchanger ..... 31

Figure 3.5 Flow energy and temperature distribution counterflow double pipe heat exchanger ..... 32

Figure 4.1 Gas turbine diagram (open cycle) for pressure ratio 9 and turbine temperature inlet 1200 K ..... 35

Figure 4.2 Calculation results open cycle diagram for pressure ratio at 9 and various temperature inlet turbines ..... 37

Figure 4.3 Calculation results of open cycle diagram for various pressure ratios and temperature inlet turbines at 1200 K ..... 38

Figure 4.4 Gas turbine diagram (1T1C) for pressure ratio 9 and turbine temperature inlet 1200 K ..... 41

Figure 4.5 Calculation results 1T1C diagram for pressure ratio at 9 and various temperature inlet turbines ..... 43

Figure 4.6 Calculation results of 1T1C diagram for various pressure ratios and temperature inlet turbines at 1200 K ..... 44

Figure 4.7 Gas turbine diagram (1T2C) for pressure ratio 9 and turbine temperature inlet 1200 K ..... 47

Figure 4.8 Calculation results 1T2C diagram for pressure ratio at 9 and various temperature inlet turbines ..... 49

Figure 4.9 Calculation results of 1T2C diagram for various pressure ratios and temperature inlet turbines at 1200 K ..... 50

Figure 4.10 Gas turbine diagram (2T2C) for pressure ratio 9 and turbine temperature inlet 1200 K ..... 53

Figure 4.11 Calculation results 2T2C diagram for pressure ratio at 9 and various temperature inlet turbines ..... 55

Figure 4.12 Calculation results of 2T2C diagram for various pressure ratios and temperature inlet turbines at 1200 K ..... 56

Figure 4.13 Combined cycle diagram (2T2C) for pressure ratio 9 and turbine temperature inlet 1200 K ..... 59

Figure 4.14 Calculation results combined cycle diagram for pressure ratio at 9 and various temperature inlet turbines ..... 61

Figure 4.15 Calculation results combined cycle diagram for pressure ratio at 9 and various temperature inlet turbines ..... 62

Figure 5.1 Double pipe heat exchanger ..... 64

# Abbreviations and Nomenclature

| | |
|---|---|
| HTGR | High Temperature Gas-cooled Reactor |
| PCS | Power Conversion System |
| SMR | Small Medium Reactor |
| CO2 | Carbon dioxide |
| EPR | Experimental Power Reactor |
| CTE | Coefficient of Thermal Expansion |
| HTR | High Temperature Reactor |
| PBMR | Pebble Bed Modular Reactor |
| HTR-PM | High Temperature Reactor- Pebble-bed Modular |
| MPa | Mega Pascal |
| MWth | Mega Watt thermal |
| MWe | Mega Watt electric |
| GTHTR | Gas Turbine High Temperature Reactor |
| GT-MHR | Gas Turbine Modular High temperature Reactor |
| RDE | Reaktor Daya Eksperimental |
| IAEA | International Atomic Energy Agency |
| GA | General Atom |
| H2O | Air |
| N2 | Nitrogen |
| H2 | Hydrogen |
| He | Helium |
| Xe | Xenon |
| LPG | Liquefied Petroleum Gas |
| TEMA | Tubular Exchanger Manufacturers Association |
| CBC | Closed Brayton Cycle |
| LMTD | Log Mean Temperature Difference |
| IHX | Intermediate Heat Exchanger |
| LPC | Low Pressure Compressor |
| HPC | High Pressure Compressor |
| SFR | Sodium Fast Reactor |

# Nomenclature

| | | |
|---|---|---|
| d | Diameter | (m) |
| $\dot{m}_{core}$ *or* $\dot{m}_1$ | Mass flow rate core or primary loop | (kg/s) |
| $\dot{m}_2$ | Mass flow rate in secondary loop | (kg/s) |
| $\dot{m}_{2,water}$ | Mass flow rate in cooler | (kg/s) |
| $h_{rx\_i/o}$ | Enthalpy reactor, input/output | (kJ/kg) |
| $h_{pump\_i/o}$ | Enthalpy pump, input/output | (kJ/kg) |
| $h_{HPC\_i/o}$ | Enthalpy HPC, input/output | (kJ/kg) |
| $h_{turb\_i/o}$ | Enthalpy turbine, input/output | (kJ/kg) |
| $h_{cooler\_hot\_i/o}$ | Enthalpy cooler, input/output | (kJ/kg) |
| $h_{cooler\_cold\_i/o}$ | Enthalpy cooler water, input/output | (kJ/kg) |
| $p_{HPC\_i}$ | Pressure HPC | (Bar) |
| $p_{recu,cold}$ | Pressure recuperator cold | (Bar) |
| $p_{turb\_i}$ | Pressure Turbine | (Bar) |
| $p_{cooler}$ | Pressure cooler | (Bar) |
| $p_{drop}$ | Pressure drop | (Bar) |
| $T_{core\_i/o}$ | Temperature reactor core, input/output | (K) |
| $T_{turb\_i/o}$ | Temperature turbine input/output | (K) |
| $T_{recu\_i/o}$ | Temperature recuperator hot, input/output | (K) |
| $T_{cooler\_i/o}$ | Temperature cooler, input/output | (K) |
| $C_p$ | Specific heat at constant pressure | (kJ/(kg.K)) |
| $C_v$ | Specific heat at constant pressure | (kJ/(kg.K)) |
| $R_e$ | Reynolds Number | |
| $\gamma$ | Gamma, ratio between $C_p$ and $C_v$ | |
| $PR\_{}_{HPC}$ | Pressure Ratio HPC | |
| $PR_{\_LPC}$ | Pressure Ratio LPC | |
| $W_{comp}$ | Compressor Work | (kW) |
| $W_{turb}$ | Turbine Work | (kW) |
| $W_{pump}$ | Pump Load | (kW) |

| | | |
|---|---|---|
| $\eta_t$ | Turbine efficiency | |
| $\eta_c$ | Compressor efficiency | |
| $\eta_{cycle}$ | Cycle efficiency | |
| $\eta_{elec}$ | Electrical efficiency or Carnot efficiency | |
| $\eta_{gen}$ | Generator efficiency | |
| $\varepsilon_{IHX}$ | IHX Effectiveness | |
| $\varepsilon_{Recu}$ | Recuperator Effectiveness | |
| $Qth_{core}$ | Reactor Power | (kW) |
| $Q_{IHX}$ | IHX Power | (kW) |
| $Q_{recu}$ | Recuperator Power | (kW) |
| $Q_{cooler}$ | Cooler Power | (kW) |
| $\dot{Q}_{cond}$ | Heat transfer rate conduction | (J/s) |
| $\dot{Q}_{conv}$ | Heat transfer rate conduction | (J/s) |
| $\frac{\partial T}{\partial x}$ | Gradien Temperature per meter | (K/m) |
| A | Area heat transfer | ($m^2$) |
| L | Length of pipe | (m) |
| $h_{i/o}$ | Heat convection coefficient input/output | ($W/m^2.K$) |
| U | Overall heat transfer coefficient | (W/m.K) |
| $\mu_{gas}$ | Dynamic viscosity gas | (Pa.s) |
| $k_{gas}$ | Thermal conductivity gas | (W/m.K) |
| v | Velocity of the fluid flow | (m/s) |
| ρ | Density of the gas | ($kg/m^3$) |
| $\Delta P$ | Pressure drop | (Pa) |
| $D_e$ | Equivalent diameter | (m) |
| $D_h$ | | |
| $D_1$ | Outside surface diameter of Inner pipe | (m) |
| $D_2$ | Inside diameter of outer pipe | (m) |
| $\Delta T_m$ | Log Mean Temperature Difference (LMTD) | |
| $Q_{tot}$ | Heat exchanger duty | (W) |
| OD/ID | Outer Diameter pipe /Inner Diameter Pipe | (Inch) |

# Acknowledgements

I would like to thank Allah Subhannahu Wa Ta'ala for giving me health and blessing in completing this report. Without His blessing, I would never manage to complete this report.

I would not have finished this thesis journey without my beautiful wife, Mita Konstantin and my sunshine kid, Maliki Jibrilian Akbar being the air of my breath. Seeing your smile is an endorphin for doing something extraordinary.

I wish to express my gratitude to my supervisors, Dr Igor Golosnoy and Prof. George Chen, who gave me helpful advice, invaluable encouragement, and extraordinary patience in guiding me throughout my study. I am deeply thankful for the moral and technical support they have given. This research project would not have been possible to be made without their guidance,

I wish to express my gratitude to my examiners Prof. Harold Chong and Prof. Meihong Wang for the helpful advice about my research in my MPhil Viva. It was an honour for me examined by great people like you.

Very deep condolence to my best friend, Faiz Faisol Makarim, a great man who struggled with the Covid pandemic. I will tell the world how we spent our young time cheerfully. Shed a tear always falls whenever remembering your banter. I will keep in touch with the others, Andang and Andri.

I am most grateful for and honoured to be awarded, a scholarship from the Ministry of Research and Technology of Indonesia (RISET-Pro) for covering all my needs throughout my study. I wish my research project will contribute to Indonesian Research and Development

# Chapter 1 Introduction

## 1.1 Background

The Paris agreement has urged countries to use a low carbon technology in the power sector to keep global temperature below 2$^{o}$C [1]. High-Temperature Gas-cooled Reactor is an advanced nuclear power plant technology which able to produce electricity in a low carbon waste. Due to high capital cost, this technology needs to be developed in small capacity and modular installation which is called Small Modular Reactor (SMR). SMR-HTGR has been estimated that could be a low carbon future electricity producer with ten times the current installed capacity up to 2050, or could at least substitute all coal-fired power plants [2]. Flexibility in installation and lower capital costs are required for a future power reactor. SMR-HTGR can be installed in a remote area. This technology offers once-time installation for 30 years lifetime reactor. Thus, there is no need for refuelling nuclear reactor for that period of time [3].

Power generation capacity in Indonesia has to be developed and increased due to population and economic growth as well as the demand for improved quality of life in Indonesian society. The society has a per capita total production of electricity of around 1967 kWh/year; however, 15% of the population in 2015 had no access to electricity [3]. The government has targeted a 26% reduction in CO2 emissions by 2025[4]. To support the government target, the National Nuclear Energy Agency will build an Experimental Power Reactor (EPR) [3]. This reactor is a preliminary project to develop national capabilities in nuclear power plant development. At the present moment, Indonesia does not have any nuclear power plant and building one from scratch is not a simple task. Thus, this power reactor would become a real-time learning tool. The technology reactor that has been chosen is based on High-Temperature Gas-cooled Reactor (HTGR) which is a nuclear reactor that uses helium (gas) as a coolant in the reactor and graphite for the structural core and can produce high-temperature heat for the power station and cogeneration purposes. Compared to light water reactors, the outlet temperature of which is limited to around 300$^{o}$C, HTGR can produce high-temperature heat around 1000$^{o}$C. EPR will apply a steam turbine or Rankine cycle as a power conversion system (PCS). Despite the maturity of Rankine cycle PCS, the capability of HTGR on producing high temperature for PCS would be one consideration to applying gas turbine or Brayton cycle PCS. Brayton cycles can accommodate high temperatures. Therefore, the Brayton cycle was chosen for PCS in this research due to its high thermal efficiency [5], simple size in design arrangement [3], and flexibility in working gas options [6].

Nuclear power plants design and installation always initiate debates on efficiency and safety of the units. The system is expected to provide noticeable benefits and to satisfy all International Atomic Energy Agency (IAEA) requirements. People in Indonesia need strong assurance to believe that nuclear power plants are safe. To learn the performances of the plant, the components of this power station have to be analyzed and selected. Five configurations of the Brayton cycle with five different working gasses will be assessed. A heat exchanger, which is one of the important components, needs to be selected. The selected components and configuration must achieve a high efficiency considering the turbine's capability to drive the compressor as well as the heat exchanger to transfer energy. Suitable working fluids for the HTGR gas turbine power station would be selected conforming to configuration and pressure ratio.

## 1.2 Research Aim, Objectives and Novel Contribution

This MPhil study aims to develop:

1. Optimal PCS performance for a SMR-HTGR 10 MWTh.

2. Sizing heat exchangers for the working gas cycle.

The aim is achieved through three objectives, which are

1. Literature review of Brayton cycle configurations in nuclear power plants as well as working gasses in this plant;
2. Assessment of five Brayton cycle configurations with five working gasses, such as Helium, Hydrogen, Carbon dioxide, Nitrogen, and Air.
3. Selection of heat exchanger for Brayton cycle.

Particular gas with particular pressure ratio using cold-gas standard assumption would be a novel contribution in PCS Brayton cycle research knowledge and development.

## 1.3 Research Methodology

A nuclear reactor will be assumed constant and performed as a heat source. The research will assess five different Brayton cycle configurations and five different working gasses. The research applies thermodynamic analysis and uses cold-gas standard assumption to assess thermal efficiency. Matlab-Simulink will be used for analytical modelling and analysis. Selection of the Brayton cycle will consider turbine capability to drive compressor, heat exchanger as well as an optimum pressure ratio.

## 1.4 Report Structure

A literature review is presented in Chapter 2 determining general knowledge of Brayton cycle configuration, basic heat transfer, and the development of the Brayton cycle as well as working gasses in a nuclear power plant. Chapter 3 comprises formulas and assumptions as to the research methodology. Thermals of various Brayton cycles with various working gas are described in Chapter 4. Chapter 5 describes the sizing of the heat exchanger. The conclusions are presented in Chapter 6.

# Chapter 2 Literature review

HTGR is a nuclear reactor and able to supply high-temperature gas for power station and cogeneration purposes. This reactor uses helium (gas) as a coolant in the reactor and graphite for the structural core. Compared to light water reactors, whose outlet temperature is limited to around 300$^{o}$C, HTGR can produce high-temperature heat around 1000$^{o}$C. HTGR core structure mainly consists of graphite which has enormous heat capacity; hence, it can conduct heat. Furthermore, graphite also has a low Coefficient of Thermal Expansion (CTE) [1]. Thus, the material is difficult to melt. This means that the HTGR has significant safety that has no concern of core meltdown or radioactivity release accidents. HTR-10 Nuclear power plant (INET-China) is one of the HTGR technologies and proved its safety systems in 2010 [3]. However, the capital cost of HTGR is expensive. This technology requires improvement, modification and enhancement of capabilities HTGR. Smaller capacity and multipurpose HTGR have been proposed to meet the economic value of HTGR.

## 2.1 HTGR Development

In the 1960s, HTGR was developed in the United Kingdom, Germany, and the United States of America. China, Russia, Japan and South Africa contributed in the following decades. Before 2000, the development focused on the opportunity of HTGR operation to support electricity with high efficiency. Although HTGR was able to produce electricity with high efficiency, the capital costs of HTGR were expensive. This was because the design specifications of HTGR were high to support high temperature and high pressure. Thus, HTGR costs were unable to compete with other nuclear power plant technology. Therefore, there is no commercial HTGR yet. More advanced improvements are required to allow the commercialization of HTGR [3]. A smaller capacity of HTGR would decrease the capital cost of this technology. Another improvement, a multipurpose reactor such as cogeneration, would enhance the capability of this technology. Thus, the capital cost of HTGR would meet economic value. SMR-HTGR has been proposed to overcome the challenge of HTGR development.

Cerelli et al. [8] explain the meaning of “small” and “modular” as follows: Small refers to the reactor power rating. While no definitive range exists, a power rating from approximately 10 to 300 MWe has generally been adopted. Modular refers to the unit assembly of the nuclear PCS which, when coupled to a power conversion system or process heat supply system, delivers the desired energy product. The unit assembly can be assembled from one or several submodules.

In the early 2000s, the Small Modular Reactor (SMR) concept offered a lower capacity between 10 MWe and 300 MWe. The design is simpler than a conventional nuclear power plant. Thus, construction time will be shorter and capital costs lower. The plant is built using modular construction. The unit can be fabricated and assembled in a module or sub-module. The deployment of this module can be added over time to match regional load growth [8]. The advantages of SMR are expected to be flexibly located, reduction in construction time as well as the ability of multi-generation (such as combined heat and power). However, there is a common issue about the lack of precise licensing requirements from the nuclear regulatory agency due to inexperience with the new technology [8]. Nevertheless, the issue would be solved by each country's policies.

Designers have started arranging conceptual designs of SMR-HTGR. HTR-10 (a test facility reactor) from China is one of the remarkable examples of such a plant. The reactor is operating now and has been running as one of the safest reactors around. Test runs done in this plant show that the reactor can operate normally without human intervention in the plant area for up to two weeks. Another example of such a plant is PBMR-400 from South Africa. Although this plant has a detailed design, the project has stopped because of management problems. In recent decades, cogeneration in HTGR has been also considered as it can improve the overall thermal efficiency of the plant. Several recent designs take into account cogeneration opportunities and multiple reactor usage. It was indicated that almost all reactor designs have finished their conceptual design phase, and are going to continue to the next phase [3]. Moreover, HTR-PM from China is under construction right now and planned to move into a commercial power plant. Some of the reactor specifications are illustrated in Table 2.1

Table 2.1 Development HTGR design [3]

| HTGR Reactor | Power | Temperature core in/out ($^{o}$C) | Pressure (MPa) | Status |
|---|---|---|---|---|
| HTR-PM<br>China | 2 x 210 MWe | 250/750 | 7/13.25 | It is a twin reactor for a single power conversion unit. The power conversion uses the Rankine cycle.<br>Status: demonstration operation |
| Starcore<br>Canada | 6 modules with various power | 280/750 | 7.4 / 6.7 | Status: conceptual design. This reactor was expected for remote area purposes. |

| | | | | |
|---|---|---|---|---|
| GTHTR 300<br>Japan | 600 MWth/100-300 MWe | 587/850<br>683/950 | 7/7 | This reactor utilizes a direct Brayton cycle for the power conversion system. The thermal efficiency of power conversion is 45-50%. This reactor is also projected for cogeneration.<br>Status: Basic design completed, Prelicensing. |
| GTMHR<br>Russia | 600 MWth/288 MWe | 490/850 | 7.2 | This reactor utilizes a direct Brayton cycle for the power conversion system.<br>Status: Preliminary design completed. |
| MHR-T<br>Russia | 4 x 600 MWth<br>4 x 200 MWe | 578/950 | 7.5 | The main purpose of this reactor is hydrogen production<br>Status: Conceptual design |
| MHR-100GT<br>Rusia | 25 MWe-87 MWe | 492/975<br>553/950 | 4-5 | Status : Conceptual design |
| Xe 100<br>USA | 200 MWth/82.5MWe | 260/750 | 6/16.5 | This reactor utilizes the Rankine cycle for the power conversion system. This reactor is also projected for cogeneration.<br>Status: Basic design. |
| SC-HTGR<br>USA | 625 MWth/272 MWe | 325/750 | 6/16 | This reactor utilizes the Rankine cycle for the power conversion system. This reactor is also projected for cogeneration and industrial process heat.<br>Status: Basic design. |
| HTR-10<br>China | 10 MWth/2.5 MWe | 250/700 | 3/4 | The main purpose of this reactor is to generate electricity and this reactor utilizes the Rankine cycle for the power conversion system |

| | | | | |
|---|---|---|---|---|
| | | | | Status: operational for research and demonstration. |
| RDE-Micro Peluit<br><br>Indonesia | 10 MWth /3 MWe | 250/750 | 3/6 | This reactor utilizes the Rankine cycle for the power conversion system. This reactor is also projected for cogeneration and industrial process heat.<br><br>Status: Licence issue since 2017 |
| PBMR<br><br>South Africa | 400 MWth/165 Mwe | 500/900 | 9 | This reactor utilizes a direct Brayton cycle for the power conversion system.<br><br>Status: The preliminary design is completed. The project was stopped in 2010. |
| AHTR-100<br><br>South Africa | 100 MWth/50 MWe | 406/1200 | 9 | This reactor was projected for combined cycle and cogeneration. |
| HTMR-100<br><br>South Africa | 100 MWth/35 MWe | 250/750 | 4 | This reactor utilizes the Rankine cycle for the power conversion system. This reactor is also projected for cogeneration.<br><br>Status: Conceptual design |
| HTTR<br><br>Japan | 30 MWth | 395/850 | 4 | This reactor produces only heat for industrial applications.<br><br>Status: Operational |

Table 2.1 shows the development of Small Modular Reactor HTGR by 2020 [3]. These developments were reported in IAEA annual reports. SMR were able to produce 300 MWe per unit. SMR-HTGR were able to support for more than one purpose, not only for an electrical generation but also industrial heat application. Hence, the utilization of HTGR was increased and would subsidize the capital cost of the HTGR core. SMR-HTGR was able to support the Rankine cycle, Brayton cycle or combined cycle. Temperature core input for Rankine cycle was 250°C-300°C while for Brayton cycle was 490°C-587°C. Temperature core output would be utilized by the power conversion system.

Temperature core output for the Brayton cycle was higher and more varied than for the Rankine cycle. Temperature core output for the Brayton cycle was 850°C-1000°C while temperature core output for the Rankine cycle was 100°C-150°C. This temperature directly affects the power conversion system. Thus, the highest temperature would lead to the highest efficiency. Although temperature core output for the Rankine cycle was capable to have the same amount as for the Brayton cycle, the temperature had less effect on the power conversion system. The hot energy from this temperature boiled water in a steam generator and produced steam. The temperature of the steam was a maximum of 200°C. Therefore, the temperature core outlet for the Rankine cycle was unnecessary to be as high as for the Brayton cycle.

Several advantages of the Brayton cycle over Rankine cycle performance comparison were noted by the authors of [5, 6]. The Brayton cycle design is simpler because it has fewer heat exchangers and pumps, reducing the total capital cost [5]. The most significant benefit is the temperature outlet of HTGR is high, which can be accommodated directly by the gas turbine. As a result, thermal efficiency from the gas turbine will be high. Another positive reason is that the working fluid in the Brayton cycle can be varied and mixed. It is possible to use various gasses in the power conversion system through a heat exchanger to enhance a higher efficiency. General Atomic (GA) did an assessment and investigation to replace a steam cycle with Closed-Brayton-Cycle (CBC) for a 2000 MWth HTGR gas turbine and OKBM in the USSR for a 1000 MWth VG-400 nuclear reactor [5]. Based on those advantages, a Brayton cycle is chosen as a power conversion system in this research.

The Brayton cycle has been used in HTGR since the 1960s. This paragraph describes the development of the HTGR Brayton cycle. Paper [5] stated that the HHT project was the first and the largest helium gas turbine in 1968 in Germany. It was rated 50 MWe at 750°C. It was experimentally tested at a high temperature, helium gas-cooled reactor. However, the heat source was generated by a fossil fuel-fired heater. In 1966, Ernest H. Feher patented a test module design of the supercritical cycle heat engine and reported the supercritical power cycle on [9]. The module was 150 kW with an outlet temperature reactor of 732°C with CO2 as working fluid. Furthermore, it was an indirect cycle with a two-shaft arrangement [10]. INET China designed a Modular High-Temperature Gas-cooled Reactor Indirect Gas Turbine (MHTGR-IGT) with a power rating of 200 MWth and outlet temperature of 850°C with fluid nitrogen used as working fluid. The plant used an indirect cycle with three compressors. The plant could reach a thermal efficiency of 48% [11]. In Japan, JAERI designed a Gas Turbine High-Temperature Reactor (GTHTR300). This design had 600 MWth with an 850°C outlet temperature. It was a direct cycle and helium was used as the working fluid. The shaft arrangement is single shaft horizontal [12]. In South Africa, PBMR Pty reported their conceptual design HTGR, Pebble Bed Modular Reactor (PBMR) with power rated 400 MWth/165 MWe and 900°C outlet temperature core. It had a direct cycle and helium was proposed as the

working fluid [13]. However, the project was stopped in 2010 after the detailed designs were presented and the test facilities were demonstrated. MIT and INEEL in the USA modified the PBMR design into an MPBR (Modular Pebble Bed Reactor). Their design had a capacity of 250 MWth/120 MWe with an outlet temperature core of 879$^{o}$C. This was an indirect cycle with helium as a working fluid and a three-shaft arrangement [14]. General Atomic (GA) and Minatom designed a GT-MHR, with a capacity of 600 MWth/286 MWe, and an outlet temperature core of 850$^{o}$C. The design used a direct cycle with helium as the working fluid. It was a single shaft configuration placed vertically [12]. GA reported a conceptual design of a GT-HTGR with the largest capacity of 2000 MWth/800 MWe and an 850$^{o}$C outlet temperature. It was a direct cycle with two transfer loops and helium used as the working fluid and a single shaft arrangement [15]. The most significant development was in China (INET). They built a test facility, HTR-10, with a 10 MWth/2.2 MWe and an outlet temperature core of 750$^{o}$C. The design was intercooled and recuperated. A direct cycle using helium as the working gas was employed in this design. It had a single shaft arrangement [16].

From the literature review, most SMR-HTGR developments are still in the design phase and the plants have not been constructed yet [3]. SMR-HTGR is one of the latest generation technologies for Nuclear Power Plant (Gen 4), thus, the general policy of SMR-HTGR construction has been in the progress [8]. Furthermore, experiences in HTGR design are a requirement to obtain a license for construction. Competitiveness of electricity prices between SMR-HTGR and conventional nuclear power plants have been compared and analyzed [8]. Electricity price SMR-HTGR and regulations are still challenging for this decade [8]. However, opportunities in the development of SMR-HTGR can reach for the next decades. China started HTGR development from design to evaluation facilities in 2000. Moreover, China launched a commercialized HTR-PM in December 2021. Other countries and nuclear power plant stakeholders have followed the roadmap since then. They also can learn policy from China's experiences.

HTGRs use Helium as a working gas. HTGR could apply the Rankine cycle or Brayton cycle as a power conversion system. Rankine cycle can accommodate temperatures from reactor between 300$^{o}$C-750$^{o}$C (temperature input for Rankine cycle) while Brayton cycle is suitable for temperatures above 750$^{o}$C (temperature input for Brayton cycle). Temperature output steam for Rankine cycle would be 100$^{o}$C-250$^{o}$C while for Brayton cycle would be above 500$^{o}$C. Brayton cycles can apply hot temperature from the reactor directly or indirectly. Hence, thermal efficiency would be higher than the Rankine cycle. A quantitative analysis regarding the value of thermal efficiency will be analyzed in the following chapter. To enhance a higher efficiency, we need to modify the configuration of the Brayton cycle.

## 2.2 Brayton Cycle Configuration

One major consideration for utilizing the high-temperature gas-cooled reactor is that this reactor provides a high core outlet temperature (> 750°C). To take advantage of the high core outlet temperature of the HTGR, a Brayton cycle is preferred. Other design considerations involve four aspects: closed-cycle versus open cycle, cycle modification, direct cycle versus indirect cycle, working fluid choice and system pressure. Figure 2.1 shows variations in Brayton cycle configuration

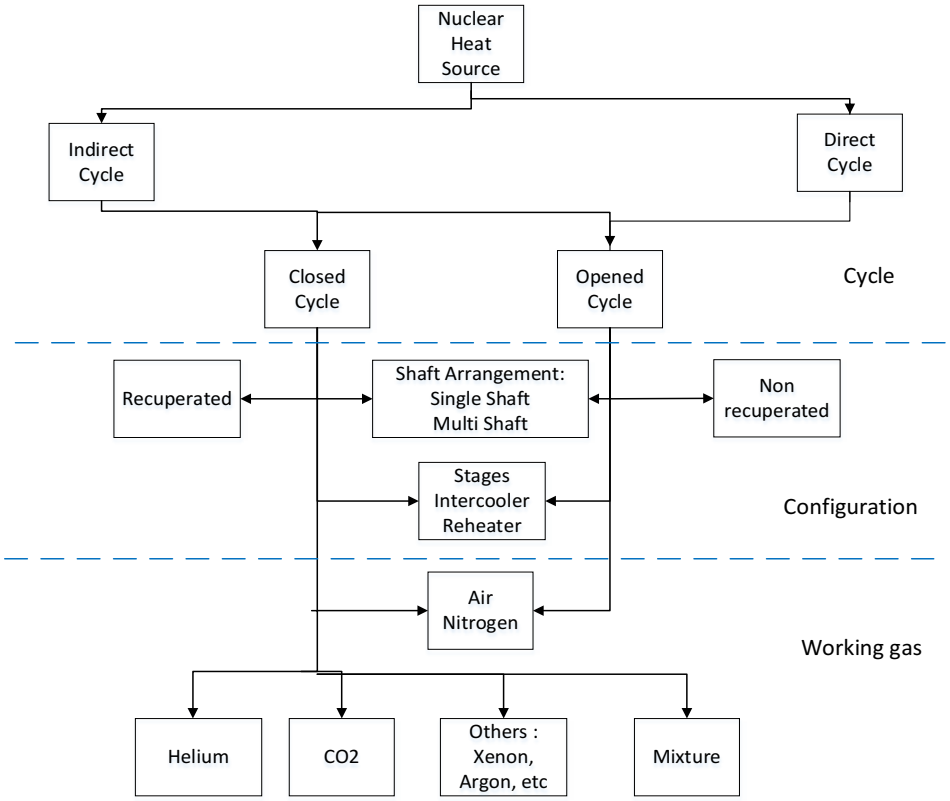


Figure 2.1 Variations in Brayton cycle configuration [17]

As can be seen, HTGR as a heat source produces energy to supply the Brayton cycle either in direct cycle mode or indirect cycle mode. Helium is not only a reactor coolant but also a working gas power conversion system in a direct cycle. This hot gas flows directly from the reactor to the turbine inlet. Thus, the working gas of this mode is only helium. The indirect cycle utilizes a heat exchanger to transfer heat energy from the reactor to the secondary system. Helium is circulated in the reactor while other gasses circulate in the secondary system after receiving hot energy in the heat exchanger. Gas flows either in open cycle mode or closed cycle mode in the secondary system. Gas exhaust from the turbine will be released into the environment in an open cycle. Thus, working gas should be safe to be released into the environment, such as air and nitrogen. Instead of releasing to the environment, the working gas in the secondary system is circulated for closed cycle mode. Thus, gas waste heat energy from turbine exhaust is exchanged in the recuperator to reheat gas

from compressor exhaust. It is possible to apply a single shaft or multiple shafts in all modes. To improve efficiency, it is also possible to apply multistage. However, multistage should be followed by an intercooler between the compressor and reheater between the turbine, as can be seen in Figure 2.2. This research will compare opportunities for various configurations of the Brayton Cycle model in Matlab-Simulink.

### 2.2.1 Direct vs Indirect Cycle

The direct cycle has a simpler configuration compared to the indirect cycle because the direct cycle does not require an intermediate heat exchanger and uses the same working fluid so the capital cost is lower. Another advantage of the direct cycle is a higher thermal efficiency because heat is transferred directly to PCS through working fluid. Hence, it circulates working fluid exiting from the reactor core directly to the power conversion unit and the working fluid exhausts from there back to the core. Thus, the working gas is helium in HTGR direct cycle. The indirect cycle utilizes an IHX to separate the primary system and the power conversion unit. The IHX transfers the thermal energy from the primary system to the working fluid of the gas turbomachines, which convert the thermal energy to mechanical energy. There are two different working loop systems separated by IHX. Although an indirect cycle yields less thermal efficiency than a direct cycle, this cycle can provide better safety due to radiological contamination from the primary system [18]. Helium should be pure and restricted from other chemical concentrations such as H2, H2O, CO, CO2, CH4, O2 and N2 [19]. A small amount of these gasses might exist in the power conversion system. H2 is removed to prevent oxidization and deoxidization of high-temperature metallic material. CO is removed to prevent carbonization and oxidization of high-temperature metallic material. CH4 is removed to prevent the carbonization of high-temperature metallic material. N2 is removed to prevent the nitridation of high-temperature metallic material [19]. Furthermore, a flexible temperature can be utilized for different applications in a parallel scheme in the secondary system without significant influence from the reactor [3]. Despite IHX operation and maintenance costs and lower thermal efficiency, utilization of IHX would be beneficial to both research and application, such as flexible combined heat and power.

### 2.2.2 Open Cycle vs Closed Cycle

This subsection describes exhaust gas conditions from the Brayton cycle. Although the open cycle has been a matured cycle method in gas turbines, the literature [14] and [17] suggested not applying this cycle in nuclear heat resources because radioactive material might contaminate PCS. In other words, in the open cycle, after flowing through the PCS, the working fluid is thrown out to the environment. Furthermore, using an open cycle in the secondary system makes the inlet

pressure in the power conversion system equal to atmospheric pressure. This pressure level would lead to an Intermediate Heat Exchanger (IHX) having a large volume.

In a closed gas turbine, the combustion process is replaced by a constant-pressure heat-addition process from an external source (nuclear resources) through IHX. Compared to the steam Rankine cycle, the closed cycle can achieve higher efficiency at higher temperatures and has simpler piping, heat exchanger, and pumps. Therefore, in this research, closed cycle will be chosen

### 2.2.3 Working Fluid

The choice of working fluid for the gas turbine cycle considerably affects the size, geometry, and performance. Some working fluids usually considered for the Closed Brayton Cycle (CBC) include air, nitrogen, carbon dioxide, helium and other noble gasses [17]. A working fluid is a gaseous or liquid substance applied for an energy conversion either in mechanical work or in heat. The majority of HTGR GT researchers who applied direct cycle also used helium as a working fluid [12, 16, 20, 21, and 22] due to its high efficiency. As stated in subsection 2.1.1 for the direct cycle, Helium from the reactor directly flew to the PCS Brayton cycle and circulated back to the reactor. Helium has been found to reach the highest efficiency mono-gas as a working fluid in CBC [23], and its specific heat transfer, Cp, was not affected by the fluctuation of temperatures [24]. However, it is not suggested to apply helium for gas turbines because it reacts with thermal neutron and produces tritium, a radioactive isotope, which is dangerous for the environment [6]. Although helium achieves the highest performance as a working fluid in HTGR, there might be a leakage in the power conversion system, as helium is a light gas [17]. This fluid also experiences a lack of sensitivity to changing pressure due to its mono-atomic gas [25]. Helium is not suggested in the second cycle due to impurities of helium with other substances [6]. Another reason is that there is limited design experience using helium as a working fluid in turbomachinery [26].

Perez-Pichel et al. [25 and El Genk and Tournier [27] have studied various working fluids. to determine an optimum steady-state performance of the noble gas (helium) and binary gas (helium mixture) [19, 27]. Perez-Pichel et al. [25] compared working gasses such as helium and helium mixture in several Rankine and Brayton cycle configurations to find the best thermal performance for Sodium Fast Reactor (SFR). El-Genk et al. [27] investigated noble gasses (He) and binary mixture gasses(He-Xe) as working fluids in a gas-cooled nuclear power plant and claimed that a good performance of the working fluid could reduce the size and number of stages in the turbomachinery units. The shaft and turbomachinery of mixture gas would be smaller than helium. However, the thermal efficiency mixture gasses were five per cent lower than single gas. Najjar [21] compared carbon dioxide, helium, air and combustion gasses in a closed Brayton cycle to investigate specific work and overall efficiency. The author stated that air and combustion gasses had similar

characteristics and were able to reach a higher efficiency than helium and carbon dioxide. A report stated [23] that applying diatomic gasses (such as nitrogen and hydrogen) as working fluid yields the highest thermal efficiency and lowest values in power per radiator area, which determines Intermediate Heat Exchanger (IHX) size.

Most recent research prefers using carbon dioxide due to the greenhouse issue. It is believed that supercritical CO2 is an advanced working fluid which has achieved a higher thermal efficiency [19,28,29]. However, the temperature of this gas decreases largely after expanding (turbine exit temperature) due to its heat capacity over temperatures in a real gas. Therefore, it requires an additional reheater to approach inlet turbine temperature. Some nuclear power plant technology uses CO2 as a working fluid in the secondary system, which requires a heat exchanger to transfer energy from the heat source (reactor core) to PCS, namely indirect SCO2 [19]. As there is no combustion, only pure CO2 flows into all components in the secondary system. However, temperature inlet/outlet components are not as high as in a direct cycle. Furthermore, indirect cycle SCO2 requires more types of recuperators (Low/Medium Temperature Recuperator (LTR and MTR)) as well as compressors (Power/Recovery Compressors) to have a high performance [29].

### 2.2.4 Modification Brayton Cycle Configuration

The arrangement of the gas turbine configuration is between the heat exchangers and the turbomachinery. The main components of the Brayton cycle are the compressor and turbine. Modification of configuration was made as an effort to improve the cycle efficiency. Additional stages and components are the most common modification of configuration. Multiple stages of compressor, turbine or both would affect a significant improvement. However, multiple stages should be followed by adding an intercooler in-between compressors or adding a reheater in-between turbines. A recuperator/regenerator utilizes waste energy from turbine exhaust to reheat energy of the compressor outlet to improve the efficiency. Figure 2.2 shows a schematic diagram for the two-stage Brayton cycle.

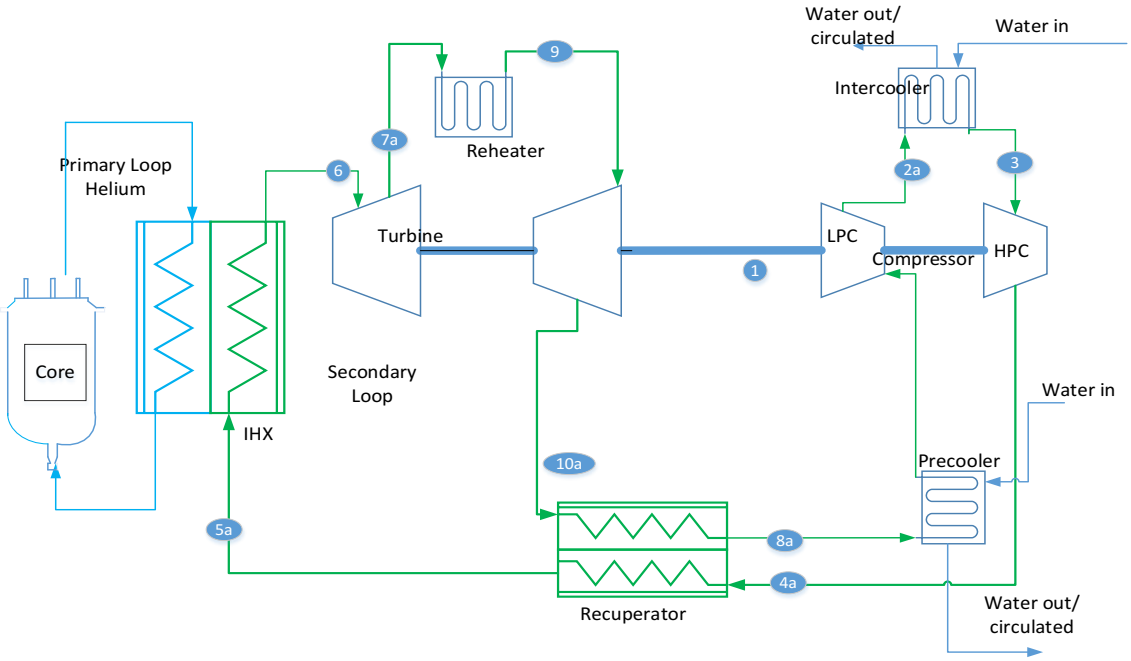


Figure 2.2 Two-stage Brayton cycle [17]

Wu et al. [16] used one turbine and two compressors (1T2C) configuration to demonstrate the feasibility of HTGR gas turbine in China using helium as the working gas. This research was an extension of a previous project, the HTGR 10 MWth Rankine cycle. Alpy et al. [30] used this configuration in the ASTRID (Advanced Sodium Technological Reactor for Industrial Development) project to compare it with the CO2 cycle using various working fluids. Since this project was SFR (Sodium Fast Reactor), it required several heat exchangers to avoid sodium entering the turbomachinery. Olumayegun [31] used the same configuration to compare a single shaft with multiple shafts in SFR using nitrogen as the working fluid.

Dostal [10] used a 1T1C diagram and CO2 as the working gas and compared pressure ratios with turbine work as well as compressor work. Kunitomi et al. [20] proposed a 1T1C gas turbine diagram for the next HTR GTHTR300 using helium as working gas. Wright et al. [32] used a micro gas turbine, which was the 1T1C gas turbine diagram, for Sandia Brayton loop 30 kWe using air as working gas.

From the literature review in this subsection, we can analyze some points. The cycle efficiency can be increased by adding stages in turbomachinery (compressor and turbine) as well as an intercooler placed between compressors and a reheater placed between turbines. Multi-stages compressor and intercooler between compressors will decrease compressor work, while multi-stages turbine and reheater between turbines will increase turbine work [30,31]. Peterson [33] applied a multi-stages Brayton cycle diagram in a Molten Coolant Gas Cycle (MCGC] project and continued using the diagram in Advanced High-Temperature Reactor (AHTR). The team compared the thermal

efficiency of helium and carbon dioxide in the second cycle for three stages Brayton cycle. Perez-Pitchell et al. [25] compared the combined cycle (single and multi-stages) and supercritical Rankine cycle by applying various binary working fluids in the second cycle in a Sodium Fast Reactor project. Supercritical Rankine cycle was able to achieve more than 40%efficiency in all working fluid schemes. The temperature input for the power conversion cycle was 525$^{o}$C. Thus, it was suitable for the Rankine cycle rather than for the Brayton cycle. Brayton cycle requires more than 550$^{o}$C to have more than 40%. However, the Supercritical Rankine cycle requires twice Heat Recovery Steam Generator (HRSG) to achieve 40 % efficiency. Thus, the design of the Supercritical Rankine cycle is more complex than the Brayton cycle. Therefore, there is still an opportunity to enhance efficiency by modifying PCS configuration. This modification should consider the capability of each component. Such as, a turbine can drive a compressor as well a heat exchanger can transfer energy from the hot side to the cold side.

## 2.3 Heat Exchanger

A heat exchanger is a device for exchanging the heat of two moving fluids at different temperatures without mixing each other. The hot fluid transfers heat to another fluid (cold fluid) through a medium such as a wall of water. The heated fluid would either be circulated to other components or cooled to a certain temperature. A high heat transfer rate and low-pressure drop among the fluids are a requirement of a good heat exchanger. In general, an enhanced heat transfer rate can be used to increase the overall heat transfer area value of the heat exchanger. A higher value can be exploited in two ways: (1) to obtain an increased heat exchange rate for fixed fluid inlet temperatures, or (2) to reduce the mean temperature difference for the heat exchange; this increases the thermodynamic process efficiency, which can reduce operating costs.

There are various classifications of heat exchangers, such as the flow arrangement (counter-flow, cross-flow, and parallel flow), the construction type and the fluid types (gas-gas, gas-liquid, and liquid-liquid) [34,35]. The most common flow arrangements are counter-flow and parallel flow. This study will use a counter-flow arrangement because of the uniformity of temperature in the entire length of the heat exchanger. This uniformity would produce a uniform heat transfer rate in the entire length and minimize thermal stress in heat exchanger material due to the large difference in temperature in heat exchangers inlets/outlets [34]. The tubular heat exchanger is the most popular construction type heat exchanger in the industry. There are hot fluid tubes inside a cold fluid tube which are separated in each tube. The temperature of the fluid would be exchanged since both fluids flow. This tubular heat exchanger is flexible to modify the core shape by changing the tube diameter, length, and arrangements. This type is also capable to serve high temperature and high pressure with lower pressure than other types [36]. This study will use a double

pipe/concentric heat exchanger which consists of a pipe and a jacket pipe around it. It is the simplest heat exchanger. The hot fluid which is desired to be heated is located inside the pipe, while the other fluid flows in the jacket. Heat is exchanged from hot fluid to cold fluid through the walls [34, 37]. According to the TEMA standard for heat exchangers, concentric heat exchangers are suitable to accommodate non-hazardous gasses as well as flexible pressure [38]. Omidi [39] reviewed the application of a double pipe heat exchanger. Most publications discussed their research on the enhancement of heat transfer rate using water, oil, or nanofluids in the pipe. Han Seo [36] designed a double pipe heat exchanger for S-CO2 by using air and LPG as heat sources. The purpose of their research was to obtain a high temperature/high-pressure double pipe heat exchanger in an SCO2 environment. Xu [40] analyzed heat transfer enhancement in a double pipe heat exchanger as well as pressure drop performance for S-CO2-Water. It was found that the velocity of the fluids affected heat transfer enhancement.

Based on the literature survey above, there is an opportunity to use a double pipe heat exchanger in HTGR although Printed Circuit Heat Exchanger (PCHE) research has been popular in the last decade. PCHE dimension are smaller than a double pipe heat exchanger since PCHE are microchannel fluid flows. However, capital cost and pressure drop PCHE are higher than double pipe heat exchangers. Thus, there is a need for some consideration of using PCHE in power plants. Double pipe heat exchangers are simple dimensions since the heat exchangers consist of conventional pipes. The capital cost of a double pipe heat exchanger is inexpensive since it is a matured technology of heat exchanger. Moreover, the pressure drop is low since the diameter of the pipes is bigger than the microchannel. Therefore, a double pipe heat exchanger would be considered in this research.

Counterflow arrangements will be used to transfer heat from hot gas to cold fluid or gas due to the uniformity of heat transfer rate in the entire length of a double pipe heat exchanger. To our knowledge, there is no publication stating interaction between helium and nitrogen or hydrogen using a double pipe heat exchanger. Thus, there is still room for research into the interaction of helium with other gasses using a double pipe heat exchanger. In this study, helium and non-helium gasses will be applied in IHX as working fluids since this research applies indirect cycle heat flow. Thus, helium in the reactor loop is circulated in the primary loop. Other helium and gasses will flow in a second cycle as well as two ways in a recuperator. The precooler and intercooler will use non-helium gas and water as the working fluids.

## 2.4 Summary

This research will apply the Brayton cycle instead of the Rankine cycle regarding HTGR's capability to provide a high temperature. Another reason is that there are some advantages of the gas turbine over the steam turbine. Since the power station is small (10 MWth) and would utilize heat for industrial applications, the plant is composed of an indirect cycle and a single shaft. Furthermore, there might be some issues regarding helium flow in turbomachinery. Initial data will be retrieved from the report [3]. There is still an opportunity to improve the efficiency of the plant by modifying the configuration of the PCS. An interesting gap would be an interaction among configuration PCS and its pressure ratio characteristics as well as working gasses capability in simulation analysis. Configuration of Brayton cycle, as well as working gas, will be assessed and selected.

The double pipe heat exchanger is inexpensive since it can utilize standard pipe. Furthermore, it is suitable for a small heat transfer request area since the power plant is small. The device can serve gasses at high temperatures and high pressure. This research will assess the performance of a double pipe heat exchanger with a low-pressure drop. Heat exchanger sizing will be done by calculating some parameters to determine an optimal overall heat transfer coefficient as well as low-pressure drop.

# Chapter 3 Power Conversion System of SMR-HTGR Model

This research will assess the thermal cycle in a gas turbine power station for HTGR 10 MWth. Data assumptions will be derived from IAEA Small Medium Reactor (SMR) report [3]. To have high efficiency, various configurations of the Brayton cycle, as well as working gas, will be assessed. Every gas has a different specific heat ratio, thus, a suitable pressure ratio would be different. Therefore, the optimum pressure ratio will be defined for each gas. The assessment will use thermodynamic analysis using the cold-gas standard assumption.

The double pipe heat exchanger is one of the simplest heat exchangers. It contains concentric pipes to exchange the heat. Sizing a double pipe heat exchanger would be calculated to find the dimensions of the heat transfer area, overall heat transfer coefficient as well as low-pressure drop. Standard pipe dimension data will be used in this calculation.

## 3.1 Thermodynamic Analysis

Thermodynamics is a physics science and scientific methodology to analyze cycles of the energy process. Thermodynamic analysis can determine a better understanding of overall system performance.

Thermodynamic phenomena in gas turbines have been modelled and analysed to know the dynamic system of this plant. This methodology can be a preliminary study because the basic learning of this methodology starts with the ideal condition of the system energy cycle. Hence, the parameters are constant and the system is in a steady-state condition.

We assumed the system was in a steady-state operation because we measure the best opportunity performance of the system. This research utilizes the cold-gas standard assumption to reduce the complexity of the gas power cycle. Parameter characteristics of the gas are constant and ideal in this assumption. Thus, it is suitable for steady-state operation. The characteristics of the cold-gas standard assumption are [24,41]:

1. The working fluid is gas, which was continuously circulated and is ideal.

2. All the processes were internally reversible.

3. Heat source was a fixed constant from the reactor to the IHX.

4. The exhaust process was circulated and restored to its initial condition

5. Kinetic and potential energy changes were negligible.

Gas turbines consist of aerodynamic components (compressor and turbine). Performances of these components should be matched with each other. When compressor and turbine are linked together on the same shaft, they should operate in the same overall pressure ratio.

Furthermore, the characteristic of the compressor-turbine should meet the following conditions:

- Mass flow through compressor = mass flow thorough turbine
- Compressor power < turbine power
- Pressure inlet compressor = pressure outlet turbine
- Temperature outlet turbine > temperature inlet IHX

The thermodynamic analysis is a function [14]:

$$Function\left(\dot{m}, \gamma, p_{01}, p_{02}, C_p, T_{01}, T_{02}\right) = 0 \quad \text{(3.1)}$$

where $\dot{m}$ is the mass flow rate. $p_{01}$is the pressure input and $p_{02}$ is the pressure output. $C_p$is the specific fuel consumption of working fluid. $T_{01}$ is the temperature input and $T_{02}$ is the temperature output. Gamma $\gamma$ ratio is the ratio between specific heat at constant pressure ($C_p$ ) and specific heat at constant volume ( $C_v$). The result of this function is a curve of performance.

A **working fluid** is a gaseous or liquid substance applied for an energy conversion either in mechanical work or in heat. The properties of working fluid in a gas turbine engine have a significant effect on the thermodynamic calculation. Physical properties of thermodynamics in working fluid such as pressure, temperature, enthalpy, entropy, specific volume and internal energy are used for the calculation of energy conversion. Therefore, the gas properties of the working fluid should be calculated precisely.

**Overall pressure ratio (PRc)** is the ratio of the stagnation pressure as measured at the front and rear of the compressor of a gas turbine engine, that is a ratio of pressure output and pressure input. The value PRc is analyzed to determine the capability of the temperatures and pressures of gas. This value also will be analyzed to determine the performance of the systems as well as the sizing of turbomachinery. The terms compression ratio and pressure ratio are used interchangeably [14].

$$\frac{Tout}{Tin} = (PRc)^{\frac{\gamma-1}{\gamma}} \quad \text{(3.2)}$$

$$PRc\ (r) = \frac{Pout}{Pin} \quad \text{(3.3)}$$

To generate net power output with a closed gas turbine cycle, the power produced by the turbine should be larger than the power consumed by a compressor with an identical pressure ratio. Decreasing the inlet temperature decreases the compressor power at the same pressure ratio. Thus, an intercooler can be used to improve the cycle efficiency. The compression process is implemented using several compressors, in which gas is cooled by a water heat exchanger

individually. This results in a significant reduction of the compressor power required to realize the compression task, and thus an increase in the cycle efficiency. The downside of adopting an intercooler is increasing the cycle complexity and the requirements for cooling water.

From Figure 2.2, the gas is compressed in a low-pressure compressor and cooled in the intercooler then recompressed in a high-pressure compressor. Ideally, the cooling process takes place at constant pressure, and the gas is cooled to the initial temperature T1 at each intercooler. To minimize compression work (cyclic devices deliver most of the work consumption) during multi-stage compression, the pressure ratio across each stage of the compressor must be the same.

Calculations have been done for the actual cycle based on fixed pressure ratio (Pr)-various temperature inlet turbine as well as fixed temperature inlet turbine-various pressure ratio. From Figure 2.2, the temperatures were the same value for its inputs as well as its outputs for multi-stage adiabatic turbomachinery. The temperature output could be defined as equations [3.4] and [3.5].

$$T_{compressor\ out} = T_{Compresoor\ in} * \left[1 + \left(\frac{(Pr_{compressor})^{\frac{\gamma-1}{\gamma}} - 1}{\eta_{compressor}}\right)\right] \quad (3.4)$$

$$T_{Turbine\ out} = T_{turbine\ in} * \left[1 - \eta_{Turbine} * \left(1 - \left(\left(\frac{1}{Pr_{Turbine}}\right)^{\frac{\gamma-1}{\gamma}}\right)\right)\right] \quad (3.5)$$

To obtain **compressor work, Wc,** we use,

$$W_C = c_p \cdot \left(T_{compressor\ out} - T_{compressor\ in}\right) \quad (3.6)$$

To obtain **turbine work, Wt,** we use,

$$W_T = c_p \cdot (T_{turbine\ in} - T_{turbine\ out}) \quad (3.7)$$

$$W_{elec} = \left(W_{turb} - \left(\sum W_{compressor}\right)\right) \quad (3.8)$$

**Mass flow rate, $\dot{m}$ (kg/s**), is mass flow rate which is the amount of mass flowing through a cross-section per unit of time. Mass flow rate expresses the energy flow associated with a fluid stream in the rating form. Mass flow rate is obtained by using the equation:

$$\dot{m}_2 = \frac{\epsilon * \dot{m}_1 * Cp_1 * (T_{Core\_o} - T_{Core\_i})}{Cp_2 * (T_{turbine\ in} - T_{compressor\ out})} \quad (3.9)$$

**Heat exchangers** are a device where two moving fluid streams exchange heat without mixing. The effectiveness of a heat exchanger is usually used to describe a regenerator's performance. It is defined by the ratio of actual regeneration of heat transfer to maximum regeneration of heat transfer. In this calculation, it is represented by enthalpy. We calculated recuperator parameters using a definition of effectiveness, ε

$$\varepsilon = \frac{q}{q_{max}} = \frac{(\dot{m}\cdot c_p)_{hot}\cdot(T_{hot,in}-T_{hot,out})}{(\dot{m}\cdot c_p)_{min}\cdot(T_{hot,in}-T_{cold,in})} \quad \text{..... (3.10)}$$

Thermal balance calculation between two gasses will determine the duty of heat exchangers or total heat exchange per unit time, Q

$$Q_{Heat\ exchanger} = (\dot{m}\cdot c_p)_{hot}\cdot(T_{hot,in}-T_{hot,out}) = (\dot{m}\cdot c_p)_{cold}\cdot(T_{cold,out}-T_{cold,in}) \quad \text{...(3.11)}$$

In the final stage, we determined efficiency, $\eta$ ,

$$\eta = \frac{Qin}{W_{net}} = \frac{Qin}{W_{turbine}-W_{compressor}} \quad \text{..... (3.12)}$$

Table 3.1 shows the assumption for the calculation of cold-gas standard calculation. Most of the core design HTGR gas turbines have a temperature inlet of 450°C-650°C and a temperature outlet of 750°C-1000°C. These temperatures depend on the thermal power production of the reactor [3]. For the initial calculation, we used maximum temperatures which could be reached in a gas turbine. The calculations used the cold-gas assumption with the temperature inlet for compressors set at 27°C while the cooling water inlet for coolers was set at 20°C [3]. The specific heat at constant pressure (Cp,) and the specific heat at constant volume (Cv) was constant, thus the specific heat ratio γ remains constant throughout the cycle. The pressure ratio (Pr) in both the compressor and the turbine was the same. Turbomachinery efficiency and heat exchanger effectiveness within the industry varies between 70% and 90% regarding power and dimension [24,41]. Thus, we assumed that turbomachinery efficiency and heat exchanger effectiveness was 85%. Parameters in table 3.1 have been compared with the literature review [3,10,14,16,30,31]. Although the nuclear power rating were different, the PCS temperatures were adaptable. Thus, data assumption which were retrieved from the papers, were suitable for cold-gas standard assumption.

We used a small capacity nuclear powerplant model, thus, the temperature in optimal condition would be at 1200K. Since the power capacity is small, the turbomachinery is classified as micro turbin generator. Micro turbine generator serves power capacity below 10 MW [9]. Most of micro turbine generator apply pressure ratio at below 15 [9]. Therefore, for an example calculation, we assumed the temperature inlet turbine was 1200K and the overall pressure ratio was 9.

Table 3.1 Data assumption

| **Parameter /Variables** | **Value** |
|---|---|
| Reactor thermal power, Qin (MW) | 10 |
| Temperature Core inlet / outlet (°C) | 950/630 |
| Pressure core inlet /outlet (bar) | 30/29 |
| Pressure maximum secondary loop (bar) | 40 |
| $Cp_{Helium}$, $Cp_{H2}$, $Cp_{CO2}$, $Cp_{N2}$, $Cp_{Air}$, $Cp_{water}$ (kJ/(kg. K) | 5.19, 14.307, 0.846, 1.039, 1.005, 4.18 |
| γ, specific heat ratio for He, H2, CO2, N2, Air | 1.667, 1.405, 1.289, 1.4, 1.4 |
| Turbine inlet temperature (°C) | 525 to 900 |
| HPC outlet pressure (bar) | 40 |
| LPC and HPC ambient inlet temperature (°C) | 27 |
| Temperature water inlet/outlet for precooler and intercooler (°C) | 20/44 |
| Turbomachinery efficiency and heat exchanger effectiveness (%)<br>Turbine/compressor efficiency<br>Recuperator /IHX effectiveness | <br>85<br>85 |
| Pressure pump and condenser Rankine cycle | 0.1 Bar |
| Pressure inlet steam generator | 46 Bar |

Figure 3.1 depicts the procedure of the Brayton cycle thermal calculation from initial data assumption to efficiency calculation. Some data resulting from this procedure will be used to calculate the sizing of the heat exchanger. The data are related to heat exchangers, such as heat exchanger duty, temperature inlets and temperature outlets of both fluids in the heat exchanger as well as mass flow rates.

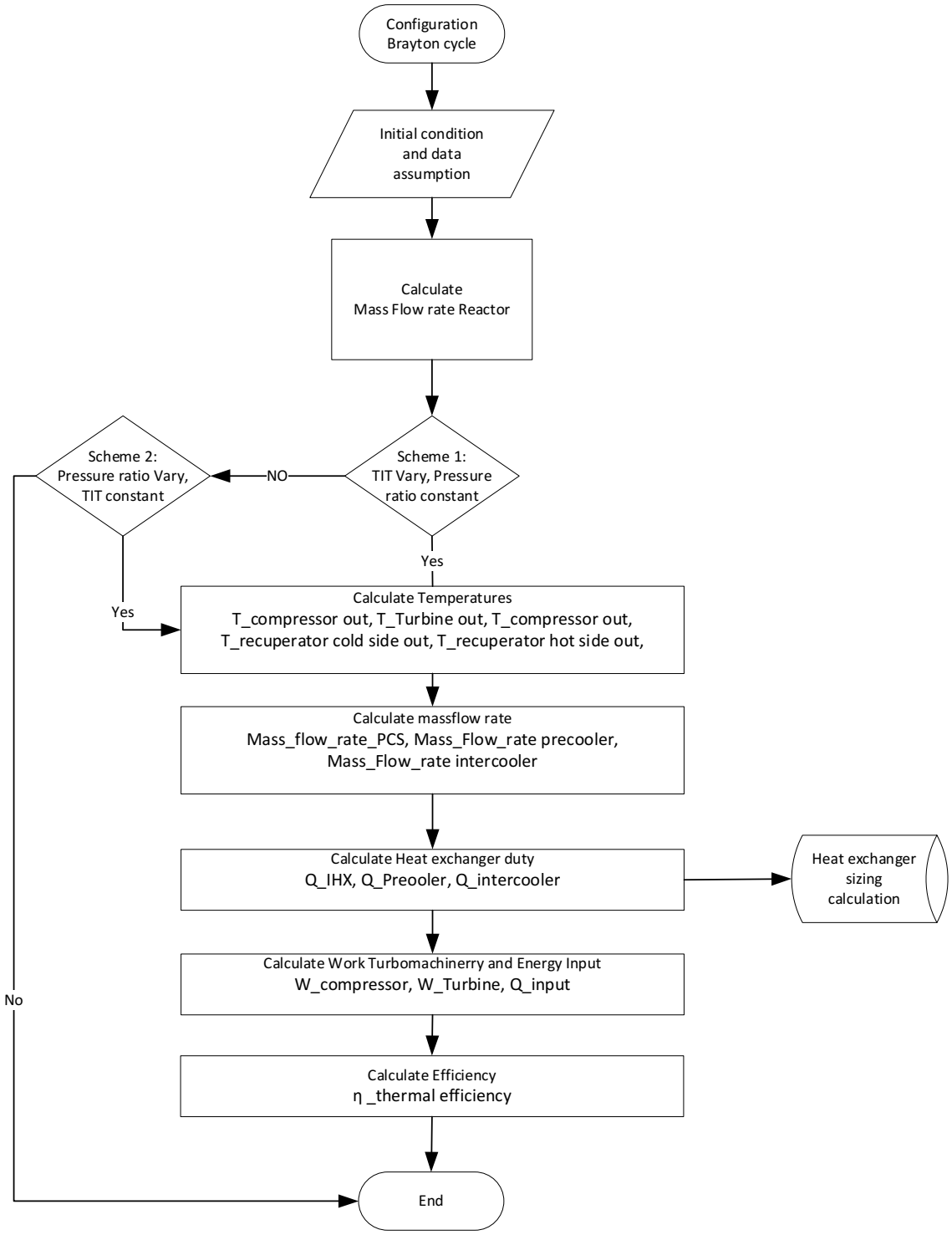


Figure 3.1 Flowchart Brayton cycle thermal calculation

Equations and parameters above were modelled and analyzed in MATLAB-SIMULINK. The diagram Simulink and equations are attached in the appendixes. The models were also considered procedures of modelling in Figure 3.1. The models of PCS have been validated by the literature [10, 14, 16, 25, 31] although nuclear power systems (heat sources) are different. We retrieve similar temperature output values as well as PCS diagrams from the literature.

## 3.2 Sizing Heat Exchanger

### 3.2.1. Heat transfer

Conduction transfers energy as heat through a stationary medium, such as a wall, water, or air. The energy is transferred because of a temperature gradient in a particular length of a medium. The heat transfer rate conduction ($\dot{Q}_{cond}$) is proportional to the thermal conductivity constant (k), area of medium (A), and temperatures gradient $\frac{\partial T}{\partial x}$ [34].

$$\dot{Q}_{cond} = \frac{k}{L} \cdot A \cdot \frac{\partial T}{\partial x} \quad \text{(3.13)}$$

The thermal conductivity value (k) of material shows the rate of displacement heat flowing in a medium. If the thermal conductivity of a medium value is high, then the heat flowing through will be large. Therefore, the thermal conductivity should be high as a good heat conductor. L is the width of the medium.

Convection transfers energy as heat through moving fluid. The energy is transferred because of the temperature gradient between surface temperature and fluid temperature. The heat transfer rate convection ($\dot{Q}_{conv}$) is proportional to convection heat transfer coefficient (h), area of medium (A), and temperatures gradient between surface temperature ($T_{surf}$) and fluid temperature ($T_{fluid}$), as seen in equation (2.17) [34]

$$\dot{Q}_{conv} = h \cdot A \cdot \left(T_{surf} - T_{fluid}\right) \quad \text{(3.14)}$$

The value of convective heat transfer coefficient (h) depends on the physical properties of the fluid (thermal conductivity, specific heat and density), and the physical situation (fluid viscosity).

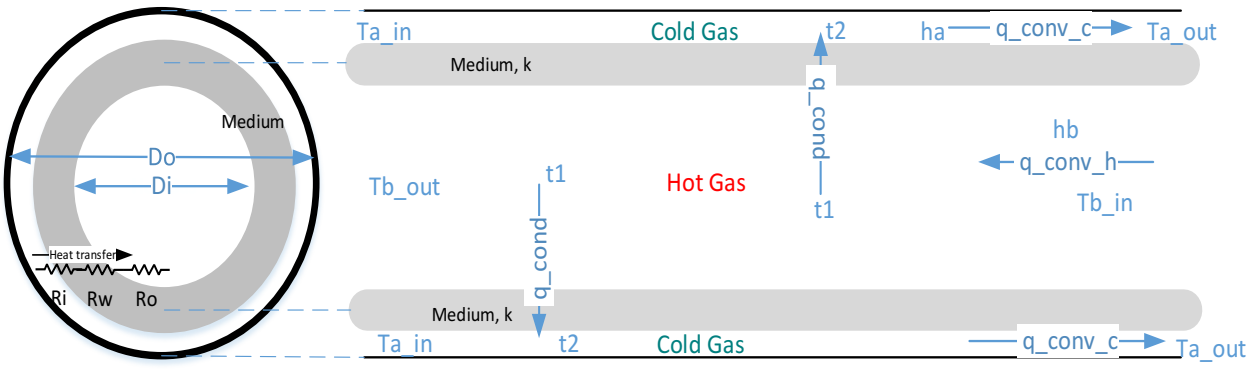


Figure 3.2 Heat transfer in double pipe

Figure 3.2 illustrates heat transfer phenomena in two pipes with different gases. The heat is transferred from hot gas in an inner pipe to cold-gas in an outer pipe. There are two pipes which have a diameter outer pipe ($D_o$) and a diameter inner pipe ($D_i$). Medium is the thickness of the metal inner pipe, hence medium is the diameter of $D_i$. Metal could be iron, aluminum, or stainless steel, thus, the thermal conductivity of the metal (k) would be different.

Areas of every heat transfer mode might not be the same dimension. Thus, the heat transfer rate equation becomes,

$$dq = U \cdot \Delta T \cdot dA \quad \text{(3.15)}$$

On the other side, the heat transfer rate is proportional to the mass flow rate,$\dot{m}$, specific heat fluid,$cp$ , and temperature difference in each fluid, $dT_A$ and $dT_B$. As can be seen in equation (3.16) [41]

$$q = -(\dot{m}_A \cdot cp_A \cdot \Delta T_A)$$

$$q = -(\dot{m}_A \cdot cp_A \cdot (T_{Ain} - T_{Aout})) \quad (3.16)$$

$$q = \dot{m}_B \cdot cp_B \cdot \Delta T_B$$

$$q = -(\dot{m}_B \cdot cp_B \cdot (T_{Bout} - T_{Bin})) \quad (3.17)$$

$$d(\Delta T) = -dq \left(\frac{1}{\dot{m}_A \cdot cp_A} + \frac{1}{\dot{m}_B \cdot cp_B}\right) \quad (3.18)$$

Substitution between equation (3.16) and (3.18) yields

$$\frac{d(\Delta T)}{(\Delta T)} = -U \left(\frac{1}{\dot{m}_A \cdot cp_A} + \frac{1}{\dot{m}_B \cdot cp_B}\right) dA \quad (3.19)$$

Figure 3.3 (a) illustrates heat from fluid A (hot fluid) is transferred to fluid B (cold fluid) through a medium surface while Figure 3.3 (b) illustrates an analogue system of total resistance for Figure A. Convection heat transfer occurred in both $T_A$-$T_1$ and $T_2$-$T_B$ areas while conduction heat transfer occurred in $T_1$-$T_2$ area.

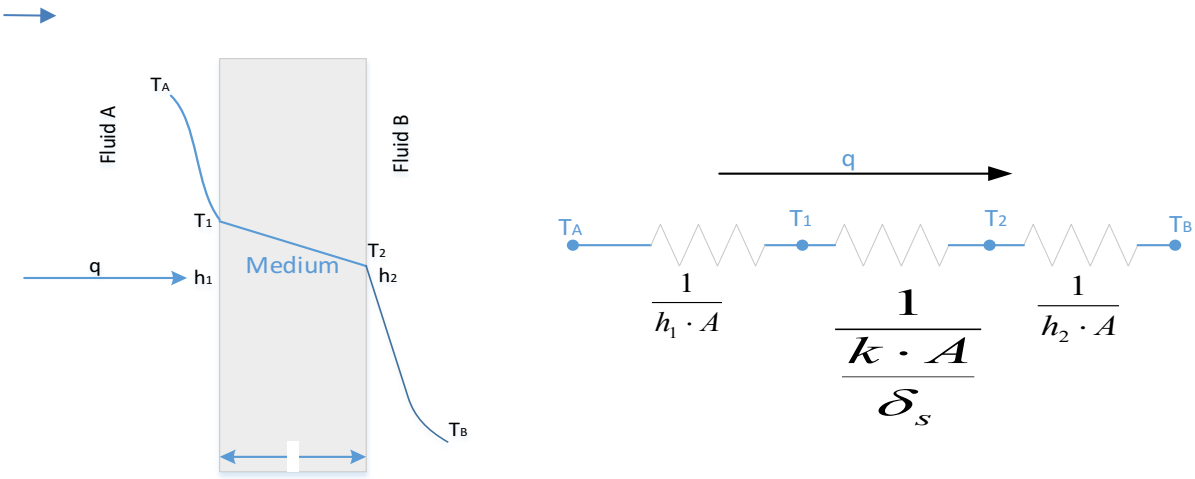


Figure 3.3 Heat transfer energy in a medium surface and electrical resistance analogy[40]

$$q = h_1 \cdot A \cdot (T_A - T_1)$$

$$q = \frac{k}{L} \cdot A \cdot (T_1 - T_2)$$

$$q = h_2 \cdot A \cdot (T_1 - T_B)$$

$$(T_A - T_1) + (T_1 - T_2) + (T_2 - T_B) = \frac{q}{A} \cdot \left(\frac{1}{h_1} + \frac{L}{k} + \frac{1}{h_2}\right)$$

$$(T_A - T_B) = \frac{q}{A} \cdot \left(\frac{1}{h_1} + \frac{L}{k} + \frac{1}{h_2}\right)$$

$$q = \frac{(T_A - T_B)}{\frac{1}{h_1 \cdot A} + \frac{1}{\frac{k}{L}A} + \frac{1}{h_2 \cdot A}} \quad \text{..... (3.20)}$$

where L is the width of medium, h is convection heat transfer coefficient, k is thermal conductivity, and A is area. Book [41] stated $\partial_s$ as a length of medium for gas and liquid medium or adjustable medium. Since the medium was metal and fixed-constant, we use L as the length of the medium. For the sake of simplification, resistant heat transfer mode is converted to overall heat transfer coefficient (U) and $\Delta T = (T_A - T_B)$ as seen in equation (3.21).

$$U = \frac{1}{R} = \frac{1}{\frac{1}{h_1} + \frac{L}{k} + \frac{1}{h_2}} \quad \text{..... (3.21)}$$

There is an electrical analogy for the above equation. As $q$ is the intensity of the heat transfer, U is the total resistance and temperature difference is a voltage. It can be illustrated in a circuit as seen in Figure 3.3

Thus, total heat transfer energy in a heat exchanger is a summation between heat transfer conduction and heat transfer convection. Heat transfer flow amongst them can be series and/or parallel. Hence, an overall heat transfer coefficient (U) can be obtained.

As can be seen from Figure 3.3, $UA$ can be represented by $R_{Total}$ . By cancelling $\Delta T$,

$$R_{Total} = R_i + R_w + R_o = \frac{1}{h_i \cdot A_i} + \frac{\ln\left[\frac{D_o}{D_i}\right]}{2\pi \cdot k_{wall} \cdot L_{pipe}} + \frac{1}{h_o \cdot A_o} \quad \text{..... (3.22)}$$

where,

$h_i \cdot A_i$ is the heat convection coefficient of the inner pipe and inner pipe area. The coefficient can be obtained by equation (3.19) while the area can be obtained by $A_i = \pi \cdot D_i \cdot L_{pipe}$.

$h_o \cdot A_o$ is the heat convection coefficient of the outer pipe and outer pipe area. The coefficient can be obtained by equation (3.19) while the area can be obtained by $A_o = \pi \cdot D_o \cdot L_{pipe}$.

In this research, we assume the wall thickness is very small and the thermal conductivity of the wall is high, the thermal resistance is neglected ( $R_w = 0$)

Equivalent Diameter, $D_e$ has four times the hydraulic radius. A hydraulic radius is a radius of the cross-sectional area of the annulus. Hydraulic radius is a ratio between the flow area and the wetted perimeter. Other studies might refer to $D_e$ as hydrodynamic diameter, $D_h$. There are two equations for wetted perimeter, for pressure drop and heat transfer.

The wetted perimeter in the annulus for heat transfer is the outer circumference of the inner pipe, diameter $D_1$. Thus, the equation $D_e$ would be

$$D_h = 4 \times Hydraulic\ Radius = \frac{4 \times flow\ area}{4 \times wetted\ perimeter} = \frac{4 \times \pi \cdot \left({D_2}^2 - {D_1}^2\right)}{4 \times \pi \cdot D_1} \quad \text{.....(3.23)}$$

The wetted perimeter in the annulus for pressure drop is the circumference of the outer pipe and inner pipe. Because friction, which is pressure drop, is not only from the outer pipe but also the outer surface of the inner pipe, thus, the equation $D_e$ would be

$$,D_h = 4 \times Hydraulic\ Radius = \frac{4 \times flow\ area}{4 \times wetted\ perimeter} = \frac{4 \times \pi \cdot \left({D_2}^2 - {D_1}^2\right)}{4 \times \pi \cdot (D_2 - D_1)} = (D_2 - D_1) \text{ .....(3.24)}$$

For annulus, $D_1$ = outside surface diameter of the inner pipe, $D_2$ = inside diameter of the outer pipe

Physical properties are molecular characteristics of the gas itself. Thermal diffusivity measures the value of the heat transfer from the hot side to the cold side. The thermal diffusivity of the gas is the thermal conductivity divided by density and specific heat capacity at constant pressure. Momentum

diffusivity is the transport of the momentum between particles (atoms or molecules) of matter, often in the fluid state. This transport of momentum can occur in any direction of the fluid flow. momentum diffusivity is defined as dynamic viscosity divided by density. This formula is also used as an analogy to determine kinematic viscosity. Thus, commonly it is an interchangeable definition. Heat transfer analysis needs to know the relation between heat diffusion and velocity (momentum). It requires a standard dimensionless number to characterize the relative thickness of the velocity and boundary layers of the fluid. It is a comparison between momentum and thermal diffusivity and called the Prandtl number (Pr); the numbers have been standardized by scholars [42]. If the Pr>>1, the momentum diffusivity dominates the behavior of the gas. Whereas for Pr<<1, the thermal diffusivity dominates the characteristics of the gas. However, it can be terminated by

$$Pr = \frac{momentum\ diffusivity}{thermal\ diffusivity} = \frac{\mu_{gas} \cdot Cp_{gas}}{k_{gas}} \quad \text{……. ……(3.25)}$$

The motion of the fluid is represented by the Reynolds number (Re). Re is a dimensionless number. Re depicts fluid flow regime whether in laminar or turbulence. The flow regime depends on the *ratio* between inertia forces and the viscosity of the fluid. The inertial force comprises a velocity $(v)$ and density$(\rho)$ and hydrometer pipe $(D_h)$ of the fluid. Otherwise, the mass flow rate $\dot{m}$ (kg/s) can replace velocity and density of the fluid while the ratio between the wetted perimeter$P_p$ and cross-sectional area $A_p$ of the pipe replace $D_h$. The relation can be seen in equation [41].

$$R_e = \frac{v \cdot \rho \cdot D_h}{\mu} = \frac{\dot{m} * P_p}{A_p \cdot \mu} \quad \text{……} \quad (3.26)$$

Re number determines the type of the flow, laminar or turbulence. If Re<2100, the flow is laminar. If Re>2100, the flow is turbulence [42].

There is drag in flow due to interaction between physical properties. Books [41,42] defines drags regarding flow velocity as well as the property of the fluid as a dimensionless number which is called the Nusselt number(Nu). It is also related to the regime of the flow because the Nu condition is constrained by the Reynolds number. Reynolds number depicts the regime of the flow turbulence or laminar. Therefore, Dittus and Boelter[41] define the Nusselt number for turbulence as

$$Nu = 0.023 \cdot Re^{0.8} \cdot Pr^{n} \quad with\ condition\ flow \quad \begin{pmatrix} 0.5 \leq Pr \leq 160 \\ 3000 \leq Re \geq 5 \times 10^{6} \\ \frac{L}{D} \geq 10 \end{pmatrix} \text{……} \quad (3.27)$$

where n = 0.4 for heating and n=0.3 for cooling of the fluid flowing in the tube.

Nusselt numbers in laminar flow are independent of Re and Pr as well as roughness and friction factor. Thus, Nu is a constant number of 3.66.

Nusselt number (Nu), is a dimensionless convection coefficient which indicates heat transfer across boundaries. Hence, Nu can define convective heat transfer coefficient per tube to support equation (3.28)

$$Nu = \frac{h \cdot D_h}{k} \quad \text{..... (3.28)}$$

h is a convective heat transfer coefficient, k (W/(m.K)) is the thermal conductivity of the fluid and $D_h$ is the perimeter of the pipe. Frictional force due to the physical properties of the fluid is also determined by the dimensionless constant, f.

If Re<2100, the flow is laminar, thus

$$f = \frac{64}{Re} \quad \text{.....(3.29)}$$

If Re > 2100, the flow is turbulence and the friction force will be

$$f = [0.79 * \ln(Re) - 1.64]^{-2} \quad \text{..... (3.30)}$$

Pressure drops $\Delta P$ depend on frictional forces, velocity and kinematic viscosity of the fluid and it also depends on how large is the hydrodynamic geometry of the channel.

$$\Delta P = f . \frac{\rho \cdot v^2 . L}{D_h} \quad \text{..... (3.31)}$$

Pressure drop determines pressure performance along with heat transfer in a heat exchanger.

Total heat transfer energy in a heat exchanger is a summation between heat transfer conduction and heat transfer convection. The heat from the hot fluid is transferred to the wall by convection, heat from the wall is transferred through the wall by conduction, and heat is transferred from the wall to the cold fluid by convection. Hence, the overall heat transfer coefficient (U) can be obtained as follows,

$$\dot{Q}_{conv\_i} = \dot{Q}_{cond} = \dot{Q}_{conv\_o} = U \cdot A \cdot \Delta T \quad \text{..... (3.32)}$$

Figure 3.4 shows the sizing double pipe heat exchanger.

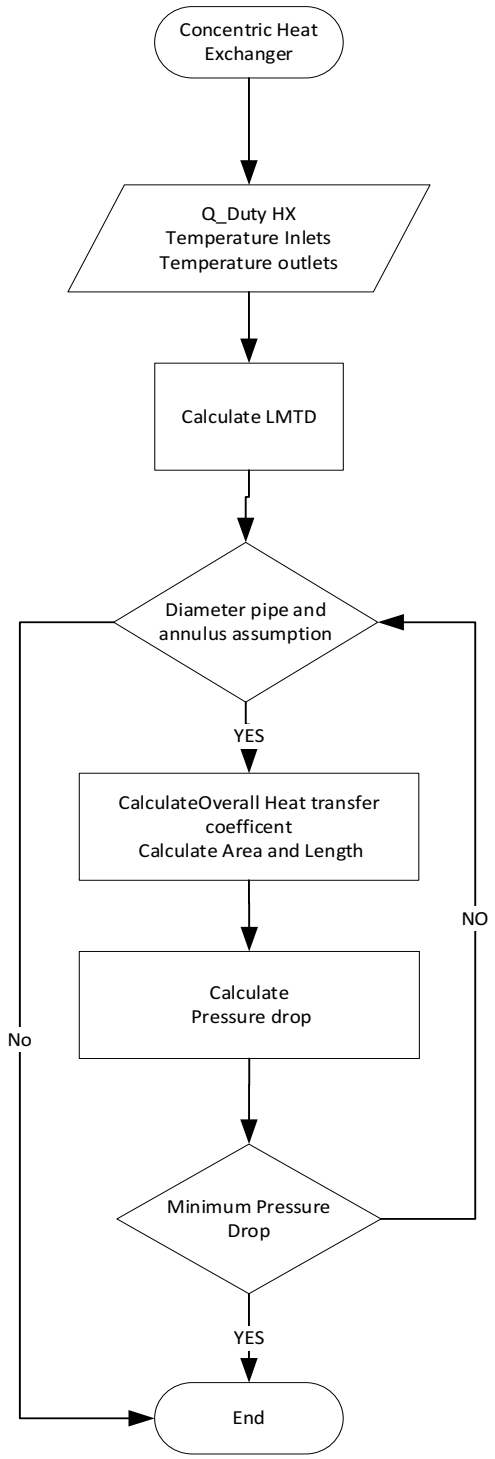


Figure 3.4 Procedure sizing a double pipe heat exchanger

### 3.2.2. Heat Exchanger Analysis: LMTD Method

Log Mean Temperature Difference (LMTD) is a method to analyze the heat capacity performance of heat exchangers. LMTD is a mean temperature difference between one point and another point of a heat exchanger per the natural logarithmic of that difference. To apply LMTD, two conditions should be assumed constant specific heat fluid (Cp) and overall heat transfer coefficient (U) due to steady-state conditions. The method covers the total heat-transfer rate, the overall heat transfer

coefficient, and the total surface area for heat transfer. This research uses a counterflow heat exchanger, thus, this subsection explains LMTD for counterflow. Figure 3.4 illustrates a description of this sub-section.

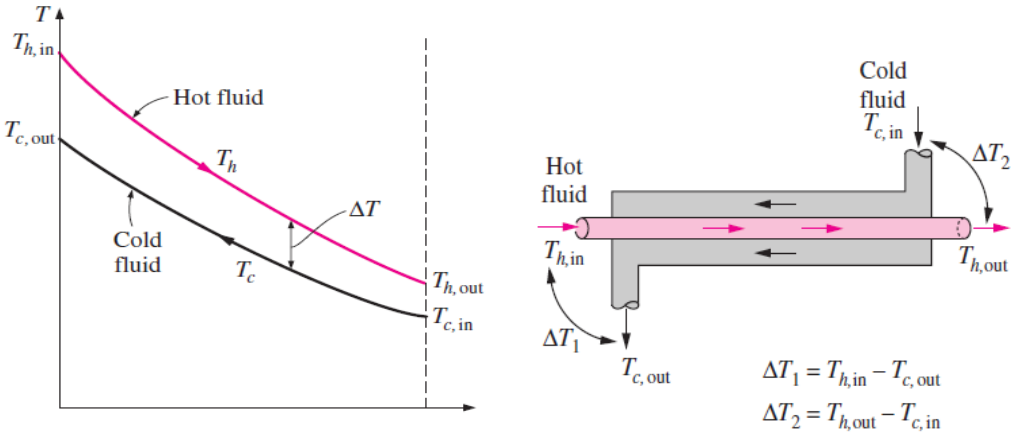


Figure 3.5 Temperature distribution and flow energy counterflow double pipe heat exchanger[41]

The flow of the fluid is opposite direction, exchanging the energy. Temperature distribution ΔT is steady and not significantly different from the input to output part. Thus, there is no significant pressure difference between hot pipe and cold pipe. On the other hand, for parallel flow/co-current flow, hot and cold fluid have the same direction through the channel/pipe. The curve shows that the temperature difference ΔT (between hot and cold) is initially large and will be decreased approaching a minimum along the channels. This condition might create a large different pressure between the hot pipe and cold pipe. Therefore, this research used a counterflow heat exchanger.

To find Log Mean Temperature Difference (LMTD), all temperatures are grouped together

$$\Delta T_m = \frac{(\Delta T_1 - \Delta T_2)}{\ln\left[\frac{(\Delta T_1)}{(\Delta T_2)}\right]} \quad \text{..... (3.33)}$$

For counter-current flow, hot and cold fluid has opposite directions through the tube/pipe. the LMTD for counter-current flow is

$$\Delta T_m = \frac{(T_{hot,in} - T_{cold\ out}) - (T_{hot,out} - T_{cold,in})}{\ln\left[\frac{(T_{hot,in} - T_{cold\ out})}{(T_{hot,out} - T_{cold,in})}\right]} \quad \text{.....(3.34)}$$

$$\ln\frac{T_{A1} - T_{B2}}{T_{A2} - T_{B1}} = UA\left(\frac{1}{\dot{m}_A \cdot cp_A} - \frac{1}{\dot{m}_B \cdot cp_B}\right) \quad \text{..... (3.35)}$$

Substituted to equation (3.32) yield

$$Q_{tot} = UA\frac{(T_{A2} - T_{B1}) - (T_{A1} - T_{B2})}{\ln\left(\frac{T_{A1} - T_{B2}}{T_{A2} - T_{B1}}\right)} \quad \text{..... (3.36)}$$

This research will analyze the Intermediate Heat exchanger(IHX) and recuperator because there is an interaction between working gas and PCS in these heat exchangers. Temperatures of inlets and outlets of heat exchangers had been obtained by using thermodynamic analysis. Hence LMTD values were determined. Sizing a double pipe heat exchanger would determine the overall heat transfer coefficient (U) and area of the heat exchanger. We calculated and analyzed various double pipe diameter configurations to find the lowest length of pipe, highest overall heat transfer coefficient as well as lowest pressure drop. Thus, the optimum performance of the heat exchanger would be selected. Pipe data have been retrieved from a heat exchanger textbook. Furthermore, a list of pipe data and gas coefficients are attached in appendix B and C.

## 3.3 Summary

Thermodynamic analysis with cold-gas standard assumption determines the performance of the system. Temperatures define the interaction between working gas and PCS. Thus, efficiencies were measured and analyzed. Thermodynamic were presented in MATLAB-Simulink. From this analysis, we obtain the best performance of a system PCS Brayton cycle with a specific working gas. The temperatures of working gas are used for sizing double pipe heat exchangers and sizing the heat exchanger determines the overall heat transfer coefficient, pressure drop, and dimension of the heat exchanger.

# Chapter 4. Thermal Efficiency Brayton cycle

This chapter compares five different working gases in a secondary loop using a cold-gas-standard assumption calculation. The working fluids are helium, hydrogen, carbon dioxide, nitrogen and air. The gasses are used in five plant configurations, such as open-cycle, 1T1C, 1T2C, 2T2C, and combined cycle. The goal of the comparison is to find the highest energy thermal efficiency among the gasses considering the capability of both regenerator and turbine to drive the compressor. Calculations have been done for the actual cycle based on fixed pressure ratio (Pr)-various temperature inlet turbines (T6) as well as fixed temperature inlet turbine- various pressure ratios. All the name temperature for actual values were followed by suffix “a”, such as, T2a, T4a, T5a, T7a, T8a and T10a. Data assumptions are tabulated in Chapter 3 Table 3.1. Physical properties in this table were constant since we use cold-gas standard assumptions. The calculation results depend on characteristics of the working fluids such as specific heat at constant pressure (Cp) as well as specific heat ratio (gamma). Based on equation (3.9), the gas which has a high Cp, requires a slow mass flow rate, and vice versa. The mass flowrate valus affect to power producing calculations.

## 4.1. Thermodynamic Analysis of Open Cycle Configuration

Open cycle gas turbines are composed of three main components: compressor, heat source and gas turbine. The heat from the nuclear core was transferred to a secondary loop through an intermediate heat exchanger (IHX). On the other side, working gas was compressed in a compressor at 300 K. This working gas would be heated in the IHX. The heated gas flowed into the turbine to drive the compressor and generate electricity. The exhaust of gas from the turbine was not circulated.

Figure 4.1 shows the temperature diagram of the open cycle gas turbine diagram for pressure ratio 9 and temperature inlet Turbine 1200 K for actual cycle values. This configuration comprises one turbine, one compressor, and IHX. There is no recuperator, hence, there is no loopback energy to the system. The gas flows through the compressor from other systems such as the environment for air or a tank for helium. Temperature gas T2a from the compressor was exchanged in IHX. The gas that came from the turbine would return to the environment or those systems. Calculation of this diagram compared efficiency between air, helium and CO2. As can be seen from Figure 4.1, CO2 experienced a lower temperature compressor out and higher temperature turbine out due to its lower gamma ratio (specific heat ratio).

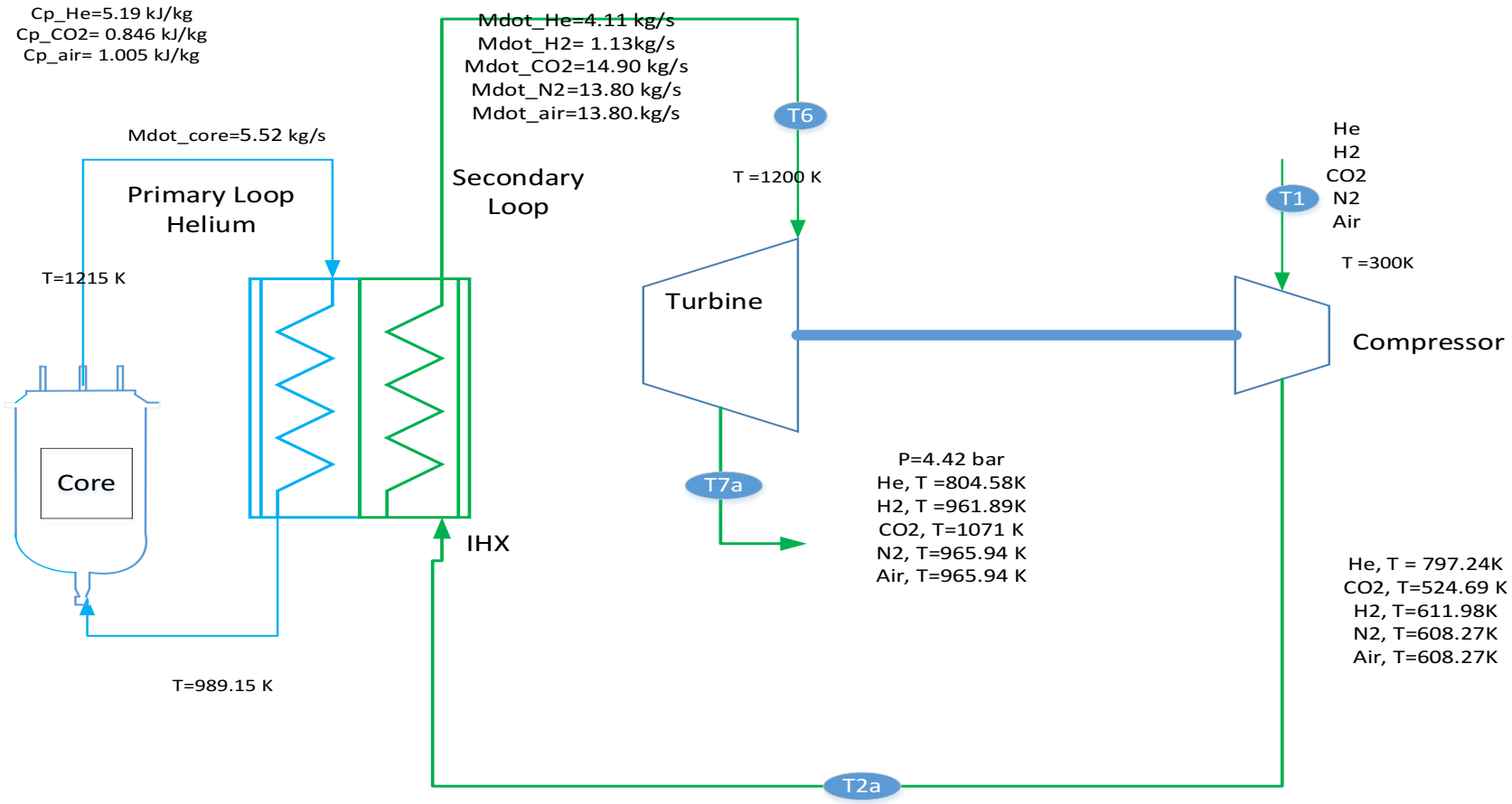


Figure 4.1. Gas turbine diagram (open cycle) for pressure ratio 9 and turbine temperature inlet 1200 K

Table 4.1. Gas turbine open cycle diagram open for pressure ratio 9 and turbine temperature inlet 1200.K

| Description | Gas | | | | |
|---|---|---|---|---|---|
| | He | H2 | CO2 | N2 | Air |
| Mass Flow rate (kg/s)<br>Reactor mass flow<br>Secondary cycle mass flow | <br>5.52<br>4.11 | <br>5.52<br>1.13 | <br>5.52<br>14.93 | <br>5.52<br>13.84 | <br>5.52<br>13.84 |
| Turbomachinery Energy (kJ/kg)<br>Turbine<br>Compressors | <br>3096<br>2580.69 | <br>6487<br>4463.51 | <br>335.66<br>190.08 | <br>477.92<br>309.84 | <br>478<br>309.8 |
| Turbomachinery Net Energy (kJ/kg) | 515.31 | 2023.49 | 145.60 | 169 | 169 |
| Q input (kJ/kg) | 2090 | 7227 | 517 | 595 | 595 |
| Thermal energy efficiency ratio | 0.25 | 0.28 | 0.25 | 0.28 | 0.28 |

As can be seen in Table 4.1, CO2 reached low turbomachinery net energy, due to lower temperature at compressor out, T2a. it because CO2 experienced a lower temperature compressor out and higher temperature turbine out due to its lower gamma ratio (specific heat ratio). On the other hand, the Q input difference between T2 and T6 was high. Hence, the ratio between Q input and turbomachinery energy was low. Therefore, the efficiency of CO2 was the lowest among the other gasses in this diagram.

Although efficiencies were above 25% for all gasses, those results did not represent the best scheme the intermediate heat exchanger was unable to regenerate energy due to the temperature inlet turbine, as T6 were lower than temperature outlet compressor 2a. Furthermore, the turbine was unable to drive the compressor due to insufficient energy for helium, as can be seen in Figure 4.2. Thus, the efficiencies were minus. Therefore, we need to determine an optimum pressure ratio for each gas.

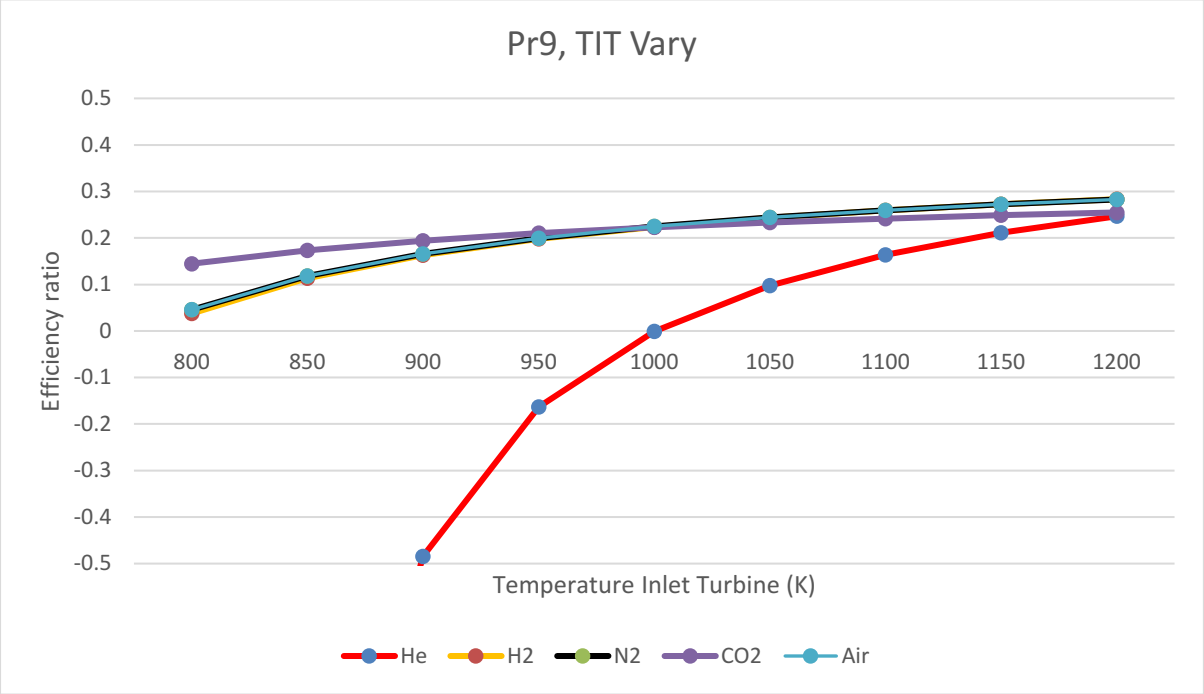


Figure 4.2. Calculation results open cycle diagram for pressure ratio at 9 and various temperature inlet turbines

Figure 4.2 illustrates the comparison efficiency calculation of five different gasses in an open cycle gas turbine diagram at various temperature inlet turbines from 800 K to 1200 K and pressure ratio 9. Although helium as working gas reached the highest efficiency, there were conspicuous values of efficiency between 700 K and 1000 K for helium. They arose because the gas turbine was unable to drive the compressor due to a lack of energy. On the other hand, other gasses were able to perform properly.

In general, all the gasses perform below 30% efficiency at a temperature of 1200 K. CO2 as working gas reached the highest efficiency, 28%, while Helium reached the lowest efficiency, 25%. Book[44] stated that open cycle gas turbine can produce electricity with efficiency 30 % depend on temperature inlet turbine, configuration of the cycles, working gas, as well as turbimachinery specification. Temperature turbine outlet T7a was still high above 400 K. Furthermore, those temperatures were sent to the environment and it was possible to utilise these waste temperatures for other purposes.

There is no recuperator, thus, energy input of turbomachinery (Qin) relied upon a fixed-temperature outlet compressor and temperature inlet turbine.

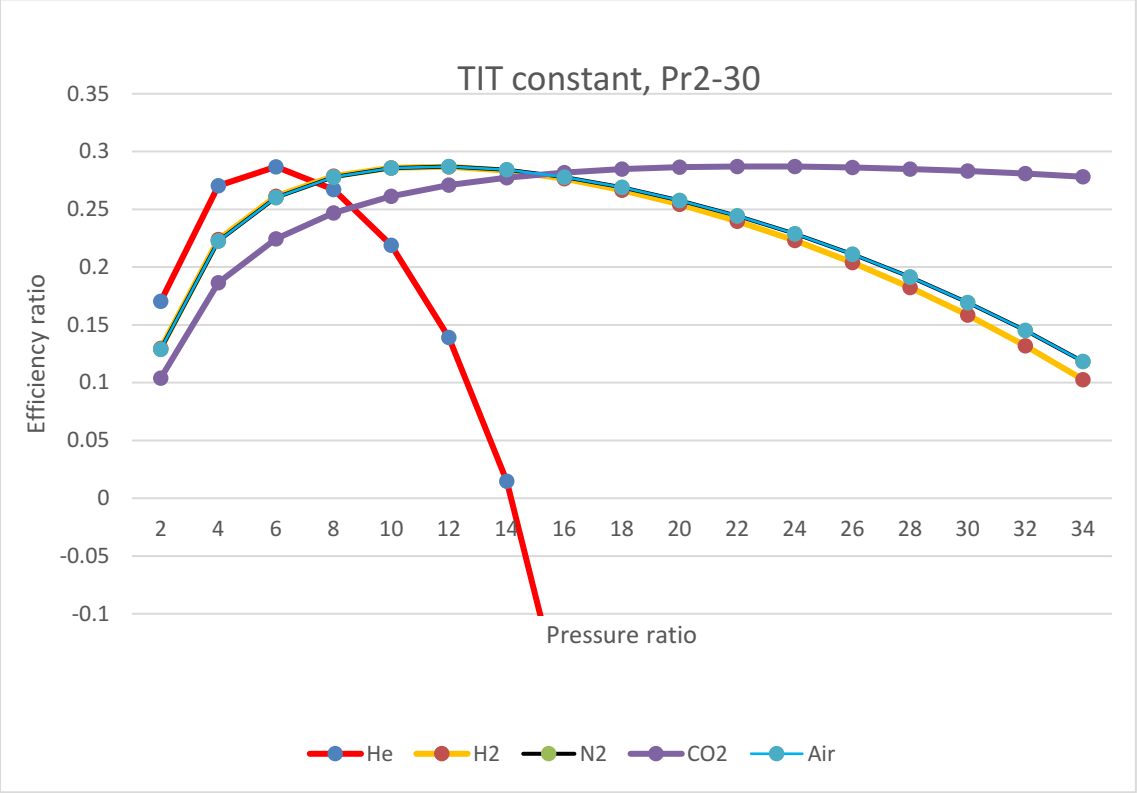


Figure 4.3. Calculation results of open cycle diagram for various pressure ratios and temperature inlet turbines at 1200 K

Figure 4.3. illustrates the comparison efficiency calculation between five different gasses in an open cycle gas turbine diagram at temperature inlet turbine 1200 K and various pressure ratios from 2 to 34. In this scheme, the system was able to produce an efficiency maximum of about 28% at a pressure ratio of 6 for helium, at a pressure ratio of 8-16 for hydrogen, air and nitrogen, as well as a pressure ratio of 14-34 for carbon dioxide. Furthermore, the turbine was unable to drive the compressor due to insufficient energy for helium at a pressure ratio of 14 and above. As stated in equation (3.2), the exponential pressure ratio affect to producing temperature outlet turbomachinery. Hence, the compressor work is higher than the turbine work. Therefore, the efficiencies were minus

There is no need to regenerate temperature, as there is no recuperator. However, the temperatures of waste gas from T7a were high. It is possible to utilize this waste gas for other purposes, such as cogeneration or combined cycle. It is also possible to have a multi-stage compressor and turbine to increase efficiency.

Figure 4.3 shows approximated range of pressure ratio for every gas while Figure 4.2 illustrates efficiencies achievement. Considering those figures' results, we determine the optimum pressure ratio. The pressure ratio would be able to accommodate the capability of both heat exchanger and turbine to drive the compressor in all temperature spans.

Table 4.2. Optimum pressure ratio at minimum temperature (800K) for open-cycle diagram

| Gas | Pressure ratio optimum | At a temperature of 800 K, | |
|---|---|---|---|
| | | Minimum efficiency ratio | Minimum potential regeneration (°K) |
| Helium | From 5 | 0.021 | 180.93 |
| | To 5.1 | 0.072 | 175.59 |
| Hydrogen | From 9 | 0.0376 | 188.02 |
| | To 9.7 | 0.016 | 173.51 |
| Carbon dioxide | From 17 | 0.0349 | 188.79 |
| | To 20 | 0.003 | 174.04 |
| Nitrogen | From 9 | 0.0457 | 191.73 |
| | To 9.7 | 0.0121 | 177.42 |
| Air | From 9 | 0.0457 | 191.73 |
| | To 9.7 | 0.0121 | 177.42 |

Table 4.2 is the optimum pressure ratio at temperatures 800 K- 1200 K. The system was able to produce an efficiency maximum of about 28%. There were ranges of optimum pressure ratios for every gas. Optimum pressure ratios were selected considering the ability to achieve the highest efficiency and potential regeneration at the lowest temperature (800 K). Thus, the open cycle can achieve maximum efficiency at 28% when working gas is

1. Helium at pressure ratio 5
2. Hydrogen at pressure ratio 9
3. Carbon dioxide at pressure ratio 17
4. Nitrogen at pressure ratio 9
5. Air at pressure ratio 9

## 4.2. Thermodynamic Analysis of 1T1C Configuration

In the Brayton cycle, the temperature of turbine exhausts was high and it was possible to re-utilize this temperature. Additionally, the recuperator re-utilized the turbine exhaust to re-heat gas from the compressor exhaust. Thus, exhausted gas from turbines was circulated through the recuperator. Before entering a compressor, the gasses were cooled in a precooler.

Figure 4.4 shows the temperature diagram of the 1T1C gas turbine diagram for pressure ratio 9 and temperature inlet turbine 1200 K for actual cycle values. Book [44] stated that this configuration is a simple CBC because it comprises one turbine, one compressor, a precooler, a recuperator and an IHX. This configuration also had been used for a model standard before modifications were made for initial CBC research activities [17].

Simple Cycle

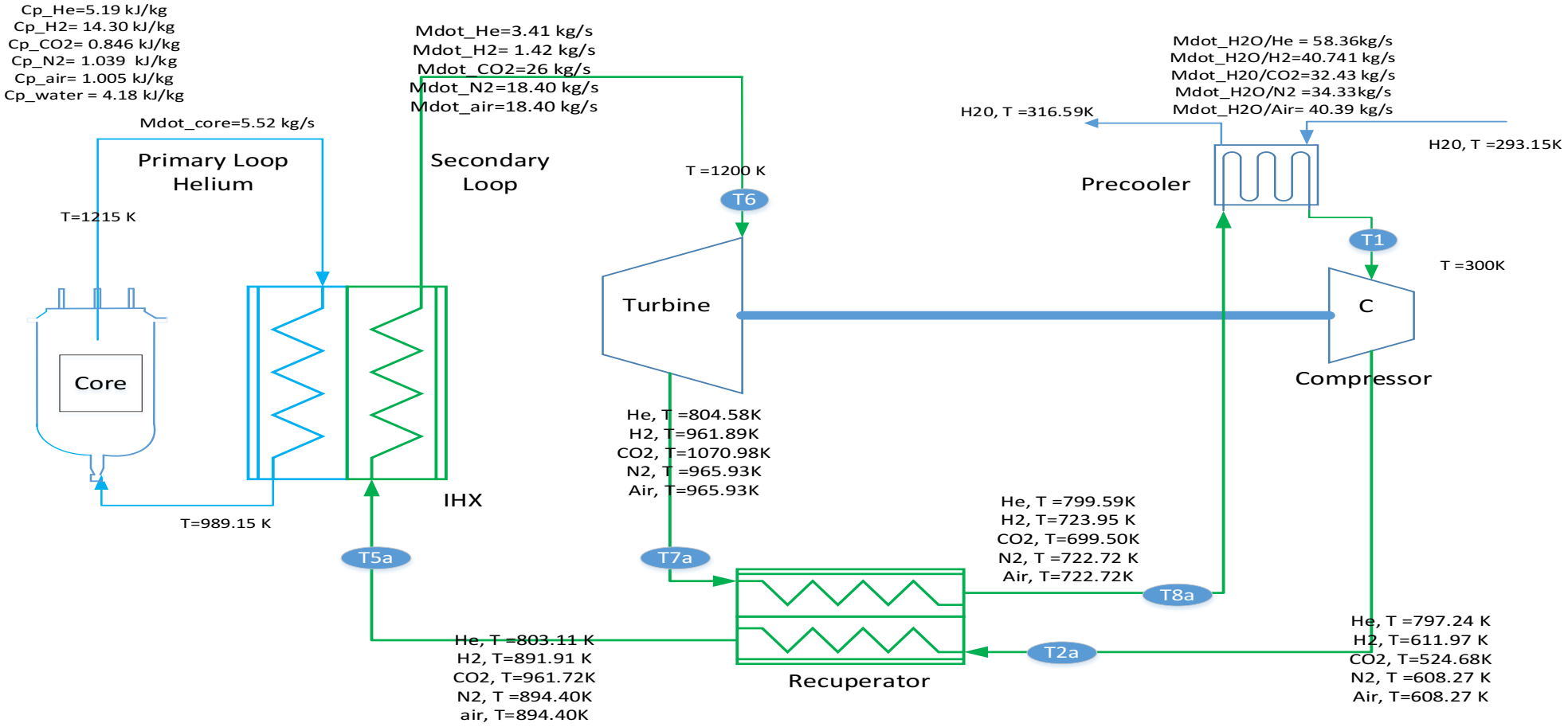


Figure 4.4. Gas turbine diagram (1T1C) for pressure ratio 9 and turbine temperature inlet 1200 K

.

Table 4.3. Gas turbine diagram (1T1C) for pressure ratio 9 and Turbine temperature inlet 1200 K

| Description | Gas | | | | |
|---|---|---|---|---|---|
| | He | H2 | CO2 | N2 | Air |
| Mass Flow rate (kg/s)<br>Reactor mass flow<br>Secondary cycle mass flow<br>Precooler water | <br>5.52<br>3.41<br>58.36 | <br>5.52<br>1.42<br>40.74 | <br>5.52<br>26<br>32.43 | <br>5.52<br>18.40<br>34.33 | <br>5.52<br>18.40<br>40.39 |
| Turbomachinery Energy (kJ/kg)<br>Turbine<br>Compressors | <br>3096<br>2580 | <br>6487<br>4463.47 | <br>335<br>190 | <br>494<br>320 | <br>494<br>320 |
| Turbomachinery Net Energy (kJ/kg) | 515 | 2383 | 145 | 174 | 174 |
| Q input (kJ/kg) | 2895 | 7160 | 382 | 518 | 518 |
| Thermal energy efficiency ratio | 0.17 | 0.33 | 0.38 | 0.33 | 0.33 |

It can be seen in Table 4.3 that, although efficiencies were above 37% for all gasses, those results did not represent the best scheme. The recuperator was unable to regenerate energy because the temperature outlet turbine T7a is lower than the temperature outlet compressor T2a. Furthermore, the turbine was unable to drive the compressor due to insufficient energy for helium, as can be seen in Figure 4.5. Thus, the efficiencies were minus. Therefore, we need to determine an optimum pressure ratio for each gas.

Calculations were made for different cases. In one case, the pressure ratio was constant at 9 and various temperature inlet turbines were from 800 K to 1200 K. In another case, the temperature inlet turbine was constant at 1200 K and various pressure ratios (from 2 to 30). Both results are illustrated in Figure 4.5 and Figure 4.6.

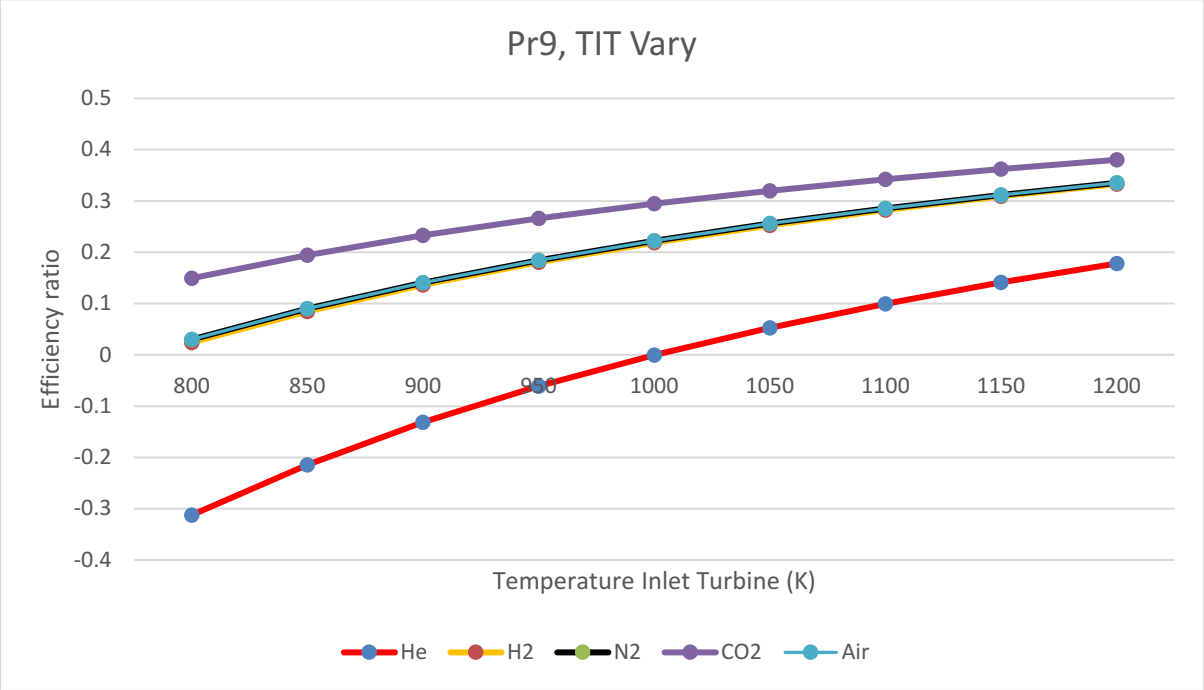


Figure 4.5. Calculation results from 1T1C diagram for pressure ratio at 9 and various temperature inlet turbines.

Figure 4.5 shows the comparison efficiency calculation for five different gasses in the 1T1C gas turbine diagram at a pressure ratio of 9 and various temperature inlet turbines from 800 K to 1200 K.

Initially, the efficiencies were minus for helium because there was insufficient energy for the turbine to drive the compressor. The turbine was able to drive the compressor when helium temperature was above 1000 K.

However, the recuperator started regenerating the temperature of the gasses, when helium temperature was 1200 K and above, temperatures of hydrogen, nitrogen and air were above 1000 K. This condition happened because the recuperator was unable to reheat the gas. Instead of reheating gas for T4a, the temperature of T8a was down and below the temperature of T4a. Using carbon dioxide as working gas, the system had the energy to regenerate temperature in the recuperator as well as to drive the compressor.

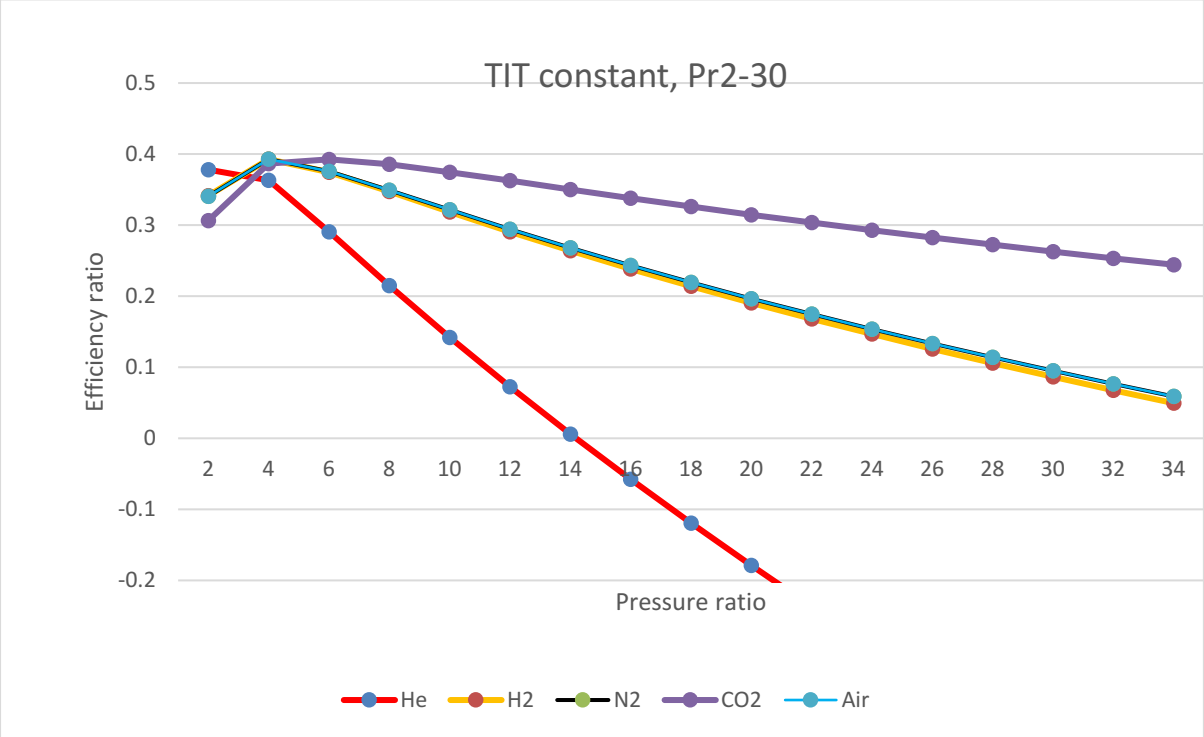


Figure 4.6. Calculation results of 1T1C diagram for various pressure ratios and temperature inlet turbines at 1200 K

Figure 4.6. Illustrates the comparison of efficiency calculation for five different gasses in 1T1C gas turbine diagram at temperature inlet turbine 1200 K and various pressure ratios from 2 to 34.

As can be seen in Figure 4.6, the system was able to produce an efficiency maximum of about 38% at pressure ratio 2 for helium, at pressure ratio 4 to 6 for hydrogen, air, and nitrogen, and at pressure ratio 4 to 10 for carbon dioxide. However, the recuperator was unable to regenerate energy at pressure ratios 8 and above for helium; 16 and above for hydrogen, nitrogen, and air. Instead of reheating gas in the recuperator, the temperature of T7a was down and below the temperature of T2a. Furthermore, the turbine was unable to drive the compressor due to insufficient energy for helium at a pressure ratio of 14 and above. Therefore, the efficiencies were going to be minus.

Figure 4.6 shows the approximated range of pressure ratio for every gas while Figure 8 illustrates efficiency achievement. Considering those figures' results, we determine the optimum pressure ratio. The pressure ratio would be able to accommodate the capability of both heat exchanger and turbine to drive the compressor in all temperature spans.

Table 4.4. Optimum pressure ratio at minimum temperature (800K) for 1T1C diagram

| Gas | Pressure ratio optimum | At a temperature of 800 K | |
|---|---|---|---|
| | | Efficiency ratio | potential regeneration (°K) |
| Helium | From 2.7 | 0.208 | 104.76 |
| | To 3.5 | 0.142 | 2.23 |
| Hydrogen | From 4 | 0.207 | 102.61 |
| | To 5.7 | 0.142 | 1.78 |
| Carbon dioxide | From 6 | 0.205 | 100.54 |
| | To 9.5 | 0.142 | 1.11 |
| Nitrogen | From 4 | 0.208 | 106.07 |
| | To 5.7 | 0.142 | 1.24 |
| Air | From 4 | 0.208 | 106.078 |
| | To 5.7 | 0.142 | 1.247 |

Table 4.4 is the optimum pressure ratio at temperatures 800 K- 1200 K. The system was able to produce an efficiency maximum of about 39%. There were ranges of optimum pressure ratios for every gas. Optimum pressure ratios were selected considering the ability to achieve the highest efficiency and potential regeneration at the lowest temperature (800 K). Thus, 1T1C can achieve maximum efficiency at 39% when working gas was

1. Helium at pressure ratio 2.7
2. Hydrogen at pressure ratio 4
3. Carbon dioxide at pressure ratio 6
4. Nitrogen at pressure ratio 4.1
5. Air at pressure ratio 4.1

## 4.3. Thermodynamic Analysis of 1T2C Configuration

This gas turbine diagram comprises two compressors with an intercooler between them, a turbine, a recuperator, and a precooler. Some scholars [16,30,31] in nuclear power plant designs used this configuration in their gas turbine analyses to improve efficiency. This configuration is applied in conventional CBC using fossil-fuels powerplant that air or nitrogen is the working gas. Therefore, scholars [17,43] sometime stated this configuration as a standard CBC configuration and called as Nitrogen cycle.

Figure 4.7 illustrates a result calculation based on T6 at 1200 K and Pressure ratio at 9 for actual cycle values in a gas turbine diagram. This gas turbine diagram comprises two compressors with an intercooler between them, a turbine, and a recuperator (1T2C). We assume T1= T3 and T2a =T4a since it is a cold-gas standard calculation

The calculations using carbon dioxide as a working fluid resulted in the lowest temperature outlet compressor, T2a, and the highest number in temperature outlet turbine, T7a. The opposite quality resulted in using helium as a working fluid. Hydrogen, nitrogen, and air results were relatively similar since H2, N2 and air have a similar gamma value.

Thus, the calculation results depend on the characteristics of the working fluids, such as specific heat at constant pressure (Cp) as well as specific heat ratio (gamma). Therefore, hydrogen requires a slow mass flow rate, while carbon dioxide requires a fast mass flow rate.

An intercooler is employed between two compressors. The gas is compressed in low-pressure compressor and cooled in intercooler then recompressed in high-pressure compressor. Ideally, the cooling process takes place at constant pressure, and the gas is cooled to the initial temperature T1 at each intercooler. To minimise compression work (The cyclic device deliver most work consumption) during multi-stage compression, the pressure ratio across each stage of the compressor must be the same. Precooler ensure temperature of the gas is cooled down and assumes that the heat is lost by precooler the change of precooler temperature rate to the net thermal power transferred to the precooler minus thermal power transferred to environment/ambient. Decreasing the inlet temperature decreases the compressor power at the same pressure ratio. Thus, intercooler and precooler can be used to improve the cycle efficiency. The compression process is implemented using several compressors, in which the inlet gas is cooled by a water heat exchanger individually. These results in a significant reduction of the compressor power required to realise the compression task, and thus an increase of the cycle efficiency.

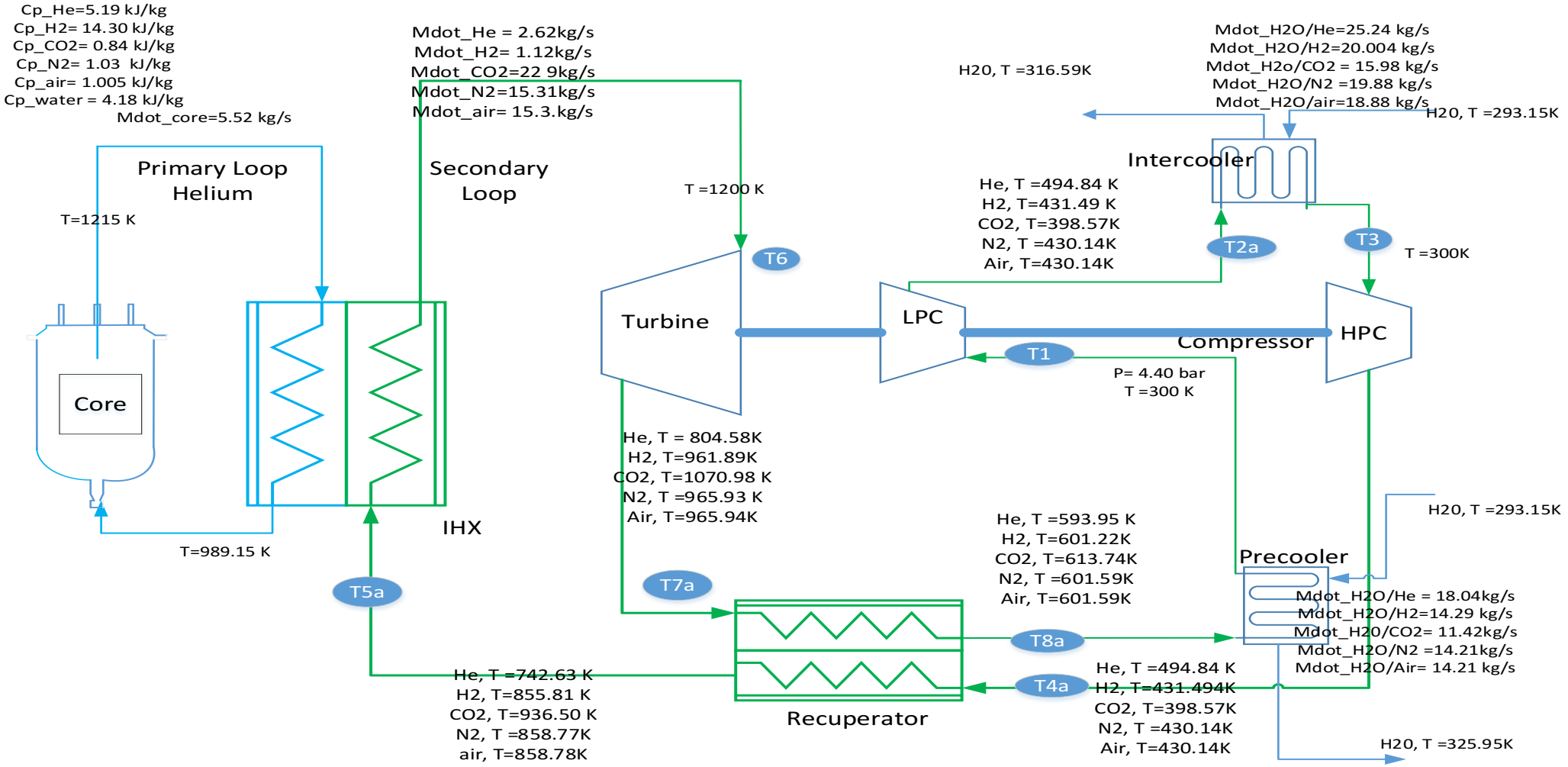


Figure 4.7. Gas turbine diagram (1T2C) for pressure ratio 9 and turbine temperature inlet 1200 K

Table 4.5. Gas turbine 1T2C diagram for pressure ratio 9 and turbine temperature inlet 1200 K

| Description | Gas | | | | |
|---|---|---|---|---|---|
| | He | H2 | CO2 | N2 | Air |
| Mass Flow rate (kg/s) | | | | | |
| Reactor mass flow | 5.52 | 5.52 | 5.52 | 5.52 | 5.52 |
| Secondary cycle mass flow | 2.62 | 1.12 | 22 | 15.31 | 15.31 |
| Precooled water | 10.60 | 10.98 | 11.424 | 10.92 | 10.92 |
| Intercooling water | 14.84 | 15.37 | 15.987 | 15.28 | 15.28 |
| Turbomachinery Energy (kJ/kg) | | | | | |
| Turbine | 3096.23 | 6847 | 335.63 | 494 | 494 |
| Compressors | 2022.43 | 3762 | 166.86 | 270.41 | 270.41 |
| Turbomachinery Net Energy (kJ/kg) | 1073 | 3084 | 168.77 | 223.62 | 223.62 |
| Q input (kJ/kg) | 3180 | 7676 | 387 | 555 | 555 |
| Thermal energy efficiency ratio | 0.33 | 0.4 | 0.43 | 0.4 | 0.4 |

As can be seen in Table 4.5, CO2 required the fastest mass flow rate due to its lowest specific heat (Cp). Calculation results using He as working gas had the lowest efficiency, about 33% while the other gasses' calculations resulted in a similar number of efficiencies, about 40%. However, H2 required the lowest mass flow rate as its Cp is high.

Those results did not represent the finest scheme because the recuperator was unable to regenerate energy due to the temperature outlet turbine T7a is lower than the temperature outlet compressor T2a for helium. Therefore, we need to determine an optimum pressure ratio for each gas

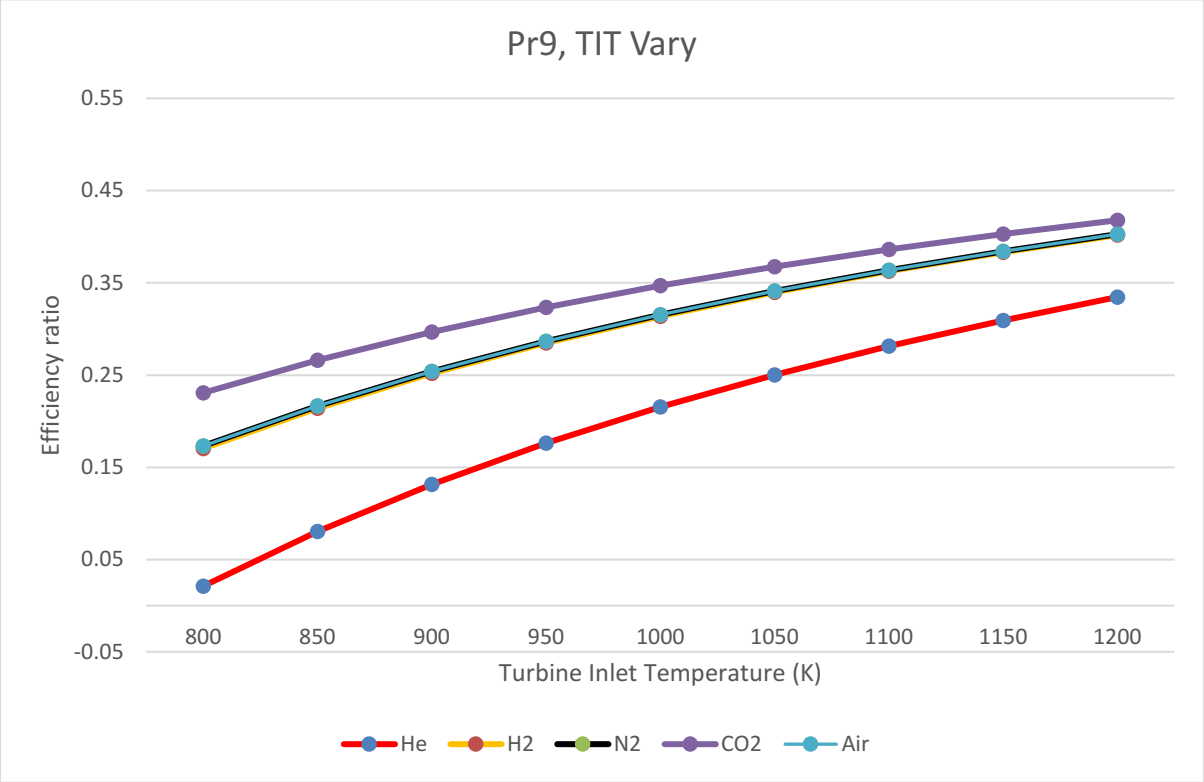


Figure 4.8. Calculation results of 1T2C diagram for pressure ratios at 9 and various temperature inlet turbines

Figure 4.8 shows the comparison efficiency calculation for five different gasses in a 1T2C gas turbine diagram at a pressure ratio of 9 and various temperature inlet turbines from 800 K to 1200 K. Overall, increasing only the turbine inlet temperature might increase their efficiencies. Helium was able to achieve maximum efficiency 34% while other gasses were about 42%.

However, the recuperator was unable to regenerate energy at a temperature below 1000 K for Helium. Instead of reheating gas in the recuperator, the temperature of T7a was lower than the temperature of T2a.

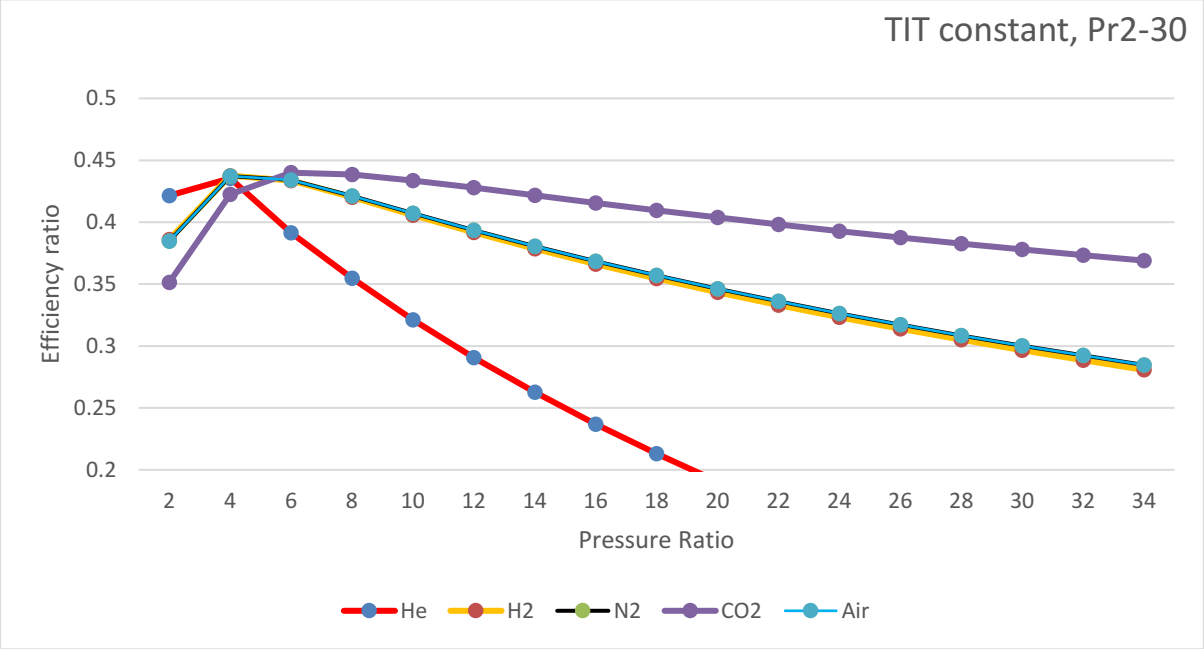


Figure 4.9. Calculation results of 1T2C diagram for various pressure ratios and temperature inlet turbines at 1200 K

Figure 4.9. Illustrates the comparison efficiency calculation for five different gasses in 1T2C gas turbine diagram at temperature inlet turbine 1200 K and various pressure ratios from 2 to 34. In this scheme, the system was able to produce an efficiency maximum of about 43% at a pressure ratio of 4 for helium, at a pressure ratio of 4-6 for hydrogen, air and nitrogen, as well as a pressure ratio of 4-14 for carbon dioxide. However, the recuperator was unable to regenerate energy at a pressure ratio of 10 and below for helium. Instead of reheating gas in the recuperator, the temperature of T2a was higher than the temperature inlet turbine, T6.

Figure 4.9 shows approximated range of pressure ratio for every gas while Figure 2 illustrates efficiencies achievement. Considering those figures' results, we determine the optimum pressure ratio. The pressure ratio would be able to accommodate the capability of both heat exchanger and turbine to drive the compressor in all temperature spans.

Overall, all curve efficiencies tend to decline along with pressure ratio increase. Initially, all the efficiency lines increased to reach their maximum efficiency and declined afterwards. Every gas has a different pressure ratio capability to reach its maximum efficiency. This capability depends on its exponential gamma, as stated in equation (3.2). Since the contant proporsional of the exponential gamma is negative over time, the quantity of Prc decreases over time and is said to be undergoing exponential decay.

Table 4.6. Optimum pressure ratio at minimum temperature (800K) for 1T2C diagram

| Gas | Pressure ratio optimum | At a temperature of 800 K | |
|---|---|---|---|
| | | Minimum efficiency ratio | Minimum potential regeneration (°K) |
| Helium | From 3.5 | 0.227 | 131.39 |
| | To 5.9 | 0.129 | 3.8777 |
| Hydrogen | From 6.5 | 0.213 | 107.146 |
| | To 11.5 | 0.132 | 7.40 |
| Carbon dioxide | From 9 | 0.230 | 136.915 |
| | To 24 | 0.128 | 2.416 |
| Nitrogen | From 7 | 0.206 | 96.88 |
| | To 12 | 0.129 | 3.9 |
| Air | From 7 | 0.206 | 96.88 |
| | To 12 | 0.129 | 3.9 |

Table 4.6 is the optimum pressure ratio at temperatures 800 K- 1200 K. The system was able to produce an efficiency maximum of about 43%. There were ranges of optimum pressure ratios for every gas. Optimum pressure ratios were selected considering the ability to achieve the highest efficiency and potential regeneration at the lowest temperature (800 K). Thus, 1T2C can achieve maximum efficiency at 43% when working gas was

1. Helium at pressure ratio 3.5
2. Hydrogen at a pressure ratio of 6.5
3. Carbon dioxide at pressure ratio 9
4. Nitrogen at pressure ratio 7
5. Air at pressure ratio 7

## 4.4. Thermodynamic Analysis of 2T2C Cycle Configuration

The cycle efficiency can be increased by adding stages in the PCS. Thus, components such as, compressors, turbines, intercooler placed between compressors, and a reheater placed between turbines are added to the system cycle. A pair compressor and an intercooler between these compressors were applied. Similar statement with sub section 4.3., the gas is compressed in a low-pressure compressor and cooled in the intercooler then recompressed in a high-pressure compressor. The gas was cooled to the initial temperature at the intercooler to minimize compression work. On the other hand, energy exhaust from a turbine would be reheated to have a similar temperature value with T6 (Temperature Inlet Turbine). This high temperature will be expanded in the second turbine. Hence, work ouput turbine would be twice higher than single turbine. Turbomachinery net energy ( energy resultant between turbine and compressor) would be higher than single turbine. Therefore, the efficiency 2T2C configuration is higher than other PCS configurations additional compressor and intercooler between compressors as well as turbine and reheater between turbines. Furthermore, there is no significant drop in the working gas temperature due to the reheater, thus, energy of the turbomachinery is still high.

Figure 4.10 shows the temperature diagram of the 2T2C gas turbine diagram for pressure ratio 9 and temperature inlet turbine 1200 K for actual cycle values. We assumed T1= T3, T2a =T4a, T6=T9 and T7a =T10a since they were a cold-gas standard calculation.

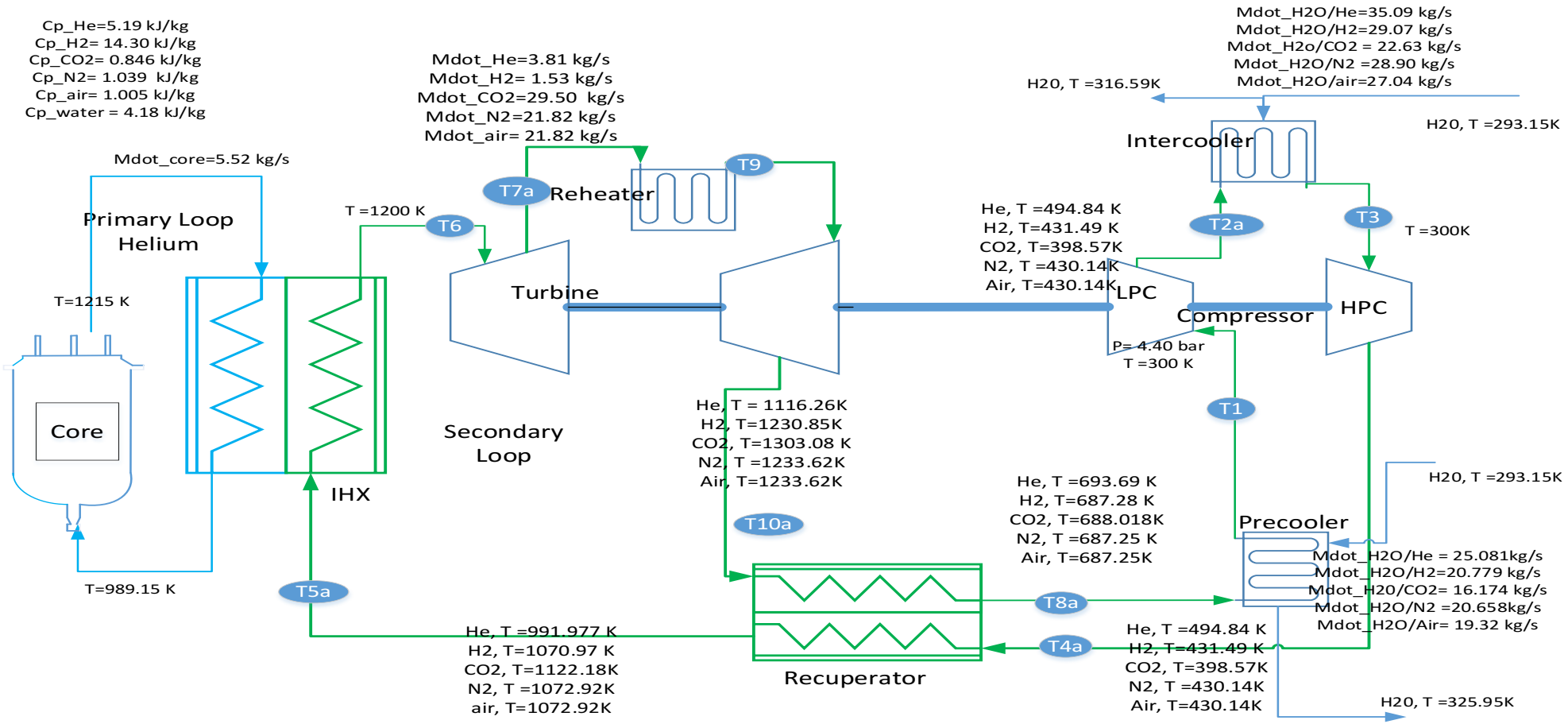


Figure 4.10 Gas turbine diagram (2T2C) for pressure ratio 9 and turbine temperature inlet 1200 K

Table 4.7 Gas turbine diagram (2T2C) for pressure ratio 9 and turbine temperature inlet 1200 K

| Description | Gas | | | | |
|---|---|---|---|---|---|
| | He | H2 | CO2 | N2 | Air |
| Mass Flow rate (kg/s) | | | | | |
| Reactor mass flow | 5.52 | 5.52 | 5.52 | 5.52 | 5.52 |
| Secondary cycle mass flow | 3.81 | 1.53 | 29.50 | 21.82 | 21.82 |
| Precooler water | 25.08 | 20.7 | 33.83 | 20.65 | 19.32 |
| Intercooling water | 35.09 | 29.07 | 22.63 | 28.90 | 27.04 |
| Turbomachinery Energy (kJ/kg) | | | | | |
| Turbine | 3765 | 7922 | 376 | 571 | 571 |
| Compressors | 2022 | 3762 | 166 | 270 | 270 |
| Turbomachinery Net Energy (kJ/kg) | 1743 | 4160 | 210 | 300 | 300 |
| Q input (kJ/kg) | 4121 | 9330 | 474 | 673 | 673 |
| Thermal energy efficiency ratio | 0.42 | 0.44 | 0.44 | 0.44 | 0.44 |

In comparison with Table 4.5, total work compressors remained the same while the total work turbine increased. Hence, turbomachinery work increased. Q input in the 2T2C diagram was also higher than in the 1T2C diagram. Therefore, all thermal efficiencies of gasses were higher than in the 1T2C diagram.

By using these configurations, there was higher efficiency among the gasses compared to Table 2. The gasses' calculations resulted in a similar number of efficiencies, about 42-44%.

Calculations have been made for different cases. In one case, the pressure ratio was constant at 9 and various temperature inlet turbines were from 800K to 1200K. In another case, the temperature inlet turbine was constant at 1200K and various pressure ratios (from 2 to 30). Both results are illustrated in Figure 4.11 and Figure 4.12.

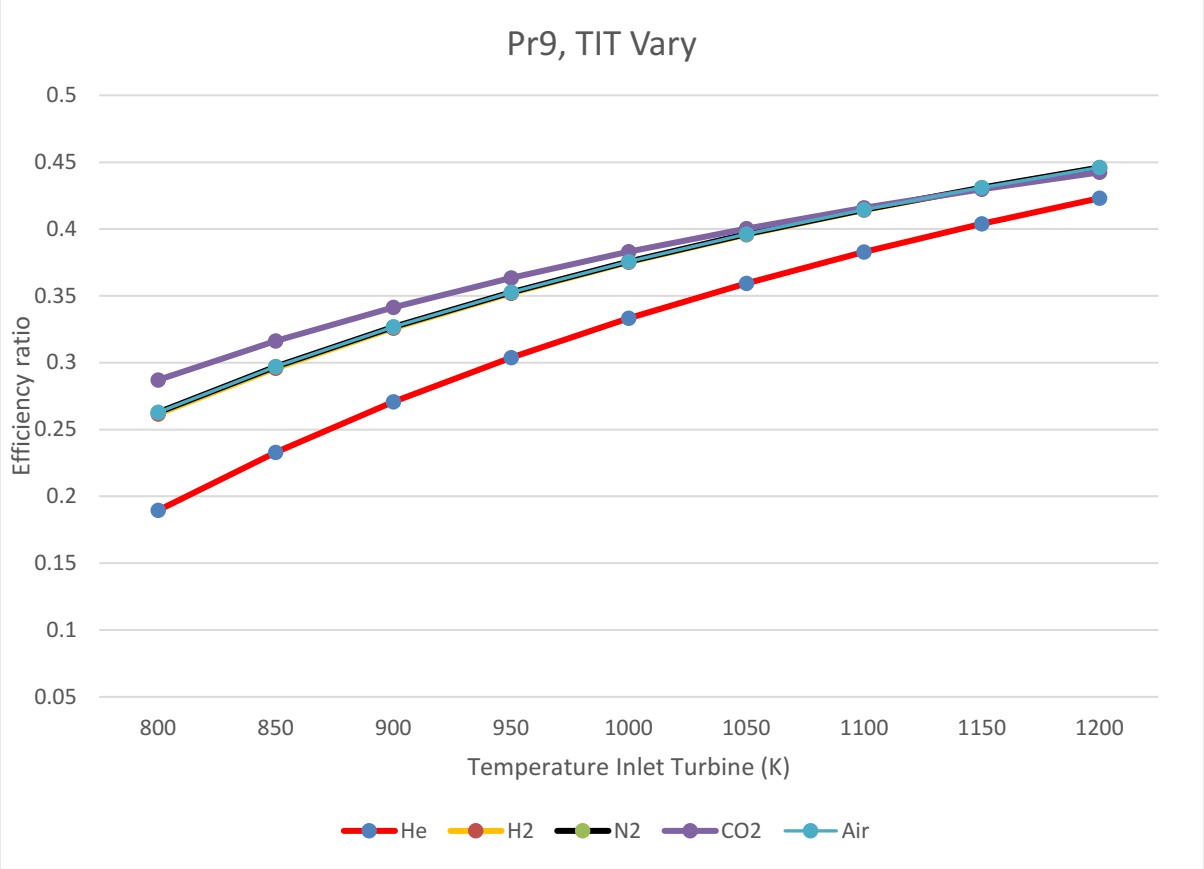


Figure 4.11. Calculation results of 2T2C diagram for pressure ratio at 9 and various temperature inlet turbines

Figure 4.11 shows the comparison efficiency calculation for five different gasses in the 2T2C gas turbine diagram at a pressure ratio of 9 and various temperature inlet turbines from 800 K to 1200 K.

Although efficiencies were above 42% for all gasses, those results did not represent the finest scheme. This scheme should consider the ability heat exchanger to transfer heat from the hot side to the cold side and the ability to achieve the highest efficiency. Therefore, we need to determine an optimum pressure ratio for each gas.

Overall, increasing only the turbine inlet temperature might increase their efficiencies.

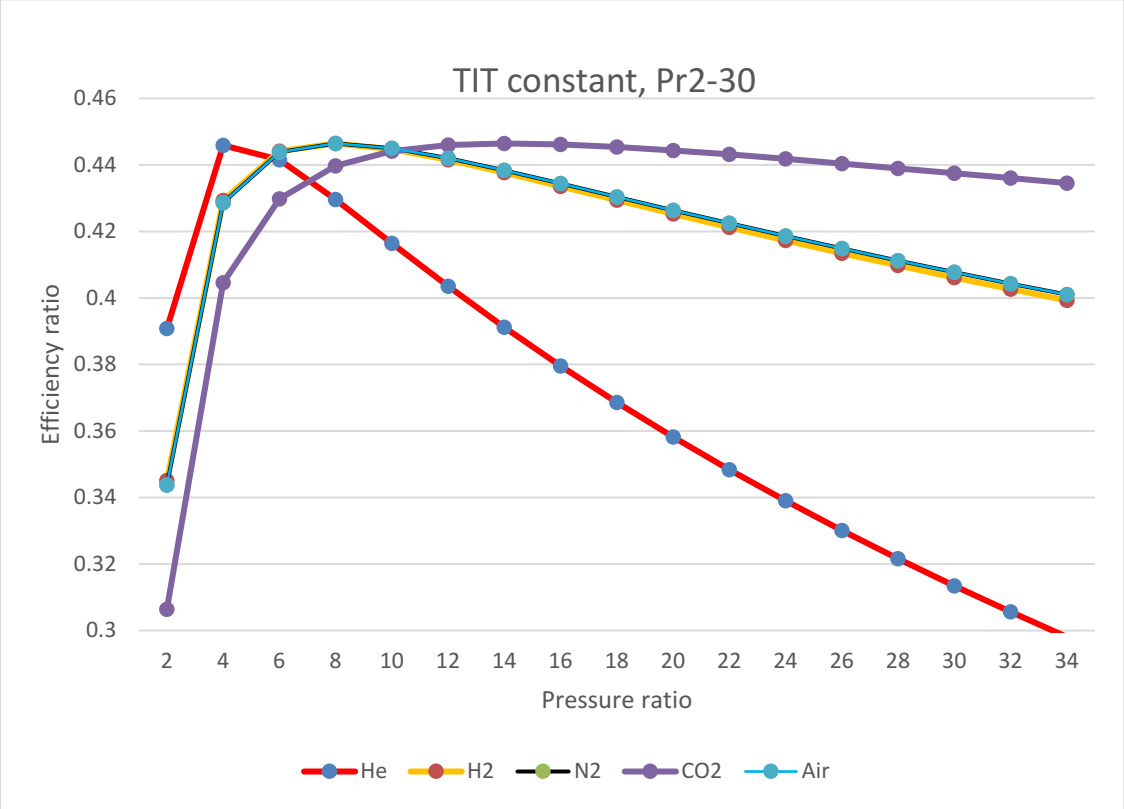


Figure 4.12. Calculation results of 2T2C diagram for various pressure ratios and temperature inlet turbine at 1200 K

Figure 4.12. Illustrates the comparison efficiency calculation for five different gasses in a 2T2C gas turbine diagram at temperature inlet turbine 1200 K and various pressure ratios from 2 to 34.

Overall, all the efficiency lines increased to reach their maximum efficiency and declined afterwards as well as every gas has a different pressure ratio capability to reach its maximum efficiency. It can be seen in Figure 4.12 that the system was able to produce an efficiency maximum of about 45% at pressure ratio 3 for helium, at pressure ratio 6-8 for hydrogen, air and nitrogen, as well as a pressure ratio of 12-18 for carbon dioxide.

Figure 4.12 shows approximated range of pressure ratio for every gas while Figure 4.11 illustrates efficiencies achievement. Considering those figures' results, we determine the optimum pressure ratio. The pressure ratio would be able to accommodate the capability of both heat exchanger and turbine to drive the compressor in all temperature spans.

Table 4.8. Optimum pressure ratio at minimum temperature (800K) for 2T2C diagram

| Gas | Pressure ratio optimum | At a temperature of 800 K | |
|---|---|---|---|
| | | Minimum efficiency ratio | Minimum potential regeneration (°K) |
| Helium | From 5 | 0.259 | 178.73 |
| | To 10 | 0.17 | 42.48 |
| Hydrogen | From 12 | 0.24 | 143.29 |
| | To 24 | 0.176 | 45.05 |
| Carbon dioxide | From 24 | 0.24 | 145.13 |
| | To 34 | 0.218 | 106.83 |
| Nitrogen | From 12 | 0.25 | 146.39 |
| | To 25 | 0.242 | 43.28 |
| Air | From 12 | 0.25 | 146.39 |
| | To 25 | 0.242 | 43.287 |

Table 4.8 is the optimum pressure ratio at temperatures 800 K-1200 K. The system was able to produce an efficiency maximum of about 45%. There were ranges of optimum pressure ratios for every gas. Optimum pressure ratios were selected considering the ability to achieve the highest efficiency and potential regeneration at the lowest temperature (800 K). Thus, 2T2C can achieve maximum efficiency at 45% when working gas was

1. Helium at pressure ratio 5.2
2. Hydrogen at pressure ratio 10
3. Carbon dioxide at pressure ratio 18
4. Nitrogen at pressure ratio 10
5. Air at pressure ratio 10

## 4.5. Thermodynamic Analysis of Combined Cycle Configuration

Figure 4.13 shows a temperature diagram of the combined cycle for pressure ratio in turbomachinery 9 and temperature inlet gas turbine 1200 K for actual cycle values. This configuration comprises two loops, the gas cycle and the steam cycle. Gas cycles consist of the turbine, one compressor, precooler, air as working gas and IHX while the steam cycle consists of a steam turbine, condenser, pump and steam as working fluid. The heat source for the steam turbine, which was from the temperature out gas turbine (T7a), was fed through a steam generator. Calculation and configuration of steam cycle followed an example in the thermodynamics textbook Chapter 10 [2] as assumptions. The pressure inlet steam generator in the steam cycle was assumed 46 Bar and the water temperature was assumed constant at 100$^{o}$C. In this diagram, three different gasses were compared: helium, carbon dioxide and air. Hydrogen and nitrogen were represented by air since these gasses had similar characteristics.

Temperature outlet gas turbine (T7a) flowed to the hot side steam generator as hot fluid for steam generator. In the steam generator, heat energy in hot side boiled water in cold side to produce steam. Temperature water in the cold side the steam generator (T2 steam cycle) would be boiled from 100$^{o}$C liquid to 300$^{o}$C vapour (T3 steam cycle). The water vapour or steam entered a steam turbine to produce electricity. The temperature exhaust steam was cooled-down and the steam was returned to liquid water in the condenser. The water was pumped and re-circulated to the steam generator. In the gas side steam generator, energy of the hot temperature working gas was exchanged and its exhaust was cooled-down in a precooler to the initial temperature gas (27$^{o}$C). Figure 4.13 showed temperature distribution at the maximum temperature (1200K) in the gas cycle. The steam cycle produced a superheated steam due to high temperature gas in the hot side steam generator.

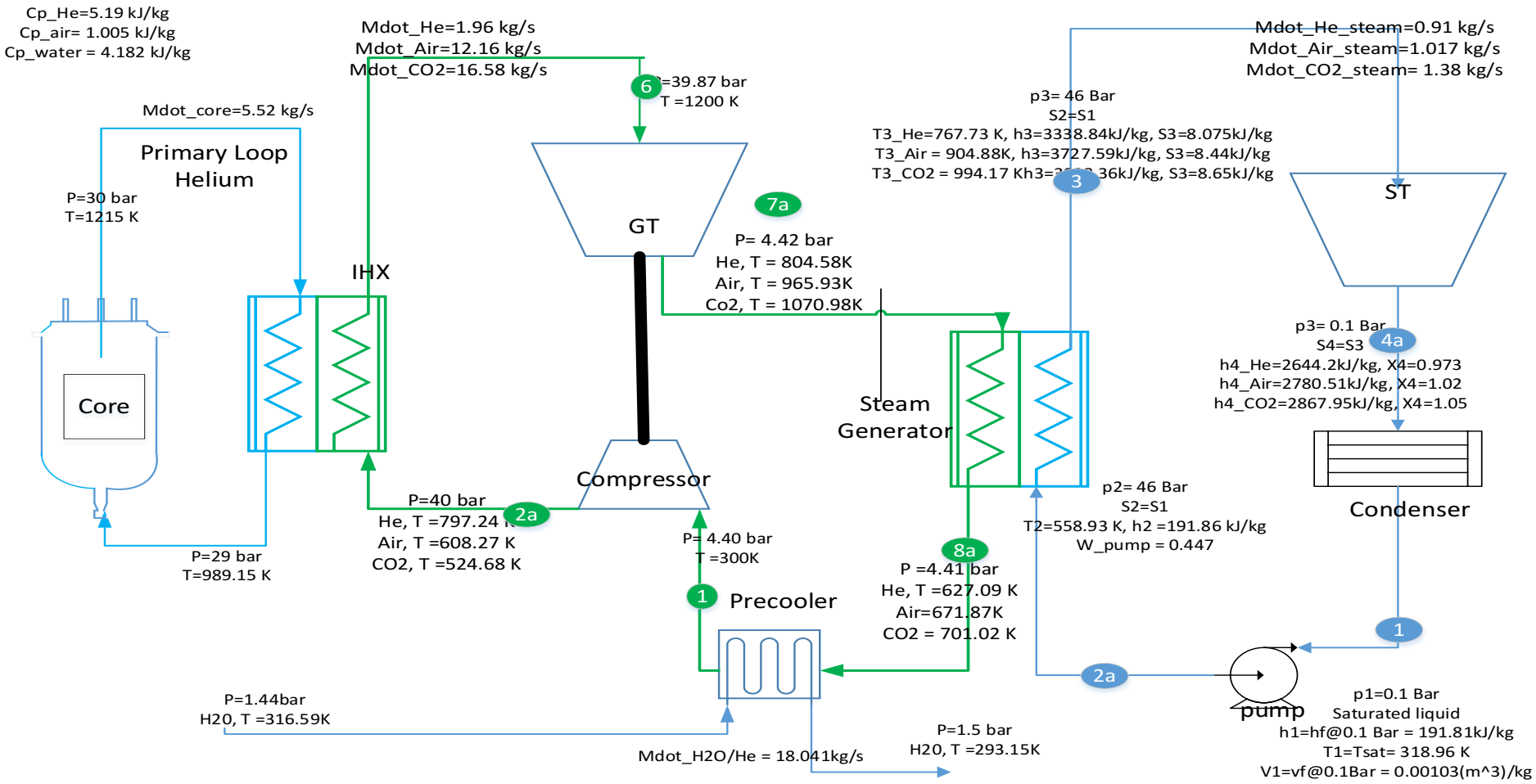


Figure 4.13. Combined cycle at pressure ratio 9 and turbine temperature inlet 1200 K

Table 4.9. Combined cycle at pressure ratio GT 9 and Turbine temperature inlet GT 1200 K

| Description | Gas | | |
|---|---|---|---|
| | He | Air | CO2 |
| Mass Flow rate (kg/s) | | | |
| Reactor mass flow rate | 3.21 | 3.21 | 3.21 |
| Gas cycle mass flow rate | 1.96 | 12.16 | 16.58 |
| Steam mass flow rate | 0.91 | 1.017 | 1.38 |
| Turbomachinery Net Energy GT (kJ/kg) | 1547.51 | 338.49 | 257.46 |
| Turbomachinery Net energy ST (kJ/kg) | 590.38 | 834.06 | 931.79 |
| Turbomachinery Net energy Combined cycle (kJ/kg) | 1855.16 | 412.94 | 338.29 |
| Q input (kJ/kg) | 4166.30 | 1030.40 | 909.71 |
| Thermal energy efficiency steam ratio | 0.18 | 0.24 | 0.25 |
| Thermal energy efficiency combined cycle ratio | 0.44 | 0.41 | 0.37 |

Turbomachinery net ST is a resultant between work steam turbine and work pump. Turbomachinery net combined cycle is the functioning ratio of mass flowrates, turbomachinery net ST, and turbomachinery GT. Since the main source originated from the reactor to the gas turbine, thus, Q input from GT calculation was used. Thermal efficiency steam is a calculation for only the steam loop while thermal efficiency combined cycle is the calculation for both gas turbine and steam turbine.

Steam generator for steam supply was fed by temperature outlet gas turbine, T7a. From that calculation, we have turbomachinery net energy and gas cycle mass flow rate. For the steam cycle, we retrieve values from a thermodynamic table in the textbook for enthalpy (h), entropy, pressure and volume. Saturated water data have been used for stage 1 and stage 2a in a steam cycle and superheated water data for 3 and 4a. Although efficiencies were above 35% for all gasses, those results did not represent the finest scheme because the steam generator was unable to regenerate energy due to temperature outlet GT T7a was lower than temperature ST 2a at some points. Thus, we need to determine an optimum pressure ratio for each gas.

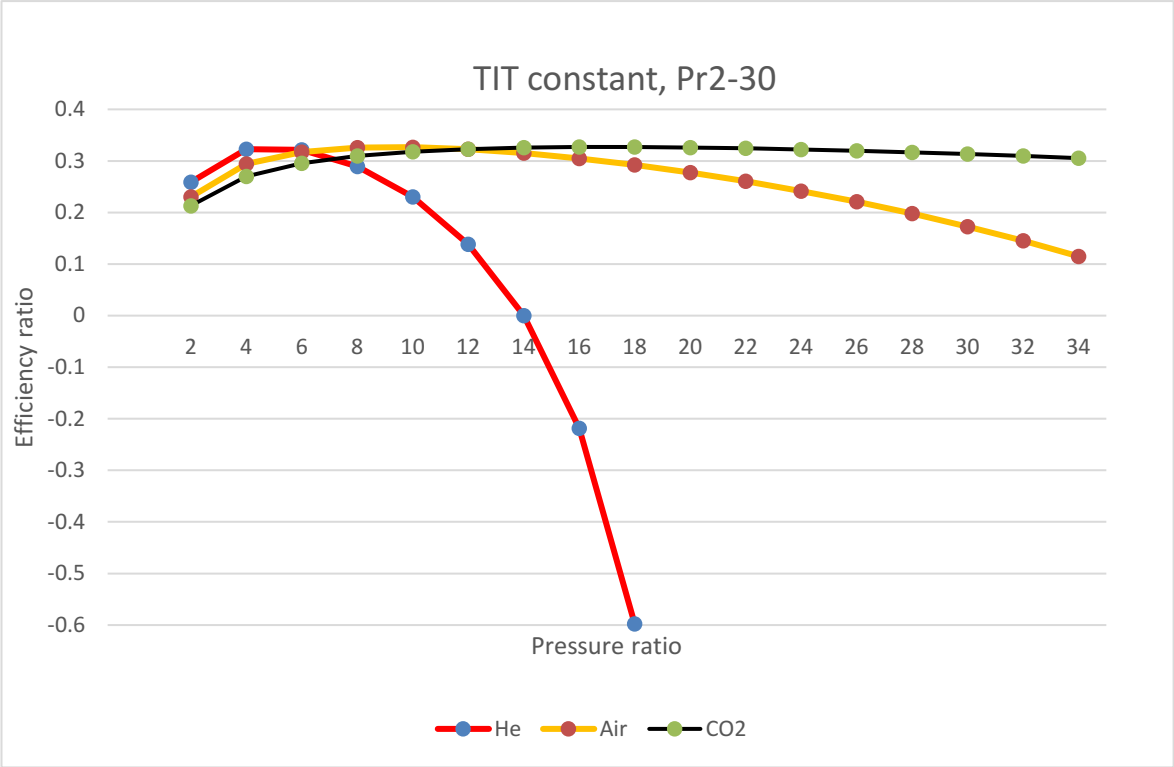


Figure 4.14. Calculation results of combined cycle diagram for various pressure ratios and temperature inlet turbine at 1200 K

Figure 4.14 Illustrates the efficiency calculation of the combined cycle using air as the working gas in the gas cycle at temperature inlet turbine 1200 K and various pressure ratios from 2 to 30. This figure arrangement was able to produce an efficiency maximum of about 32% at a pressure ratio of 4-6 for helium, at a pressure ratio of 6-12 for air and a pressure ratio of 10-28 for carbon dioxide. However, the turbine was unable to drive the compressor due to insufficient energy for helium at a pressure ratio of 14 and above. Therefore, the efficiencies were going to be a minus.

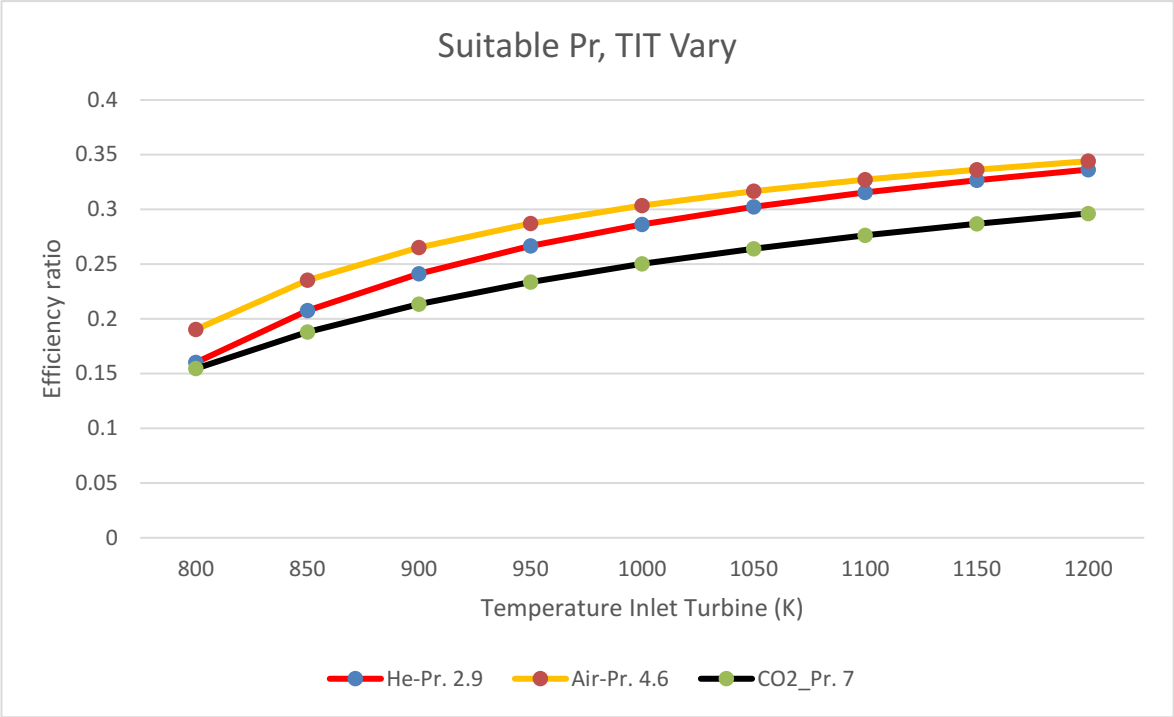


Figure 4.15. Calculation results of combined cycle diagram for suitable pressure ratio and various temperature inlet turbines

Figure 4.15 Illustrate the efficiency calculation of the combined cycle using helium, air and CO2 as the working gas in the gas cycle at various temperature inlet turbines from 800 K to 1200 K. Every gas conformed to a particular pressure ratio. There were ranges of optimum pressure ratios for every gas. Optimum pressure ratios were selected considering the ability to achieve the highest efficiency and potential regeneration at the lowest temperature (800 K). The pressure ratio would be able to accommodate the capability of both heat exchanger and turbine to drive the compressor in all temperature spans. Therefore, based on some calculations, we determine the optimum pressure ratio for helium at 2.9, for air at 4.6 as well as for CO2 at 7.

Helium and air as working gas reached 34% the efficiency while CO2 reached the lowest efficiency, 29%. Since specific heat at constant pressure (Cp) of CO2 is the lowest, the turbin work was the lowest among other gases according to equation (3.7) in the same model scheme. Overall, since the pressure ratio was fixed constant, the turbomachinery net energy was constant as well. Q input rose along with turbine inlet temperature.

## 4.6. Summary

There were ranges of optimum pressure ratios for every gas. The optimum pressure ratio was selected considering the ability to achieve the highest efficiency and potential regeneration at the lowest temperature (800K). The capabilities of the cycle with optimum pressure ratio were summarized in table 4.10. It was seen from table 4.10 that a Brayton cycle configuration with a

particular pressure ratio was able to achieve a range of efficiency at a temperature between 800K and 1200K. From this study, we can learn capabilities Brayton cycle configuration to reach maximum efficiencies such as, 1T1C configuration was at 40%, 2T2C configuration at 45%, 1T2C configuration was at 43%, open cycle configuration was at 33%, and combined cycle was at 29-34%. Overall, Brayton cycle would be able to achieve efficiency more than at 30% [44].

Despite having the lowest Cp, carbon dioxide would be considered a working fluid. As a working gas, carbon dioxide was capable to achieve high performance with respect to high efficiency, the capability of heat transfer as well as a turbine to drive the compressor. Luyben[21] depicted carbon dioxide as the lowest capital cost among the pressure ratios span. Furthermore, the author also stated that a lower pressure ratio would also decrease capital costs. However, carbon dioxide as working gas would require the fastest mass flow rate hence it might require a pump to to flow the gas faster.

The 1T2C configuration would be the selected system regarding the efficiencies performance although its efficiency ratio was lower than the 2T2C configuration. However, the capability difference efficiency between these diagrams was not much. Furthermore, an expansion machine is expensive in terms of capital cost. Therefore, one turbine and lower pressure ratio were adequate with respect to efficiency

Table 4.10. Optimum pressure ratio vs efficiency ratio

| | He | H2 | CO2 | N2 | Air |
|---|---|---|---|---|---|
| 1T1C | η = 0.2-0.4<br>Pr = 2.7 | η = 0.2-0.4<br>Pr = 4.5 | η = 0.2-0.4<br>Pr = 6.5 | η = 0.2-0.4<br>Pr = 4.5 | η = 0.2-0.4<br>Pr = 4.5 |
| 2T2C | η = 0.25-0.45<br>Pr = 5.2 | η = 0.25-0.45<br>Pr = 10 | η = 0.25-0.45<br>Pr = 18 | η = 0.25-0.45<br>Pr = 12 | η = 0.24-0.45<br>Pr = 12 |
| 1T2C | η = 0.16-0.43<br>Pr = 3.5 | η = 0.21-0.43<br>Pr = 6.5 | η = 0.21-0.43<br>Pr = 9 | η = 0.2-0.43<br>Pr = 7 | η = 0.2-0.43<br>Pr = 7 |
| Open cycle | η = 0.007-0.33<br>Pr = 5.1 | η = 0.0016-0.33<br>Pr = 9.7 | η = 0.0035-0.33<br>Pr = 17 | η = 0.012-0.33<br>Pr = 9.7 | η = 0.012-0.33<br>Pr = 9.7 |
| CC | η = 0.16-0.34<br>Pr = 2.9 | | η = 0.15-0.29<br>Pr = 7 | | η = 0.21-0.34<br>Pr = 4.5 |

# Chapter 5. Double Pipe Heat Exchanger

Figure 5.1 Double pipe heat exchanger[40]

It had been decided that 1T2C with carbon dioxide as working gas would be a suitable configuration for this research. Temperature maximum at 1215 K and 989.15 K in hot side intermediate heat exchanger (IHX) as well as Helium as working gas were set. Carbon dioxide as working gas as well as temperature input and output for cold side IHX at 694.15 K and 1200 K were set. This chapter described heat exchanger sizing in this configuration. Only gas to gas heat exchangers would be described in this chapter due to the simplicity of phase change. Thus, this chapter determines the sizing intermediate heat exchanger and recuperator. A double pipe heat exchanger would be employed for both heat exchangers due to being simple and inexpensive. We used Iron Pipe Size (IPS) data to calculate the sizing heat exchanger[43]. The list of pipe size were tabulated in appendix C. Some conditions of heat exchanger sizing were assumed[43], such as,

1. The system is in a steady-state operation
2. The pipes were smooth and no fouling, thus, dirt factors were negligible
3. Kinetic and potential energy was negligible.
4. Fluid properties were constant
5. Heat loss to the surrounding was negligible.
6. The thermal resistance of conduction from pipe material was negligible since it was very small compared to thermal resistance from convection.
7. Constrain for Re and Pr were stated in the Nusselt number equation (3.26)

8. A pipe below 6 inches was unable to be applied. Reynolds numbers were calculated using these pipes and the result was over the constraints. Thus, combination pipes over 6 inches will be used since it was a single double pipe heat exchanger.
9. Constraint had been set up regarding capability Reynolds number.
10. All the flow was in a turbulent regime since the Re number was above two thousand.

the objectives of these analyses are to have the smallest area as well as the length of the heat exchanger and the smallest pressure drop Lowest pressure drop became the main consideration since it would affect the pressure requirement of the system. Furthermore, it would determine the power pump as well as its cost. The length of pipes, as well as the area of the heat exchanger, also would affect the capital cost of the plant, thus, the plant requires the smallest dimension. The maximum length of a horizontal pipe is 6 meters and it is extendable by applying a bend that is called a hairpin. The purpose of assessing both tubes was to determine a better performance for hot gas placed either in pipe or annulus.

## 5.1. Intermediate Heat Exchanger (IHX)

It had been known from the previous chapter that the temperature inlet and outlet in hot side IHX were 1200K and 980 K and the working gas was Helium. Carbon dioxide as working gas would be employed in cold side IHX and the temperature input and output were 695 K and 1200K. Hence, LMTD for IHX would be determined and it was 112 K. Both side mass flow rates have been known that were 8.199 kg/s for the Helium side and 19.861 kg/s for the carbon dioxide side. The property of the gases can be seen in table 5.1.

Table 5.1 Properties of the gases

| | |
|---|---|
| Cp Helium, Cp carbondioxide , (J/kg.K), | 5190, 846 |
| $\rho_{He}, \rho_{CO2}$ , (kg/m$^3$) | 0.1786, 1.98 |
| Thermal conductivity, $k_{He}, k_{CO2}$, (W/m.K) | 0.149, 0.01663 |
| Dynamic viscosity, $\mu_{He}, \mu_{CO2}$, (Pa.s) | 0.00002, 0.000025 |
| Mass flow rate, $\dot{m}_{He}, \dot{m}_{CO2}$ (kg/s) | 8.199, 19.861 |

Sizing IHX comprised of calculation of overall heat transfer coefficient as well as pressure drop. Data tubes or pipes were derived from IPS tube data in the appendix. Hot gas and cold gas were assessed both in the annulus as well as in the tube to determine the performance of heat transfer and pressure drop.

A combination pipe with a diameter of six required a large area and a longer pipe. Re number was high and beyond the constraint in this diameter. Therefore, diameter six was not suitable in the IHX of these schemes.

A significant difference between inside and outside diameter resulted in a major value of diameter equivalent, De. This condition required a larger area as well as a longer pipe. It is because the difference between inside tube diameter and outside tube diameter was twice.

Helium is hot gas in an intermediate heat exchanger. The heat from Helium will be transferred to carbon dioxide. There were some noticeable points when Carbon dioxide was in the pipe and Helium in the annulus. It was noticed that the Re number was higher due to the mass flow rate of carbon dioxide being high. Furthermore, Re numbers in the pipe were beyond the constraint. Although Re number CO2 in the tube were high, the pressure drop in the tube was lower compared to helium in the annulus as well as the dimension, area, and length of the tube. The pressure drop in the annulus was high due to the low mass flow rate of Helium. However, the constraint should be committed.

It had been investigated that the Re number on both sides performed adequately when Helium was in the tube and carbon dioxide in the annulus. Most of them were similar and under constraint.

Table 5.2 result calculation sizing IHX

| IPS OD/ID inch | Gas | | Annulus | | | pipe | | | U | A | L |
|---|---|---|---|---|---|---|---|---|---|---|---|
| | Annulus | Pipe | Re | h1 | ΔP | Re | h2 | ΔP | | | |
| Inch | | | | W/(m.K) | Pa | | W/(m.K) | Pa | W/(m.K) | $m^2$ | m |
| 10 by 6 | He | CO2 | 2E+06 | 1180.083 | 707656 | 7E+06 | 777.5787 | 113112 | 444.0131 | 170.9409 | 30 |
| | CO2 | He | 3E+06 | 3344.339 | 222639 | 4E+06 | 274.3763 | 392138 | 233.636 | 324.8644 | 57 |
| 10 by 8 | He | CO2 | 7E+06 | 12096.34 | 1.3E+07 | 5E+06 | 474.3912 | 41618 | 423.5979 | 179.1794 | 24 |
| | CO2 | He | 3E+06 | 2040.34 | 12034.3 | 1E+07 | 2812.471 | 7E+06 | 1143.688 | 66.36426 | 9 |
| 12 by 6 | He | CO2 | 1E+06 | 646.6745 | 436262 | 7E+06 | 777.5787 | 148217 | 338.8497 | 223.9932 | 39 |
| | CO2 | He | 3E+06 | 3344.339 | 303662 | 3E+06 | 150.3557 | 244628 | 132.2051 | 574.1082 | 101 |
| 12 by 8 | He | CO2 | 3E+06 | 1999.725 | 1187909 | 5E+06 | 474.3912 | 48977 | 359.9545 | 210.86 | 28 |
| | CO2 | He | 3E+06 | 2040.34 | 89832.3 | 5E+06 | 464.9479 | 648733 | 355.3101 | 213.6163 | 29 |
| 14 by6 | He | CO2 | 9E+05 | 304.5507 | 281763 | 7E+06 | 777.5787 | 235463 | 213.2963 | 355.8431 | 63 |
| | CO2 | He | 3E+06 | 3344.339 | 506614 | 2E+06 | 70.80984 | 160861 | 63.59179 | 1193.551 | 210 |

| | | | | | | | | | | | |
|---|---|---|---|---|---|---|---|---|---|---|---|
| 14 by 8 | He | CO2 | 1E+06 | 732.5401 | 413580 | 5E+06 | 474.3912 | 64227 | 274.486 | 276.5169 | 37 |
| | CO2 | He | 3E+06 | 2040.34 | 126335 | 3E+06 | 170.3199 | 229402 | 146.3019 | 518.7905 | 70 |
| 14 by 10 | He | CO2 | 3E+06 | 2291.477 | 1468264 | 4E+06 | 314.9763 | 28429 | 260.2444 | 291.649 | 32 |
| | CO2 | He | 2E+06 | 1354.702 | 506060 | 5E+06 | 532.7821 | 27204 | 363.3915 | 208.8657 | 23 |
| 16 by 6 | He | CO2 | 6E+05 | 167.393 | 224239 | 7E+06 | 777.5787 | 370586 | 135.5242 | 560.0475 | 98 |
| | CO2 | He | 3E+06 | 3344.339 | 828183 | 1E+06 | 38.91987 | 130202 | 35.25444 | 2152.921 | 378 |
| 16 by 8 | He | CO2 | 1E+06 | 355.9006 | 234818 | 5E+06 | 474.3912 | 89695 | 196.5473 | 386.1666 | 52 |
| | CO2 | He | 3E+06 | 2040.34 | 185284 | 2E+06 | 82.74901 | 132192 | 73.8008 | 1028.444 | 139 |
| 16 by 10 | He | CO2 | 2E+06 | 840.5096 | 447755 | 4E+06 | 314.9763 | 34002 | 217.5854 | 348.8287 | 38 |
| | CO2 | He | 2E+06 | 1354.702 | 64389.7 | 3E+06 | 195.4235 | 18693 | 160.5635 | 472.7102 | 51 |
| 16 by 12 | He | CO2 | 3E+06 | 2378.953 | 1647694 | 3E+06 | 224.6324 | 18693 | 195.4999 | 388.2356 | 35 |
| | CO2 | He | 2E+06 | 966.1363 | 456046 | 5E+06 | 553.1208 | 17326 | 339.943 | 223.2728 | 20 |

Although some configurations were able to achieve the Reynolds number constrain in table 5.2, those configurations were not able to accommodate a new Reynolds number constraint for pressure drop calculation. The Reynolds number values in the table were derived from equation (3.26) and equation (3.26) for overall heat transfer coefficient calculation. A new Reynolds number should be determined by using equations (3.25) and (3.27). By using equations (3-27), (3-25), and equations (3-30), pressure drops were calculated. The resulted pressure drop values can be seen in table 5.2. The last consideration is the lowest pressure drop and shortest pipe.

OD/ID: 14/8 and OD/ID: 16/10 size had a decent performance. Both had similar capabilities. Regarding lower diameter, OD/ID: 14/8 would be employed as pipes in IHX This configuration was able to achieve an adequate pressure drop and length. The length of the tube is about thirty-seven meters; thus, it will be approximately seven double pipes which are connected in series by using a hairpin (bend connection). The pressure drops were 413580 Pa for the hot side and 64227 for the cold side.

## 5.2. Recuperator

Carbon dioxide was the working gas in the recuperator. The physical properties of carbon dioxide were assumed constant. From the previous chapter, the temperature outlet turbine would become the inlet temperature hot side for the recuperator while the temperature outlet compressor would become the inlet temperature cold side recuperator. We retrieved temperatures data from the previous chapter at a temperature maximum of 1T2C 1200K, as follows,

Temperature outlet turbine = temperature inlet recuperator hot side = $T_{Hot\_in}$= 732.4K

Temperature input precooler = temperature outlet recuperator hot side = $T_{Hot\_out}$= 525.67K

Temperarture outlet compressor = temperature outlet recuperator cold side = $T_{cold\_in}$= 413.375K

Temperature inlet IHX = temperature outlet recuperator cold side = $T_{cold\_out}$= 694.122K

Mass flow rate were constant and the same in both side recuperator = 19.861 kg/s

physical properties of carbon dioxide can be referred from table 5.1

| IPS | Gas | | Hot side | | | Cold side | | | U | A | L |
|---|---|---|---|---|---|---|---|---|---|---|---|
| OD/ID | Annulus | Pipe | Re | h1 | ΔP | Re | h2 | ΔP | | | |
| inch | | | | W/(m.K) | Pa | | W/(m.K) | Pa | W/(m.K) | $m^2$ | m |
| 12 by 8 | CO2 | CO2 | 5E+06 | 453.9024 | 4E+06 | 5E+06 | 474.3912 | 381079 | 223.1557 | 147.9916 | 19.977 |
| | CO2 | CO2 | 5E+06 | 463.1214 | 336309 | 5E+06 | 464.9479 | 5E+06 | 223.0356 | 148.0713 | 19.988 |
| 14 by 8 | CO2 | CO2 | 3E+06 | 166.2737 | 2E+06 | 5E+06 | 474.3912 | 705171 | 120.5947 | 273.8526 | 36.966 |
| | CO2 | CO2 | 5E+06 | 463.1214 | 665186 | 3E+06 | 170.3199 | 3E+06 | 117.5872 | 280.8569 | 37.912 |
| 14 by 10 | CO2 | CO2 | 5E+06 | 520.1251 | 5E+06 | 4E+06 | 314.9763 | 190174 | 187.661 | 175.9831 | 19.062 |
| | CO2 | CO2 | 4E+06 | 307.4936 | 159395 | 5E+06 | 532.7821 | 5E+06 | 189.9053 | 173.9034 | 18.836 |
| 16 by 8 | CO2 | CO2 | 2E+06 | 80.78217 | 888256 | 5E+06 | 474.3912 | 709201 | 68.22665 | 484.0102 | 65.34 |
| | CO2 | CO2 | 5E+06 | 463.1214 | 700883 | 2E+06 | 82.74901 | 824731 | 65.70676 | 502.6145 | 67.846 |
| 16 by 10 | CO2 | CO2 | 3E+06 | 190.7809 | 2E+06 | 4E+06 | 314.9763 | 308623 | 115.6369 | 285.5937 | 30.934 |
| | CO2 | CO2 | 4E+06 | 307.4936 | 280319 | 3E+06 | 195.4235 | 2E+06 | 114.3904 | 288.7059 | 31.271 |
| 16 by 12 | CO2 | CO2 | 5E+06 | 540.1138 | 5E+06 | 3E+06 | 224.6324 | 115398 | 152.7604 | 216.1894 | 19.741 |
| | CO2 | CO2 | 3E+06 | 219.296 | 93932 | 5E+06 | 553.2572 | 6E+06 | 154.6504 | 213.5472 | 19.499 |

Although OD/ID:16/12 configurations were able to achieve a good performance, this configuration was not able to accommodate a new Reynolds number constraint for pressure drop calculation. The Reynolds number values in the table were derived from equation (3.25) and equation (3.26) for overall heat transfer coefficient calculation. A new Reynolds number should be determined by using equations (3.25) and (3.27).

By using equations (3-27), (3-25), and equations (3-30), pressure drops were calculated. The resulted pressure drop values can be seen in table 5.3.

OD/ID: 16/8 tube size would be employed as pipes in recuperator since this pair of the tube was able to accommodate Reynolds number constraint regarding turbulent flow. Only this configuration was able to achieve an adequate pressure drop. The length of the tube is about 70 meters, thus it will be approximately 10 double pipes which are connected in series by using hairpins (bend connection). The pressure was 700883 Pa for the hot side and 824731 Pa for the cold side

# Chapter 6. Conclusion

1. The 1T2C configuration with pressure ratio 9 was considered an options system and carbon dioxide would be a working fluid with the capability to achieve high performance concerning high efficiency, capability heat transfer in heat exchangers, as well as a turbine to drive. This configuration was able to achieve efficiency at 52%.
2. The calculation result depends on the characteristic of the working fluid, such as specific heat ratio (gamma) and specific heat at constant pressure Cp. The values of gamma affect the temperature output of turbomachinery. Since gamma is high, the temperature output will be decreased. Cp effect mass flow rate. Since Cp is high, the mass flow rate will be below.
3. Increasing the turbine inlet Temperature in a closed cycle might increase their efficiencies while increasing the pressure ratio might affect turbomachinery net energy. The assessment of the cycle is not only to determine the highest efficiency but also the capabilities of the heat exchanger to transfer heat as well as the capability turbine to drive the compressor.
4. Increasing only the turbine inlet temperature may increase their efficiencies, as can be seen in the curves for Pr9, TIT various-scheme calculation. Carbon dioxide as working gas reached the highest efficiency while Helium reached the lowest in recuperated cycle diagram. On the other hand, the opened cycle using Helium as working gas had the highest efficiency while CO2 as working had the lowest efficiency.
5. The efficiencies of the Ideal cycle in the recuperated diagram (closed cycle) depend on loopback energy (Qin) from the recuperator while the non-recuperated diagram (opened cycle) depends on pressure ratio and gamma ratio from the compressor.
6. Sizing heat exchangers should accommodate parameter constraints regarding flow regime for both calculations of overall heat transfer coefficient and pressure drop.
7. OD/ID: 14/8 would be employed as pipes in IHX. The length of the tube is about 37 meters, thus it will be approximately 7 double pipes which are connected in series by using hairpins (bend connection). The pressure drops were 413580 Pa for the hot side and 64227 for the cold side.
8. OD/ID: 16/8 tube size would be employed as pipes in the recuperator. The length of the tube is about 70 meters, thus it will be approximately 10 double pipes which are connected in series by using hairpins (bend connection). The pressure was 700883 Pa for the hot side and 824731 Pa for the cold side

# List of References

[1] UNO,2015, Framework Convention on Climate Change, Adoption of the Paris Agreement, 21st Conference of the Parties Tech. rep., United Nations (2015) Paris

[2] V. Knapp, D. Pevec, Promises and limitations of nuclear fission energy in combating climate change Energy Pol., 120 (Sep 2018), pp. 94-99]

[3] ] International Atomic Energy Agency, Advances in Small Modular Reactor Technology: High-Temperature Gas-cooled Reactor Small Modular Reactor. A supplement to IAEA Advanced Reactor Information System (ARIS) 2020 edition Vienna (2020).

[4] Presidential Regulation No. 22/2017: General Plans of National Energy. The Ministry of Law and Human Rights of Indonesia, 2017

[5] H. Brey, "Development history of the gas turbine modular high-temperature reactor," *Technical Committee meeting of Gas turbine power conversion systems for modular HTGRs,* p. 21, 12-18 November 2000

[6] Bahman Zohuri, "Nuclear energy for hydrogen generation through intermediate heat exchanger," Switzerland: Springer, 2016

[7] ] Xiang-wen Zhou, Ya-ping Tang, Zhen-ming Lu, Jie Zhang, Bing Liu, Nuclear graphite for high temperature gas-cooled reactors, NEW CARBON MATERIALS Volume 32, Issue 3, Jun. 2017, https://doi.org/10.1016/S1872-5805(17)60116-1

[8] M.D. Carelli, D.T. Ingersoll, Handbook of Small Modular Nuclear Reactor 2014

[9] Feher. EG, "Supercritical cycle heat engine". United State of America Patent US3237403 A, 1966

[10] V. Dostal, “A Supercritical Carbon Dioxide Cycle for Next Generation Nuclear Reactors,” PhD thesis, Massachusetts Institute of Technology, 2004

[11] Zhang Z, Jiang Z, “Design of Indirect Gas Turbine Cycle for a Modular High-Temperature Gas-cooled Reactor”, in Gas turbine power conversion systems for modular HTGRs, Report of technical committee meeting, International Atomic Energy Agency (IAEA), Vienna-Austria, 2001

[12] A I. Kiryushin, N.G. Kodochigov, N.G. Kouzavkov, N.N. Ponomarev-Stepno, E.S Gloushkov, V.N Grebennik, “Project of the GT-MHR High-Temperature Helium Reactor with Gas Turbine”. Nuclear Engineering Design Journal 1997;173:119–29, Elsevier 1997. http://dx.doi.org/10.1016/S0029-5493(97)00099-X

[13] A. Koster, H.D. Matzner, and D.R. Nichols. “PBMR design for the future”, Nuclear Engineering Design Journal 2003;222:231–45, Elsevier 2003. http://dx.doi.org/10.1016/S0029-5493(03)00029-3

[14] C. Wang, Design, analysis and optimization of the power conversion system for the modular Pebble Bed Reactor System, USA: Massachusetts Institute of Technology, 2003

[15] International Atomic Energy Agency (IAEA), "Gas-Cooled Reactor Design and Safety," International Atomic Energy Agency (IAEA), Vienna-Austria, 1990

[16] Y. Xu, S. Hu, F. Li, S.Yu. "High-Temperature Reactor Development in China". Progress Nuclear Energy 2005;47:260–70, Elsevier 2005. http://dx.doi.org/10.1016/j.pnucene.2005.05.026

[17] Olumide Olumayegun, Meihong Wang, Greg Kesall, "Closed-cycle gas turbine for power generation: A state-of-the-art review," Fuel, vol. 180, no. 2016, pp. 694-717, 15 September 2016.

[18] Tim Abram, Sue Ion, "Generation-IV nuclear power: A review of the state of the science," Energy Policy, vol. 36, no. 2008, pp. 4223-4330, 2008

[19] Tocio D, et al, "Helium leak and chemical impurities control technology in HTTR", Journal of Nuclear Science and Technology, 2014, https://doi.org/10.1080/00223131.2014.921126

[20] K Kunitomi S.Katanishi, S. Takada, T. Takizuka, X Yan, "Japan's future HTR—the GTHTR300," in Nuclear Engineering and Design journal 2004, Nuclear Engineering and Design 233 (2004) 309–327, Elsevier 2004. http://doi:10.1016/j.nucengdes.2004.08.026

[21] Y.S.H. Najjar, M.S. Zaamout. "Comparative performance of closed-cycle gas turbine engine with heat recovery using different gases". Heat Recovery System and CHP P Vol. 12, No. 6, pp. 489--495, 1992, Pergamon Press Ltd, Great Britain 1992.

[22] R.A Moore, M.E Kantor, "HTGR experience, programs, and future applications," Nuclear Engineering and Design, vol. 72, no. 2, pp. 153-174, 2 September 1982.

[23] J. Tarlecki, N. Lior, N. Zhang. "Analyses of Thermal Cycle and Working Fluids for Power Generation in Space". In Energy Conversion and Management Journal, Energy Conversion and Management 48 (2007) 2864-2878, Elsevier 2007. http://doi:10.1016/j.enconman.2007.06.039

[24] Cengel Y and Boles, Thermodynamic an Engineering approach,8th edition. M, Mc-Grawhill New York 2015

[25] G.D. Perez-Pichel, J.I. Linares, L.E. Herranz, B.Y. Moratilla, "Potential application of Rankine and He-Brayton cycles to sodium fast reactors," in Nuclear Engineering and Design journal 2011, Nuclear Engineering and Design 241 (2011) 2643-2652, Elsevier 2011. http://doi:10.1016/j.nucengdes.2011.04.038

[26] Y.S.H. Najjar, M.S. Zaamout. "Comparative performance of closed-cycle gas turbine engine with heat recovery using different gases". Heat Recovery System and CHP P Vol. 12, No. 6, pp. 489--495, 1992, Pergamon Press Ltd, Great Britain 1992.

[27] M.S El-Genk, J.M Tournier, “On the use of noble gases and binary mixtures as reactor coolants and CBC working fluids,” in Energy Conversion and Management journal 2008, Energy Conversion and Management 49 (2008) 1882–1891, Elsevier 2008. http://doi:10.1016/j.enconman.2007.08.01.

[28] Hee Cheon No, Ji Hwan Kim, Hyeu Min Kim, "A review of helium gas turbine technology for high-temperature gas-cooled reactors," Nuclear Engineering and Technology, vol. 39, pp. 21-30, 2007

[29] Ahn Y, et al, “Review of supercritical CO2 power cycle technology and current status of research and development”, Journal of Nuclear Engineering Technology vol. 47, 2015.

[30] N. Alpy, et.al “Gas Cycle testing opportunity with ASTRID, the French SFR prototype”, Supercritical CO2 Power Cycle Symposium, May 24-25, 2011, Boulder, Colorado.

[31] Olumayugen O, Wang M, Kelsali G. Thermodynamic analysis and preliminary design of closed Brayton cycle using nitrogen as working fluid and coupled to small modular Sodium-cooled fast reactor (SM-SFR), J Applied Energy 191(2017) 436-463 http://dx.doi:10.1016/j.apenergy.2017.01.009.

[32] S. A. Wright, R. Fuller, R.J Lipinski, K. Nichols, and N. Brown, “Operational result of a Brayton cycle test-loop,” in Space Technology and Application International Forum-STAIF 2005, AIP Conference Proceedings 746, 699 (2005, edited by M. S. El-Genk et al. (AIP Publishing, Albuquerque, New Mexico (USA), 2005), pp. 699–710); http://doi:10.1063/1.1867189620.

[33] Peterson P, Multiple-reheat Brayton Cycles for nuclear power conversion with molten coolants, Nuclear Technology, 144:3, 279-288, 2017 DOI: 10.13182/NT144-279. https://doi.org/10.13182/NT144-279.

[34] F. P. Incorpera, D. P. DeWitt, T. L. Bergman, A. S. Lavine, “Fundamentals of Heat and Mass Transfer-7 th Edition”, John Wiley, New, 2011, New York.

[35] . K. Shah, D. P. Sekulic, Fundamental of Heat Exchanger Design, John Wiley, 2003, New York

[36] Han Seo, Jae Eun Cha, Jaemin Kim, Injin Sah and Yong-Wan Kim,. “Design and Performance Analysis of a Supercritical Carbon Dioxide Heat Exchanger”, Applied Science 2020-10(13)-4545, MDPL publisher, Swiss 2020. https://doi.org/10.3390/app10134545.

[37] Kakaç, S., H. Liu, A. Pramuanjaroenkij, Heat Exchangers: Selection, Rating, and Thermal Design, 3rd Edition, CRC Press, 2012

[38] https://www.enggcyclopedia.com/2012/06/typical-datasheet-shell-tube-heat-exchanger/

[39] Mohamad Omidi, Mousa Farhadi, Mohamad Jafari,. “A comprehensive review on double pipe heat exchangers”, Applied Thermal Engineering 110(2017) 1075-7090., Elsevier 2016. http://dx.doi.org/10.1016/j.applthermaleng.2016.09.027.

[40] X.Y.Xu, Q.W.Wang, L.Li, Y.T.Chen, T.Ma., “Study on thermal resistance distribution and local heat transfer enhancement method for SCO2–water heat exchange process near pseudo-critical temperature”., International Journal of Heat and Mass Transfer Volume 8 Pages 179-188, Elsevier 2015. https://doi.org/10.1016/j.ijheatmasstransfer.2014.11.029.

[41] Moran MJ et al, Principles engineering thermodynamics SI Version, John Wiley & sons, Singapore 2015.

[42] Cengel Y, Heat Transfer a practical approach,2nd edition. M, Mc-Grawhill New York 2015. www.mhhe.com/cengel/

[43] D.Q Kern, Process Heat Transfer: International student edition, Mc-Grawhill International Book Company, Japan 1983.

[44] P.P. Walsh and P. Fletcher, Gas Turbine Performance: second edition, Blackwell Science Ltd, United Kingdom 2004

**Equations**

There two conditions, ideal values calcukation and actual values calculations. Ideal values are the value without considering tolerance in the machine, hence, the turbomachinery is 100% without loss. However, there are always losses tolerance in the turbomachinery. Thus, actual values consider some tolerances such as, the turomachinery efficiency and the heat exchangers effectiveness.

A. **Ideal values calcukation**

**1.** Mass flowrate core

$$\dot{m}_{core} = \frac{Q_{th\_core}}{Cp_{He}(T_{core\_o} - T_{core\_i})} \quad \#\frac{kg}{s} \quad \text{.....(1)}$$

**2. High Pressure Compressor calculation**

# Temperature output HPC

$$T_{HPC\_i} = T_{LPC\_i}$$

$$T_{HPC\_o} = \left((\pi_{HPC})^{\frac{\gamma_{N2}-1}{\gamma_{N2}}}\right) * T_{HPC_i} \quad \#K \quad \text{..... (2)}$$

**3. Pressure recuperator cold side out**

$$p_{rec\_cold\_o} = \left(p_{HPC\_O} - \left(p_{HPC\_o} * p_{drop\_recu}\right)\right) \quad \#Bar \quad \text{..... (3)}$$

**4. Turbine calculation**

$$p_{Turb\_i} = \left(p_{rec\_cold\_o} - \left(p_{rec\_cold\_o} * p_{drop\_IHX}\right)\right) \quad \#Bar \quad \text{..... (4)}$$

$$p_{turb\_o} = \frac{p_{Turb\_i}}{\pi_{Turb}} \quad \#bar \quad \text{.....(5)}$$

$$T_{turb\_o} = \left(\left(\frac{1}{\pi_{Turb}}\right)^{\frac{\gamma_{N2}-1}{\gamma_{N2}}}\right) * T_{Turb\_i} \quad \#K \quad \text{..... (6)}$$

**5. Recuperator calculation**

$$p_{rec\_cold\_i} = p_{HPC\_o}$$
$$T_{rec\_cold\_i} = T_{HPC\_o}$$
$$p_{rec\_hot\_i} = p_{turb\_o}$$
$$T_{rec\_hot\_i} = T_{turb\_o}$$

$$T_{rec\_cold\_o} = T_{HPC\_o} + \left(\varepsilon_{recu}\left(T_{rec\_hot\_i} - T_{HPC\_o}\right)\right) \quad \text{..... (7)}$$

$$p_{rec\_hot\_o} = \left(p_{rec\_hot\_i} - \left(p_{rec\_hot\_i} * p_{drop\_recu}\right)\right) \quad \text{..... (8)}$$

$$T_{rec\_hot\_o} = T_{HPC\_o} + TTD \quad \text{..... (9)}$$

**6. Precooler calculation**

$$p_{precooler\_i} = p_{rec\_hot\_o} \quad \#Bar$$
$$T_{precooler\_i} = T_{rec\_hot\_o} \quad \#K$$
$$T_{precooler\_o} = T_{HPC\_i}$$

$$p_{precooler\_o} = \left(p_{precooler\_i} - \left(p_{precooler\_i} * p_{drop\_precooler}\right)\right) \quad \#Bar \quad \text{.....(10)}$$

**7. Low Pressure Compressor calculation**

$$p_{LPC\_i} = p_{precooler\_o} \ \#Bar$$
$$T_{LPC\_i} = T_{precooler\_o}$$

$p_{LPC\_o} = \pi_{LPC} * p_{LPC\_i} \quad \#bar$ ..... (11)

$T_{LPC\_o} = \left((\pi_{LPC})^{\frac{\gamma_{N2}-1}{\gamma_{N2}}}\right) * T_{LPC_i} \quad \#K$ ..... (12)

**8. Intercooler calculation**

$$T_{intercooler\_i} = T_{LPC\_o}$$
$$p_{intercooler\_i} = p_{LPC\_o} \ \#Bar$$
$$T_{intercooler\_o} = T_{HPC\_i} \ \#K$$

$p_{intercooler\_o} = \left(p_{intercooler\_i} - \left(p_{intercooler\_i} * p_{drop\_precooler}\right)\right) \ \#Bar$ .....(12)

$$p_{HPC\_i} = p_{intercooler\_o} \ \#Bar$$

**9. Pump Calculation**

$T_{pump\_i} = T_{rec\_cold\_o} + TTD\_IHX$ ..... (13)

$p_{pump\_o} = \left(p_{core} * \left(1 - p_{loss\_pump}\right)\right) \ \#Bar$ ..... (14)

**10. Duty heat exchangers and mass flowrates**

$Q_{IHX} = \dot{m}_{core} * Cp_{He} * \left(T_{core\_o} - T_{pump\_i}\right)$ ..... (15)

$\dot{m}_2 = \frac{Q_{IHX}}{Cp_{N2}*\left(T_{rec\_cold\_o} - T_{turb\_i}\right)}$ ..... (16)

$Q_{precooler} = \dot{m}_2 * Cp_{N2}\left(T_{precooler\_i} - T_{precooler\_o}\right)$ ..... (17)

$\dot{m}_{precooler\_water} = \frac{Q_{precooler}}{Cp_{water}*\left(T_{water\_precooler\_o} - T_{watter\ precooler\ i}\right)}$ ..... (18)

$Q_{intercooler} = \dot{m}_2 * Cp_{N2}\left(T_{intercooler\_i} - T_{intercooler\_o}\right)$ ..... (19)

$\dot{m}_{intercooler\_water} = \frac{Q_{intercooler}}{Cp_{water}*\left(T_{water\_intercooler\_o} - T_{watter\ intercooler\ i}\right)}$ ..... (20)

**11. Works and efficiency**

$W_{HPC} = \dot{m}_2 * Cp_{N2}\left(T_{HPC\_o} - T_{HPC\_i}\right)$ ..... (21)

$W_{LPC} = \dot{m}_2 * Cp_{N2}\left(T_{LPC\_o} - T_{LPC\_i}\right)$ ..... (22)

$W_{Turb} = \dot{m}_2 * Cp_{N2}\left(T_{Turb\_i} - T_{Turb\_o}\right)$ ..... (23)

$W_{pump} = \dot{m}_{core} * Cp_{He}\left(T_{core\_i} - T_{pump\_i}\right)$ ..... (24)

$W_{elec} = \left(W_{turb} - \left(W_{HPC} + W_{LPC}\right)\right) - W_{pump}$ ..... (25)

$\eta_{cycle} = \frac{W_{elec}}{Q_{th\_core}}$ ..... (26)

B. **Actual values**

Calculations have been done for the actual cycle based on fixed pressure ratio (Pr)-various temperature inlet turbine (T6) as well as fixed temperature inlet turbine-various pressure ratio. For multi-stage adiabatic equipment, the temperatures were the same value for its inputs (T1=T3 for the compressor) as well as its outputs (T2a=T4a for the compressor).

**Actual values for compressors and turbine**

1. Mass flowrate core

$$\dot{m}_{core} = \frac{Q_{th\_core}}{Cp_{He}(T_{core\_o} - T_{core\_i})} \quad \#\frac{kg}{s} \quad \text{.....(27)}$$

2. **High Pressure Compressor calculation**

# Temperatures and enthalpies

$$T_{HPC\_i} = T_{LPC\_i}$$

$$T_{HPC\_o} = \left((\pi_{HPC})^{\frac{\gamma_{N2}-1}{\gamma_{N2}}}\right) * T_{HPC_i} \quad \#K \quad \text{..... (28)}$$

$$h_{HPC\_i} = Cp_{N2} * T_{HPC\_i} \quad \text{..... (29)}$$

$$h_{HPC\_o} = Cp_{N2} * T_{HPC\_o} \quad \text{..... (30)}$$

From thermodynamic textbook p.512, work compressor is calculated using enthalpy in equation (31) .

$$W_{HPC\_s} = h_{HPC\_o} - h_{HPC\_i} \quad \text{.....(31)}$$

Assume $\eta_{HPC} = 0.88$, we will obtain enthalpy HPC output actual and Temperature HPC output actual using equation (32) and (33)

$$\boldsymbol{\eta_{HPC}} = \frac{W_{HPC\_s}}{W_{HPC\_actual}} \cong \frac{h_{HPC\_o} - h_{HPC\_i}}{h_{HPC\_o\_actual} - h_{HPC\_i}}$$

$$h_{HPC\_o\_actual} = \frac{W_{HPC\_s}}{\eta_{HPC}} + h_{HPC\_i} \quad \text{..... (32)}$$

$$T_{HPC\_o\_actual} = \frac{h_{HPC\_o\_actual}}{\boldsymbol{Cp_{N2}}} \quad \text{..... (33)}$$

3. **Pressure recuperator cold side out**

$$p_{rec\_cold\_o} = \left(p_{HPC\_O} - \left(p_{HPC\_o} * p_{drop\_recu}\right)\right) \quad \#Bar \quad \text{..... (34)}$$

4. **Turbine calculation**

$$p_{Turb\_i} = \left(p_{rec\_cold\_o} - \left(p_{rec\_cold\_o} * p_{drop\_IHX}\right)\right) \quad \#Bar \quad \text{..... (35)}$$

$$p_{turb\_o} = \frac{p_{Turb\_i}}{\pi_{Turb}} \quad \#bar \quad \text{.....(36)}$$

$$T_{turb\_o} = \left(\left(\frac{1}{\pi_{Turb}}\right)^{\frac{\gamma_{N2}-1}{\gamma_{N2}}}\right) * T_{Turb\_i} \quad \#K \quad \text{..... (37)}$$

$$h_{turb\_i} = Cp_{N2} * T_{turb\_i} \quad \text{..... (38)}$$

$$h_{turb\_o} = Cp_{N2} * T_{turb\_o} \quad \text{..... (39)}$$

Similar with HPC, work of the turbine is calculated using enthalpy in equation (40) .

$$W_{turb\_s} = h_{turb\_i} - h_{turb\_o} \quad \text{.....(40)}$$

Assume $\eta_{turb} = 0.93$, we will obtain enthalpy turbine output actual and temperature turbine output actual using equation (41) and (42)

$$\boldsymbol{\eta_{turb}} = \frac{W_{turb\_s}}{W_{turb\_actual}} \cong \frac{h_{turb\_i} - h_{turb\_o}}{h_{turb\_i} - h_{turb\_o\_actual}}$$

$h_{turb\_o\_actual} = h_{turb\_i} - \frac{W_{turb\_s}}{\eta_{turb}}$ ..... (41)

$T_{turb\_o\_actual} = \frac{h_{turb\_o\_actual}}{\boldsymbol{cp_{N2}}}$ ..... (42)

**5. Recuperator calculation**

$$p_{rec\_cold\_i} = p_{HPC\_o}$$

$$T_{rec\_cold\_i} = T_{HPC\_o\_actual}$$

$$p_{rec\_hot\_i} = p_{turb\_o}$$

$$T_{rec\_hot\_i} = T_{turb\_o\_actual}$$

$T_{rec\_cold\_o} = T_{HPC\_o\_actual} + \left(\varepsilon_{recu}\left(T_{rec\_hot\_i} - T_{HPC\_o\_actual}\right)\right)$ ..... (43)

$p_{rec\_hot\_o} = \left(p_{rec\_hot\_i} - \left(p_{rec\_hot\_i} * p_{drop\_recu}\right)\right)$ ..... (44)

$T_{rec\_hot\_o} = T_{HPC\_o\_actual} + TTD$ ..... (45)

**6. Precooler calculation**

$$p_{precooler\_i} = p_{rec\_hot\_o} \ \#Bar$$

$$T_{precooler\_i} = T_{rec\_hot\_o} \ \#K$$

$$T_{precooler\_o} = T_{HPC\_i}$$

$p_{precooler\_o} = \left(p_{precooler\_i} - \left(p_{precooler\_i} * p_{drop\_precooler}\right)\right) \ \#Bar$ .....(46)

**7. Low Pressure Compressor calculation**

$$p_{LPC\_i} = p_{precooler\_o} \ \#Bar$$

$$T_{LPC\_i} = T_{precooler\_o}$$

$p_{LPC\_o} = \pi_{LPC} * p_{LPC\_i} \quad \#bar$ ..... (47)

$T_{LPC\_o} = \left(\left(\pi_{LPC}\right)^{\frac{\gamma_{N2}-1}{\gamma_{N2}}}\right) * T_{LPC_i} \quad \#K$ ..... (48)

$h_{LPC\_i} = Cp_{N2} * T_{LPC\_i}$ ..... (49)

$h_{LPC\_o} = Cp_{N2} * T_{LPC\_o}$ ..... (50)

From thermodynamic textbook p.512, work of the low pressure compressor is calculated using enthalpy in equation (51) .

$$W_{LPC\_s} = h_{LPC\_o} - h_{LPC\_i} \quad \text{.....(51)}$$

Assume $\eta_{HPC} = 0.89$, we will obtain enthalpy LPC output actual and Temperature LPC output actual using equation (52) and (53)

$$\boldsymbol{\eta_{LPC}} = \frac{W_{LPC\_s}}{W_{LPC\_actual}} \cong \frac{h_{LPC\_o} - h_{LPC\_i}}{h_{LPC\_o\_actual} - h_{LPC\_i}}$$

$h_{LPC\_o\_actual} = \frac{W_{LPC\_s}}{\eta_{LPC}} + h_{LPC\_i}$ ..... (52)

$T_{LPC\_o\_actual} = \frac{h_{LPC\_o\_actual}}{\boldsymbol{Cp_{N2}}}$ ..... (53)

**8. Intercooler calculation**

$$T_{intercooler\_i} = T_{LPC\_o\_actual}$$

$$p_{intercooler\_i} = p_{LPC\_o} \ \#Bar$$

$$T_{intercooler\_o} = T_{HPC\_i} \ \#K$$

$$p_{intercooler\_o} = \left(p_{intercooler\_i} - \left(p_{intercooler\_i} * p_{drop\_precooler}\right)\right) \ \#Bar \quad \text{.....(54)}$$

$$p_{HPC\_i} = p_{intercooler\_o} \ \#Bar$$

**9. Pump Calculation**

$T_{pump\_i} = T_{rec\_cold\_o} + TTD\_IHX$ ..... (55)

$p_{pump\_o} = \left(p_{core} * \left(1 - p_{loss\_pump}\right)\right) \ \#Bar$ ..... (56)

$h_{pump\_i} = Cp_{He} * T_{pump\_i}$ ..... (57)

$h_{core\_i} = Cp_{He} * T_{core\_i}$ ..... (58)

Work of the pump is calculated using enthalpy in equation (59) .

$$W_{pump} = h_{core\_i} - h_{pump\_i} \quad \text{.....(59)}$$

**10. Duty heat exchangers and mass flowrates**

$Q_{IHX} = \dot{m}_{core} * Cp_{He} * \left(T_{core\_o} - T_{pump\_i}\right)$ ..... (60)

$\dot{m}_2 = \frac{Q_{IHX}}{Cp_{N2} * \left(T_{rec\_cold\_o} - T_{turb\_i}\right)}$ ..... (61)

$$Q_{precooler} = \dot{m}_2 * Cp_{N2}\left(T_{precooler\_i} - T_{precooler\_o}\right) \quad \text{(62)}$$

$$\dot{m}_{precooler\_water} = \frac{Q_{precooler}}{Cp_{water}*\left(T_{water\_precooler\_o} - T_{watter\ precooler\ i}\right)} \quad \text{(63)}$$

$$Q_{intercooler} = \dot{m}_2 * Cp_{N2}\left(T_{intercooler\_i} - T_{intercooler\_o}\right) \quad \text{(64)}$$

$$\dot{m}_{intercooler\_water} = \frac{Q_{intercooler}}{Cp_{water}*\left(T_{water\_intercooler\_o} - T_{watter\ intercooler\ i}\right)} \quad \text{(65)}$$

**11. Works and efficiency**

$$W_{elec} = \dot{m}_2 * \left(W_{turb} - (W_{HPC} + W_{LPC})\right) - \dot{m}_{core} * W_{pump} \quad \text{(66)}$$

$$\eta_{cycle} = \frac{W_{elec}}{Q_{th\_core}} \quad \text{(67)}$$

Flow chart in figure 3.1 shows a procedure simulation, appendix A describes equations for modelling, and appendix B depicts model of PCS Brayton cycle in software Matlab-Simulink. All the equations are put in Matlab - Simulink as a model of PCS. Input and output as well as run the model will be done in discrete simulation for each gas and its thermal property parameters. Figures in appendix B are examples modelling and simulation for Helium as working gas in the gas cycle. Since simulation have been run in discrete mode, the iteration results were collected and gathered in Microsoft Excel . The graph of the results were figured in Microsoft Excel.

Appendix B: Open cycle diagram Simulink-Model

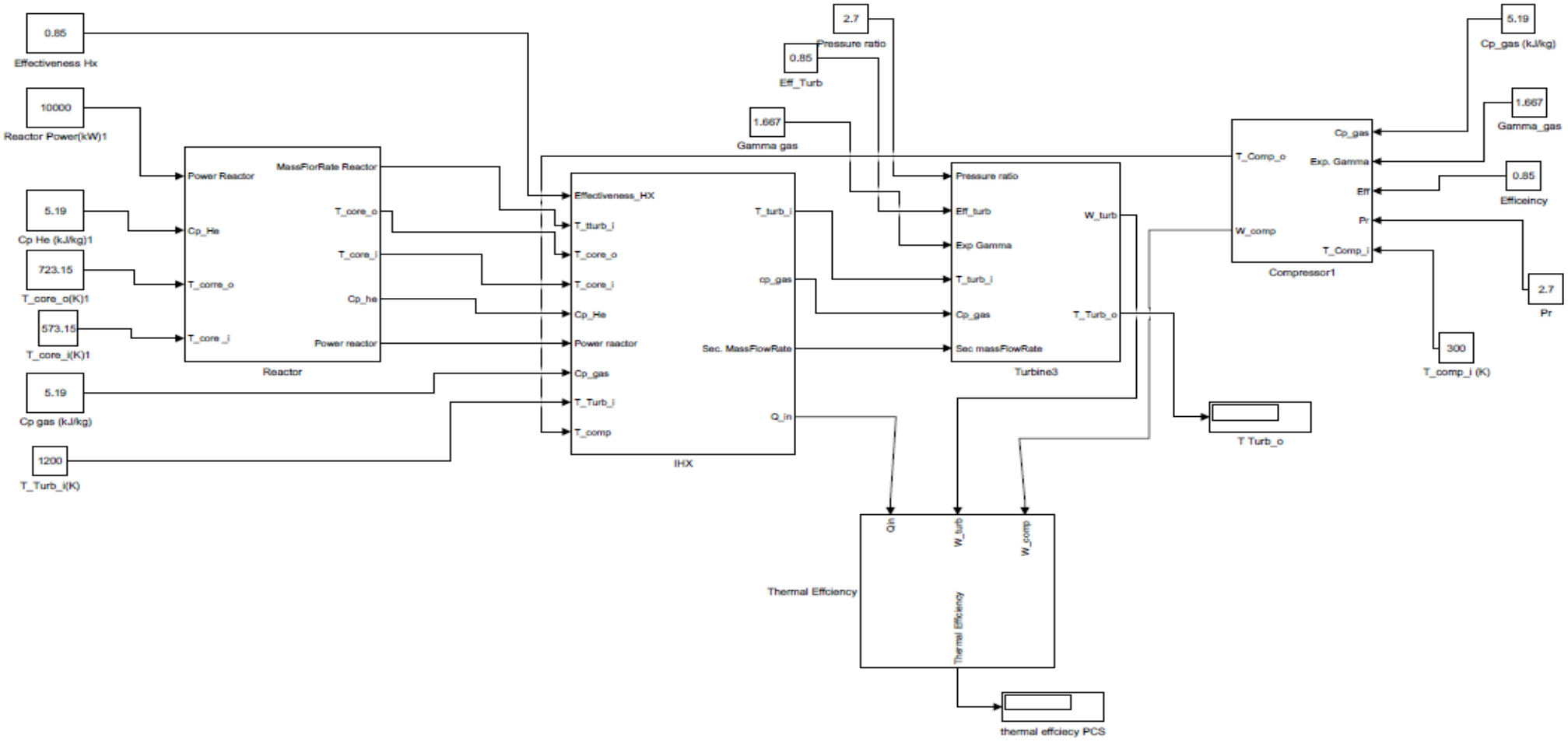

Appendix B: 1T1C diagram Simulink-Model

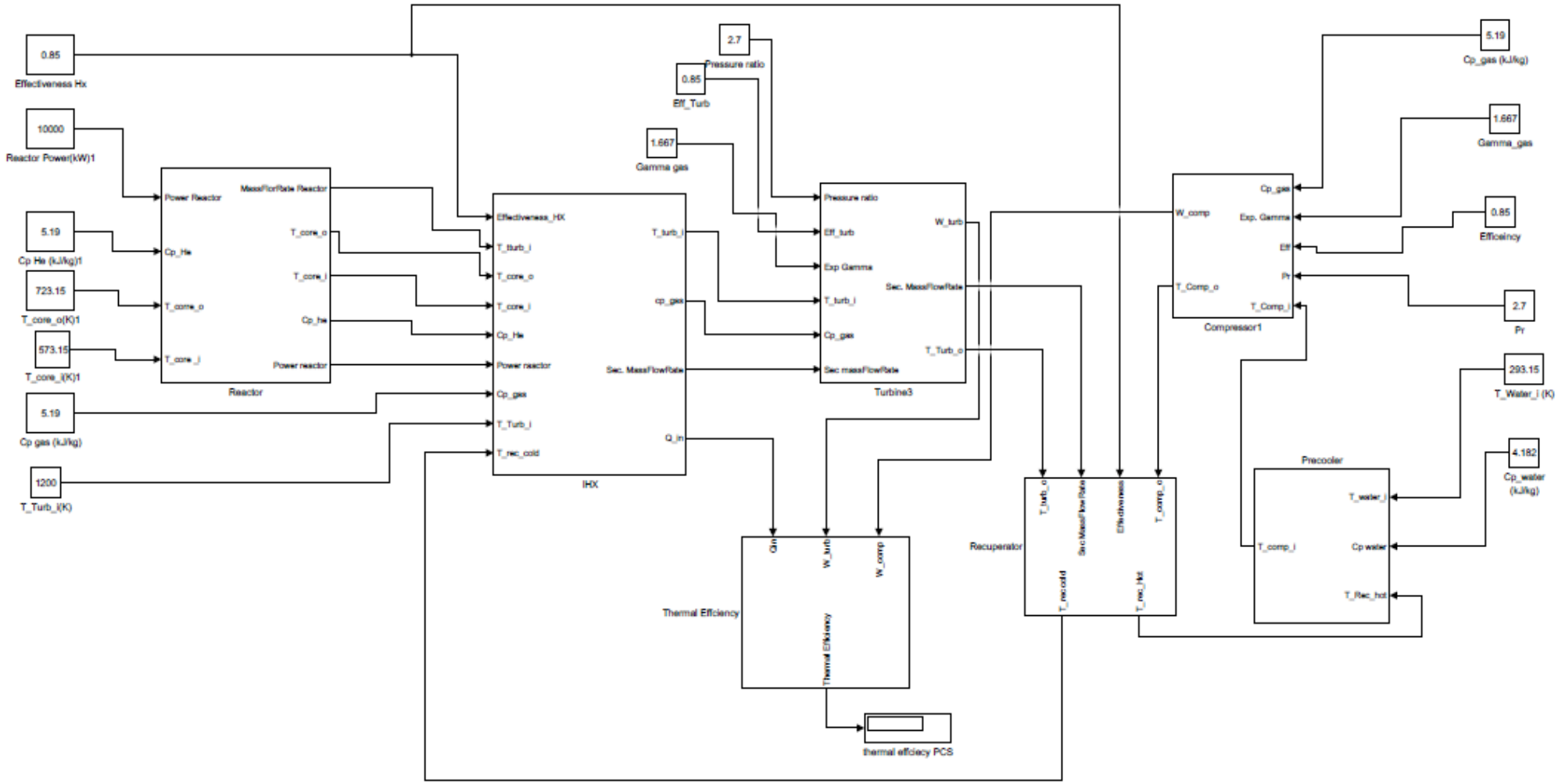

Appendix B: 1T2C diagram Simulink-Model

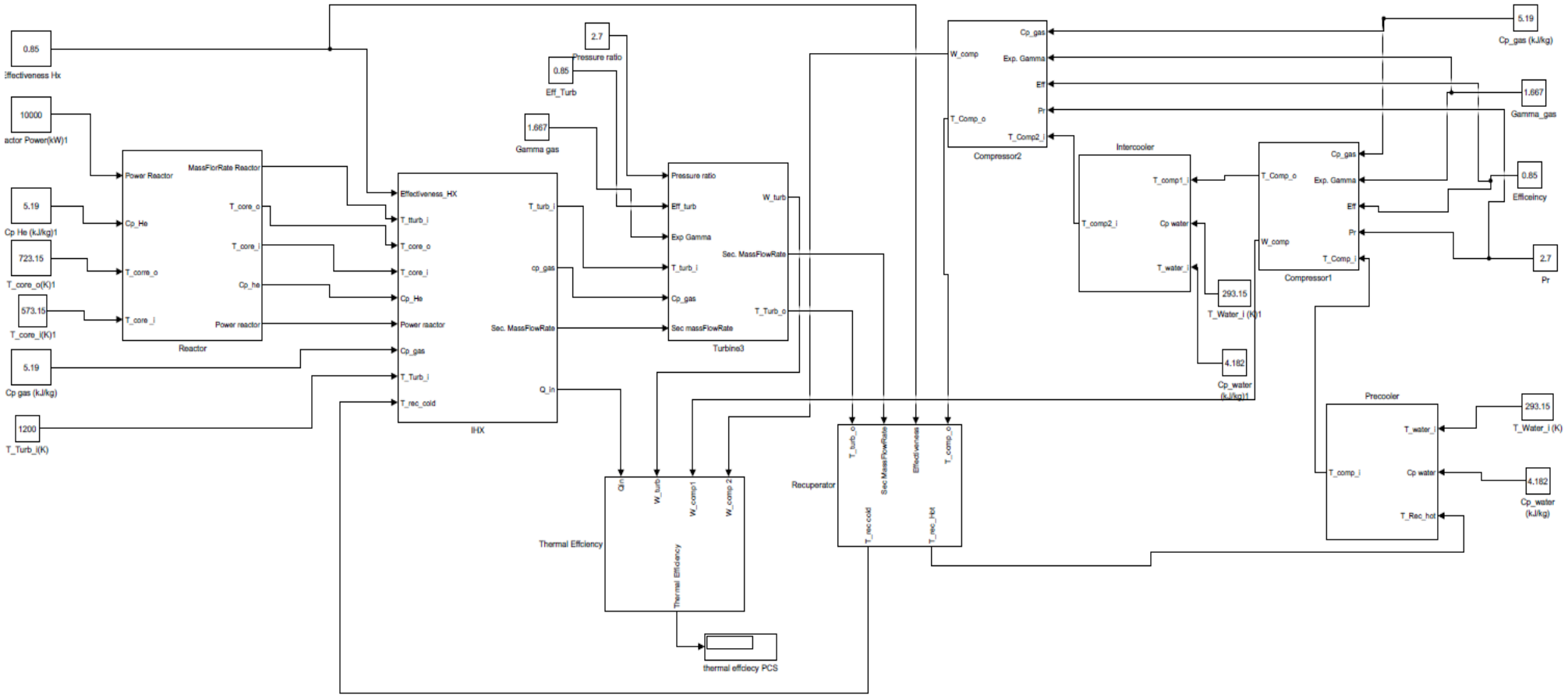

Appendix B: 2T2C diagram Simulink-Model

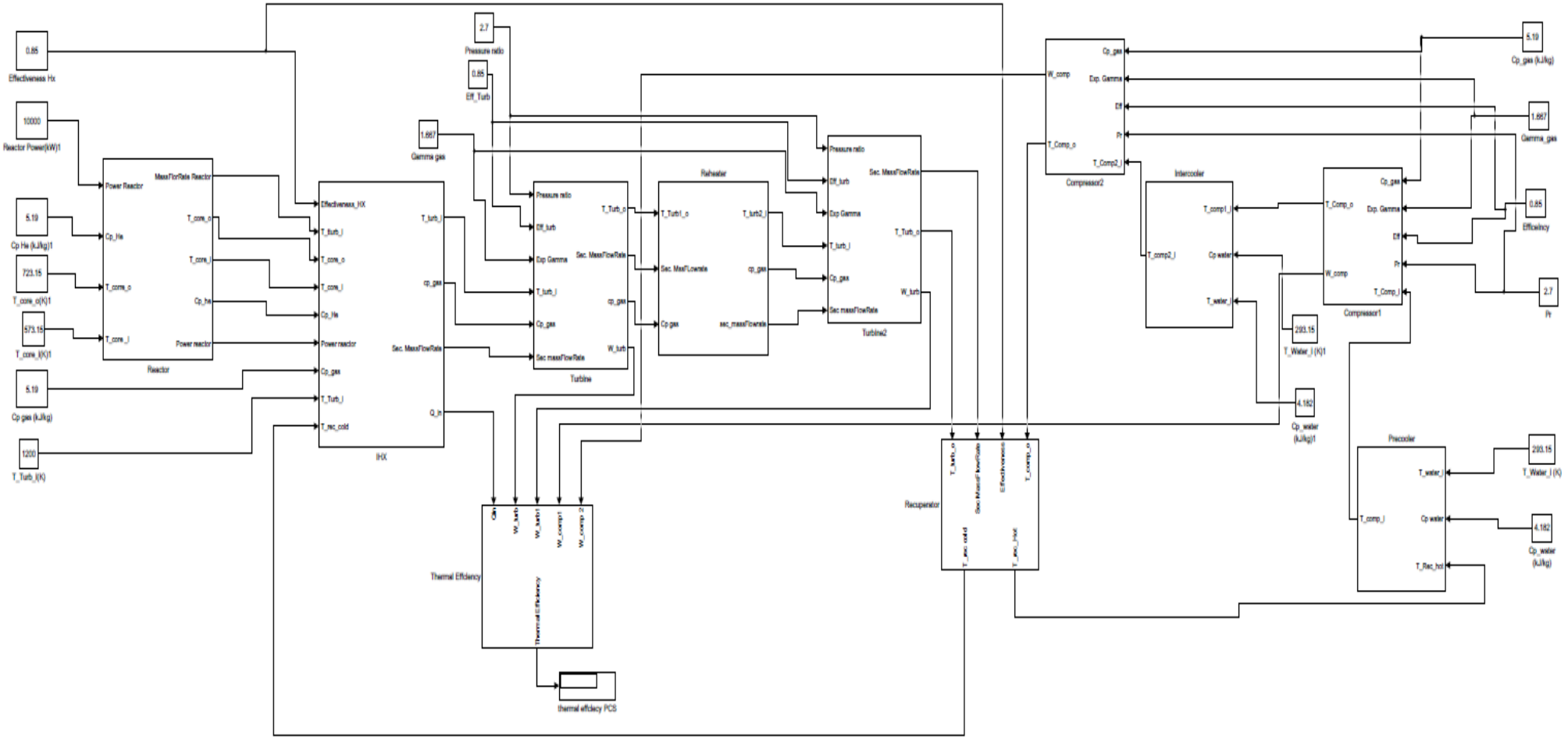

Appendix B: Combined cycle Simulink Diagram

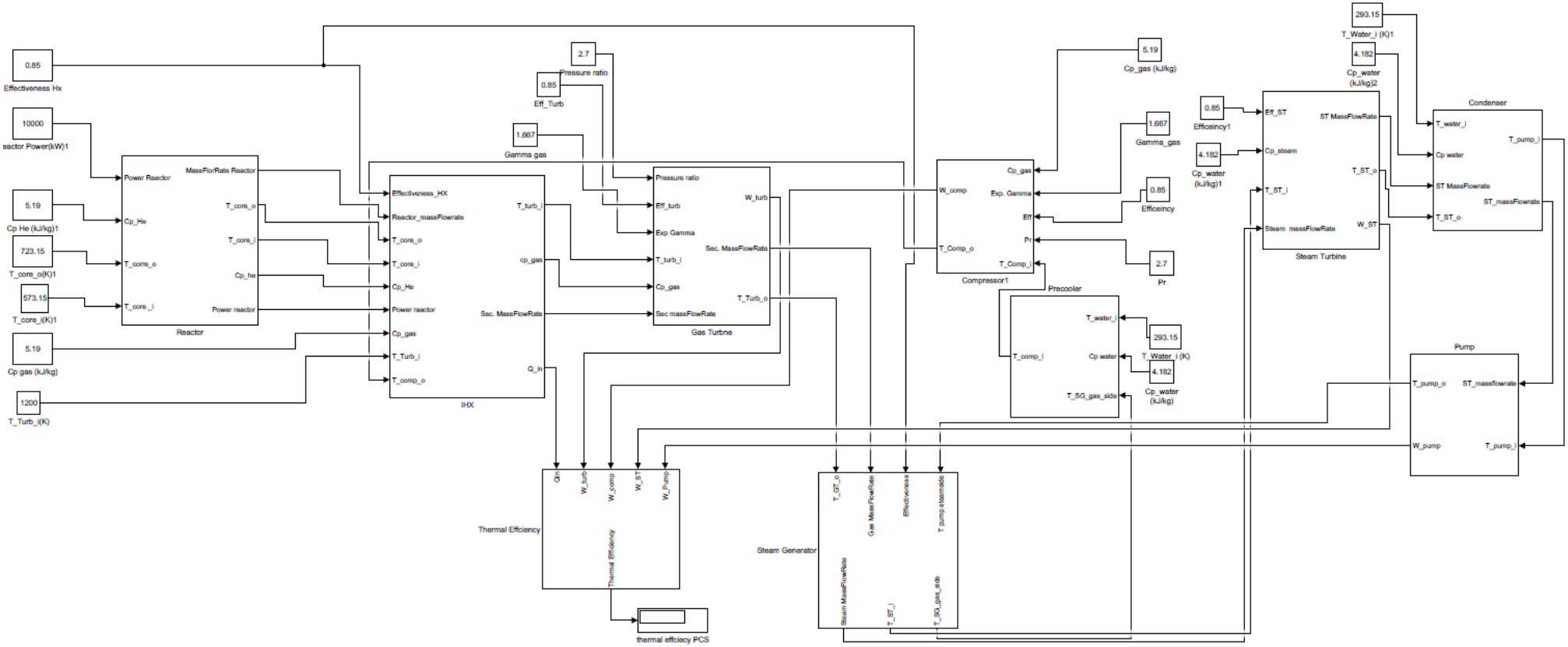

**Dimension of Iron Pipe Size (IPS) [43]**

| Nominal pipe size, IPS, in. | OD, in. | Schedule No. | ID, in. | Flow area per pipe, in.² | Surface per lin ft, ft.²/ft. | | Weight per lin ft, lb steel |
|---|---|---|---|---|---|---|---|
| | | | | | Outside | Inside | |
| ⅛ | 0.405 | 40* | 0.269 | 0.058 | 0.106 | 0.070 | 0.25 |
| | | 80† | 0.215 | 0.036 | | 0.056 | 0.32 |
| ¼ | 0.540 | 40* | 0.364 | 0.104 | 0.141 | 0.095 | 0.43 |
| | | 80† | 0.302 | 0.072 | | 0.079 | 0.54 |
| ⅜ | 0.675 | 40* | 0.493 | 0.192 | 0.177 | 0.129 | 0.57 |
| | | 80† | 0.423 | 0.141 | | 0.111 | 0.74 |
| ½ | 0.840 | 40* | 0.622 | 0.304 | 0.220 | 0.163 | 0.85 |
| | | 80† | 0.546 | 0.235 | | 0.143 | 1.09 |
| ¾ | 1.05 | 40* | 0.824 | 0.534 | 0.275 | 0.216 | 1.13 |
| | | 80† | 0.742 | 0.432 | | 0.194 | 1.48 |
| 1 | 1.32 | 40* | 1.049 | 0.864 | 0.344 | 0.274 | 1.68 |
| | | 80† | 0.957 | 0.718 | | 0.250 | 2.17 |
| 1¼ | 1.66 | 40* | 1.380 | 1.50 | 0.435 | 0.362 | 2.28 |
| | | 80† | 1.278 | 1.28 | | 0.335 | 3.00 |
| 1½ | 1.90 | 40* | 1.610 | 2.04 | 0.498 | 0.422 | 2.72 |
| | | 80† | 1.500 | 1.76 | | 0.393 | 3.64 |
| 2 | 2.38 | 40* | 2.067 | 3.35 | 0.622 | 0.542 | 3.66 |
| | | 80† | 1.939 | 2.95 | | 0.508 | 5.03 |
| 2½ | 2.88 | 40* | 2.469 | 4.79 | 0.753 | 0.647 | 5.80 |
| | | 80† | 2.323 | 4.23 | | 0.609 | 7.67 |
| 3 | 3.50 | 40* | 3.068 | 7.38 | 0.917 | 0.804 | 7.58 |
| | | 80† | 2.900 | 6.61 | | 0.760 | 10.3 |
| 4 | 4.50 | 40* | 4.026 | 12.7 | 1.178 | 1.055 | 10.8 |
| | | 80† | 3.826 | 11.5 | | 1.002 | 15.0 |
| 6 | 6.625 | 40* | 6.065 | 28.9 | 1.734 | 1.590 | 19.0 |
| | | 80† | 5.761 | 26.1 | | 1.510 | 28.6 |
| 8 | 8.625 | 40* | 7.981 | 50.0 | 2.258 | 2.090 | 28.6 |
| | | 80† | 7.625 | 45.7 | | 2.000 | 43.4 |
| 10 | 10.75 | 40* | 10.02 | 78.8 | 2.814 | 2.62 | 40.5 |
| | | 60 | 9.75 | 74.6 | | 2.55 | 54.8 |
| 12 | 12.75 | 30 | 12.09 | 115 | 3.338 | 3.17 | 43.8 |
| 14 | 14.0 | 30 | 13.25 | 138 | 3.665 | 3.47 | 54.6 |
| 16 | 16.0 | 30 | 15.25 | 183 | 4.189 | 4.00 | 62.6 |
| 18 | 18.0 | 20‡ | 17.25 | 234 | 4.712 | 4.52 | 72.7 |
| 20 | 20.0 | 20 | 19.25 | 291 | 5.236 | 5.05 | 78.6 |
| 22 | 22.0 | 20‡ | 21.25 | 355 | 5.747 | 5.56 | 84.0 |
| 24 | 24.0 | 20 | 23.25 | 425 | 6.283 | 6.09 | 94.7 |

Appendix D: Viscosity of Gases [43]

| Gas | $X$ | $Y$ |
|---|---|---|
| Acetic acid | 7.7 | 14.3 |
| Acetone | 8.9 | 13.0 |
| Acetylene | 9.8 | 14.9 |
| Air | 11.0 | 20.0 |
| Ammonia | 8.4 | 16.0 |
| Argon | 10.5 | 22.4 |
| Benzene | 8.5 | 13.2 |
| Bromine | 8.9 | 19.2 |
| Butene | 9.2 | 13.7 |
| Butylene | 8.9 | 13.0 |
| Carbon dioxide | 9.5 | 18.7 |
| Carbon disulfide | 8.0 | 16.0 |
| Carbon monoxide | 11.0 | 20.0 |
| Chlorine | 9.0 | 18.4 |
| Chloroform | 8.9 | 15.7 |
| Cyanogen | 9.2 | 15.2 |
| Cyclohexane | 9.2 | 12.0 |
| Ethane | 9.1 | 14.5 |
| Ethyl acetate | 8.5 | 13.2 |
| Ethyl alcohol | 9.2 | 14.2 |
| Ethyl chloride | 8.5 | 15.6 |
| Ethyl ether | 8.9 | 13.0 |
| Ethylene | 9.5 | 15.1 |
| Fluorine | 7.3 | 23.8 |
| Freon-11 | 10.6 | 15.1 |
| Freon-12 | 11.1 | 16.0 |
| Freon-21 | 10.8 | 15.3 |
| Freon-22 | 10.1 | 17.0 |
| Freon-113 | 11.3 | 14.0 |
| Helium | 10.9 | 20.5 |
| Hexane | 8.6 | 11.8 |
| Hydrogen | 11.2 | 12.4 |
| $3H_2 + 1N_2$ | 11.2 | 17.2 |
| Hydrogen bromide | 8.8 | 20.9 |
| Hydrogen chloride | 8.8 | 18.7 |
| Hydrogen cyanide | 9.8 | 14.9 |
| Hydrogen iodide | 9.0 | 21.3 |
| Hydrogen sulfide | 8.6 | 18.0 |
| Iodine | 9.0 | 18.4 |
| Mercury | 5.3 | 22.9 |
| Methane | 9.9 | 15.5 |
| Methyl alcohol | 8.5 | 15.6 |
| Nitric oxide | 10.9 | 20.5 |
| Nitrogen | 10.6 | 20.0 |
| Nitrosyl chloride | 8.0 | 17.6 |
| Nitrous oxide | 8.8 | 19.0 |
| Oxygen | 11.0 | 21.3 |
| Pentane | 7.0 | 12.8 |
| Propane | 9.7 | 12.9 |
| Propyl alcohol | 8.4 | 13.4 |
| Propylene | 9.0 | 13.8 |
| Sulfur dioxide | 9.6 | 17.0 |
| Toluene | 8.6 | 12.4 |
| 2, 3, 3-Trimethylbutane | 9.5 | 10.5 |
| Water | 8.0 | 16.0 |
| Xenon | 9.3 | 23.0 |

Appendix D : Viscosity of Gases (the graph) [43]